AEDC-TDR-64-121

117p ~ $2.50

RESEARCH STUDY OF THERMODYNAMIC SYSTEMS FOR TEMPERATURE CONTROL OF HEAT SINKS IN SPACE SIMULATION CHAMBERS

By

C. B. Hood, Jr., W. W. Vogelhuber,
C. B. Barnes, and R. F. Barron
CryoVac, Inc.
Columbus, Ohio

TECHNICAL DOCUMENTARY REPORT NO. AEDC-TDR-64-121

June 1964

AFSC Program Area 850E, Project 7778, Task 777801

(Prepared under Contract No. AF 40(600)-1032 by CryoVac, Inc., Columbus, Ohio.)

ARNOLD ENGINEERING DEVELOPMENT CENTER
AIR FORCE SYSTEMS COMMAND
UNITED STATES AIR FORCE

NOTICES

Qualified requesters may obtain copies of this report from DDC, Cameron Station, Alexandria, Va. Orders will be expedited if placed through the librarian or other staff member designated to request and receive documents from DDC.

RESEARCH STUDY OF THERMODYNAMIC SYSTEMS FOR TEMPERATURE CONTROL OF HEAT SINKS IN SPACE SIMULATION CHAMBERS

By

C. B. Hood, Jr., W. W. Vogelhuber, C. B. Barnes, and R. F. Barron

CryoVac, Inc.

Columbus, Ohio

June 1964

ABSTRACT

The selection of a specific type of thermodynamic system for temperature control of the heat sink (and cryopanel) surfaces in a space simulation chamber is vitally important for several reasons including:

1. Facility first cost
2. Facility operating cost
3. Facility usefulness or flexibility
4. Ease of operation and use
5. Reliability
6. Effect on heat sink design

Several systems which could be utilized for effecting temperature control of the heat sink surfaces in the range between 20°K and 373°K were examined in the light of these considerations. Also, where several systems could provide the same temperatures, an economical comparison was made. Thus, the first cost and operating cost of an air separation plant was compared to a nitrogen reliquefier, and the break-even point between a nitrogen reliquefier and a nitrogen subcooled circulation system was evaluated.

Considerable attention was also given to a more basic consideration, that is, to determine the relationship between the heat sink temperature and/or temperature profile and the simulator performance or capability. The areas of cryopumping, vehicle equilibrium temperature and the simulation temperature error as determined by an electrical network analogy were investigated. In addition, several generalized parameters were developed regarding the heat sink warm-up process from operating temperatures to some elevated temperature utilizing helium or nitrogen gas for the heat transfer fluid. ( )

PUBLICATION REVIEW

This report has been reviewed and publication is approved.

John D. Peters

JOHN D. PETERS, Lt Col, USAF
Chief, Technology Division
DCS/Plans and Technology

W. F. McRae

W. F. McRAE, Flt Lt, RCAF
Experimental Branch
Technology Division
DCS/Plans and Technology

CONTENTS

ILLUSTRATIONS

Figure

TABLES

NOMENCLATURE

A	Surface area, ft^2
A_h	Area of convection heat transfer, ft^2
A_p	Cross-sectional area of heat sink panel, ft^2
B	Breakeven point
C	Proportionality constant
C_r	Reliquefier installed first cost, $
C_s	Subcooler installed first cost, $
C_t	Heat transfer parameter as defined
D	Diameter, ft
E	Effectiveness of heat transfer process
E_s	Thermal "potential" of the solar source
E_s'	Thermal "potential" of the sun
E_v	Thermal "potential" of a vehicle inside a space simulator
E_v'	Thermal "potential" of a vehicle in space
E_w	Thermal "potential" of a heat sink wall
E_w'	Thermal "potential" of space
F	View factor
G	Incident thermal radiation per unit area on a surface
H	Thermal radiation per unit area leaving surface
I	Radiation emission per unit area for a black body
J	Mass flow rate per unit area leaving surface
K	Ratio of thermal currents, Q_2/Q_1
L	Length of panel in direction of gas flow, ft

M	Molecular weight
M_g	Mass of gas or fluid, lb_g
M_s	Mass of heat sink, lb_m
N_c	LN_2 cost, $/gal
P	Pressure
P_c	Power cost, $/KW-hr
P'	Vapor pressure
P''	Ionization gauge pressure reading
Q	Heat load and heat transfer rate, BTU/hr
Q_1, Q_2	Thermal "currents" representing net radiation heat transfer
R	Universal gas constant
R_1, R_2	Thermal "resistances"
RE	Refrigeration effect, BTU/lb gas compressed
S	Pumping speed
T	Absolute temperature, °R or °K
T_g	Fluid temperature
T_p	Heat sink panel temperature
T_s	Temperature of solar simulation source
T_s'	Temperature of surface of sun
T_v	Actual vehicle temperature
T_v'	Ideal vehicle temperature or, alternately, the temperature of a vehicle in space
T_w	Heat sink mean wall temperature

T_w'	Equivalent temperature of space
V	LN_2 requirements, gal/hr
V_g	Volume of gas, ft^3
W	Outgassing rate, i.e. generated mass flow rate per unit area leaving surface
W_k	Cycle input work, BTU/lb gas compressed
W_r	Reliquefier power requirements, KW
W_s	Subcooler power requirements, KW
X_r	Heat capacity ratio
Z_r	Reliquefier maintenance and operating costs, $/hr
Z_s	Subcooler maintenance and operating costs, $/hr
c	constant
$\bar{c}_p$	fluid specific heat, BTU/lb-°R
$\bar{c}_s$	mean heat sink specific heat, BTU/lb-°R
d	prefix for incremental element
e_s	heat sink emissivity
f	fraction of total (as defined)
f_c	capture fraction (of incident molecules)
f_r	friction factor
h	enthalpy, BTU/lb
h_c	convection heat transfer coefficient, BTU/hr-ft^2-°F
k_s	thermal conductivity of heat sink panel, BTU/hr-ft-°F

q	specific heat addition, BTU/lb_g
m_g	mass flow rate per unit area, $lb/hr\ Ft^2$
r	radius, ft
t	time, hr
v	molecular velocity
w	fluid flow rate, lb/hr
x_e	by-pass fraction
β	heat transfer parameter as defined
γ	heat transfer parameter as defined
Δ	prefix indicating finite difference
∂	prefix indicating partial derivative
θ	angle as defined
θ'	function as defined
ρ	density, lb/Ft^3
$\bar{\rho}$	mean density, lb/Ft^3
σ	Stefan-Boltzmann Constant
ϕ	Arcsin (A_1/A_2)
Ω	solid angle
η	function as defined
ξ	cycle efficiency
ξ_c	Carnot efficiency

ABBREVIATIONS

ave	average
GN_2	gaseous nitrogen
LN_2	liquid nitrogen
max.	maximum
min	minimum
press	pressure
ref	refrigeration
temp	temperature

BLANK PAGE

1.0 INTRODUCTION

This study was conducted to ascertain what thermodynamic systems are available for control of heat sink, and cryopanel temperatures in space simulation chambers and to evaluate the relative merits of the available units. The evaluation was predominantly technical but some systems were compared from an economical standpoint as well.

Before specific systems could be considered, the relationship, between (1) the requirements for temperature control of the various surfaces, (2) the temperature level, and (3) the temperature distribution provided by the thermodynamic systems, was determined.

Many of the systems which were examined during the course of this study have already been utilized in simulation facilities (as well as other areas).

This study was initiated on March 15, 1963 and completed on April 15, 1964.

2.0 SUMMARY

The relationship between the heat sink temperature level and the capability of the space simulation chamber was examined. The cryopumping speed, ultimate chamber pressure, and the sensitivity of the vacuum gauge to position in the chamber were determined. The simulation error of the vehicle exposed to heat sinks at various temperatures was defined and evaluated employing an electrical network analogy. The equilibrium vehicle temperature as a function of heat sink temperature was also determined. The effect of non-uniform heat sink temperatures on vehicle temperature was evaluated. A considerable variation in temperature between 2 points on the heat sink was shown to introduce a negligible error into the equilibrium temperature of the vehicle during radiation heat transfer studies.

The types, operating cycles, cycle characteristics, and the relative performances of a number of thermodynamic systems which are available for control of heat sink temperature in the 20°K to 373°K range were examined. In particular, an economic comparison was made between an air separation plant and a nitrogen reliquefier based on systems supplying 1000 KW refrigeration effect and, the break-even point was determined between a total loss nitrogen subcooler system and a no loss nitrogen reliquefier. The latter calculation was also again based upon systems supplying 1000 KW refrigeration effect. A graph showing the relationship between the break-even point, and LN_2 costs for two different power costs is included. Other systems examined included neon reliquefier, hydrogen reliquefier and a dense gas helium refrigerator.

The various techniques for warm-up of the heat sinks to near ambient temperatures following operation at cryogenic temperatures were examined. Expressions relating the fluid properties, the heat sink configuration, and the warm-up time were developed. The resulting non-dimensional parameters are plotted in various combinations to facilitate calculations of unknown variables for a specific application. Sample problems of these calculations showing typical procedures are included in Appendix A.

3.0 CRYOPUMPING

3.1 SURFACE TEMPERATURE AND CRYOPUMPING SPEED

Consider a test vehicle at temperature T_1, in a simulation chamber, surrounded by a heat sink which is cooled to some low temperature T_2. When molecules leave the relatively warm test vehicle, they move at a velocity greater than the velocity of other molecules which have been reflected from the surrounding heat sink. For purposes of calculations, the heat sink is taken as a sphere of area A_2 with a uniform capture fraction, f_{c2}. Similarly, the test vehicle is approximated by a warm sphere of area A_1 which is located concentrically within the heat sink.

In the following development it will be assumed that free molecular conditions exist, i.e. that collisions between molecules and the heat sink surfaces are much more likely than intermolecular collisions. From equilibrium conditions, the free molecular flow from any surface A_i to any other surface, A_j, is the same as the free molecular flow from A_j to A_i, if A_i and A_j are both molecularly rough (so that the cosine distribution law applies) and if both surfaces are at the same temperature. Therefore, the molecular flow rate from a finite area to an infinitesimal area is equal to the flow rate from the infinitesimal area outward to the finite area, assuming the same molecular speed in both cases. Because the cosine distribution implies complete randomness, the number of molecules leaving an infinitesimal surface element, dA, per unit solid angle per unit volume in any permitted direction would be the same as in any other direction. Expressed differently, the flow rate per unit solid angle per unit volume leaving dA and going to a finite area A_i subtending a solid angle Ω_i at dA would be everywhere the same within Ω_i and would be zero outside of Ω_i. This is graphically depicted on figure 1-a.

The molecules moving from A_i to dA cause a molecular density, defined as the number of molecules per unit volume, to exist adjacent to dA. The fraction of those molecules leaving A_i and moving within a total solid angle Ω_i (as measured from dA to A_i) which have directions of motion enclosed in a small solid angle $d\Omega$ is $d\Omega / \Omega_i$. The density of molecules adjacent to dA and having directions of motion toward dA and within $d\Omega$, making some angle θ with the normal to dA, is consequently

$$\rho_{i,dA} \cdot \frac{d\Omega}{\Omega_i}$$

The density $\rho_{i,\,dA}$ includes those molecules moving from A_i to dA and no others, and is measured adjacent to dA.

The mass flow toward a capturing surface such as dA varies with the molecular speed, v, and is biased by the cosine law. Thus $m_{i,\,dA}$, the mass flow rate from A_i to dA, is given by

$$\frac{m_{i,\,dA}}{dA} = \int_{\Omega_i} \rho_i \; v_i \cos\theta \; \frac{d\Omega}{\Omega_i} \tag{1}$$

where v_i represents the speed of molecules which leave A_i at temperature T_i. Because $\rho_{i,\,dA}$, Ω_i, and v_i are constant with respect to variations of $d\Omega$ within Ω_i, $m_{i,\,dA}$ can be written as

$$\frac{m_{i,\,dA}}{dA} = \left(\frac{\rho_{i,\,dA}\, v_i}{\Omega_i} \right) \int_{\Omega_i} \cos\theta \; d\Omega \tag{2}$$

Thus, in the actual problem of interest, the density of molecules adjacent to A_2 caused by molecules moving from the vehicle surface, A_1, is given by

$$\frac{m_{12}}{A_2} = \frac{\rho_{12}\, v_1}{\Omega_{12}} \int_{\theta\,=\,0}^{\phi} \cos\theta \; d\Omega \tag{3}$$

or

$$\rho_{12} = \frac{m_{12} \quad \Omega_{12}}{A_2 v_1 \int_{\theta\,=\,0}^{\phi} \cos\theta \; d\Omega} \tag{4}$$

where ϕ is depicted on figure 1-b, Ω_{12} is the solid angle subtended by A_1 at any point on A_2, and m_{12} is the mass flow rate from A_1 to A_2.

Since

$$\int_{\theta=0}^{\phi} \cos\theta \, d\Omega = \int_{\theta=0}^{\phi} \cos\theta \cdot 2\pi \sin\theta \, d\theta = \pi \sin^2\phi$$

and

$$\Omega_{12} = \int_{\theta=0}^{\phi} d\Omega = \int_{\theta=0}^{\phi} 2\pi \sin\theta \, d\theta = 2\pi(1-\cos\phi)$$

Then

$$\rho_{12} = \frac{2\, m_{12}(1-\cos\phi)}{A_2 v_1 \sin^2\phi} \tag{5}$$

In a similar manner, the density of molecules adjacent to A_2 caused by molecules going directly from A_2 to other parts of A_2 is given by

$$\rho_{22} = \frac{2\, m_{22}}{A_2 v_2 \cos\phi} \tag{6}$$

where m_{22} is the mass flow rate from A_2 to A_2. Finally, the density of molecules adjacent to A_2 caused by molecules leaving A_2 is given by

$$\rho_2 = \frac{2\, m_2}{A_2 v_2} \tag{7}$$

where m_2 is the mass flow rate leaving A_2. The total density adjacent to surface A_2 is ρ where

$$\rho = \rho_{12} + \rho_{22} + \rho_2 \tag{8}$$

or

$$\rho = \left[m_{12} \cdot \left(\frac{2}{v_1}\right)\left(\frac{1-\cos\phi}{\sin^2\phi}\right) + m_{22} \cdot \left(\frac{2}{v_2}\right)\left(\frac{1}{\cos\phi}\right) + m_2 \cdot \left(\frac{2}{v_2}\right)\right] \frac{1}{A_2} \tag{9}$$

The total mass flow rate leaving A_1 is composed of both the outgassing from A_1 and a fraction, F_{21}, of the mass of molecules which leave A_2. The fraction, F_{21} is the view factor similar to that used in radiation heat transfer calculations. Its use is justified because both molecular and radiant reflections are assumed to follow Lambert's cosine law. The total mass flow rate leaving A_2 consists of the outgassing from A_2 as well as the mass of molecules which leave A_1 (all of which strike A_2) and are not captured by A_2, and the mass of molecules which leave A_2, by-pass A_1, and strike A_2 again without being captured.

These statements may be expressed as

$$J_1 A_1 = W_1 A_1 + J_2 A_2 F_{21} \tag{10}$$

$$J_2 A_2 = W_2 A_2 + (1-f_{c2}) \left[J_1 A_1 + J_2 A_2 (1-F_{21}) \right] \tag{11}$$

where f_{c2} = capture fraction of surface A_2

J_1 = mass flow rate per unit area leaving the surface A_1.

J_2 = mass flow rate per unit area leaving the surface A_2.

W_1 = outgassing, i.e. generated, mass flow rate per unit area leaving A_1.

W_2 = outgassing rate per unit area leaving A_2.

Equations (10) and (11) can be solved for J_1 and J_2, using $F_{21} = A_1/A_2$.

$$J_1 = \left(1 + \frac{F_{21}}{f_{c2}} - F_{21}\right) W_1 + \frac{W_2}{f_{c2}} \tag{12}$$

$$J_2 = \left(\frac{1-f_{c2}}{f_{c2}}\right) F_{21} W_1 + \frac{W_2}{f_{c2}} \tag{13}$$

By definition

$$m_2 = J_2 A_2 \tag{14}$$

$$m_{12} = J_1 A_1 \tag{15}$$

$$m_{22} = J_2 (1-F_{21}) A_2 \tag{16}$$

Also, referring to Figure 1-b

$$\sin^2 \phi = (r_1/r_2)^2 = \left(\frac{A_1}{A_2}\right) = F_{21} \tag{17}$$

Substituting the relationships (12) through (17) in equation (9), and utilizing the relationship

$$v_1/v_2 = \sqrt{T_1/T_2} \tag{18}$$

where T_1 and T_2 are the absolute temperatures of surfaces A_1 and A_2 respectively, the expression for total density can be written as

$$\rho = \left\{\left[1 + \frac{F_{21}}{f_{c2}} - F_{21} + \frac{W_2}{f_{c2}W_1}\right]\cdot\left[1 - \sqrt{1-F_{21}}\right] + \sqrt{\frac{T_1}{T_2}}\left[F_{21}\left(\frac{1-f_{c2}}{f_{c2}}\right) + \frac{W_2}{f_{c2}W_1}\right]\left[1 + \sqrt{1-F_{21}}\right]\right\}\frac{2W_1}{v_1} \tag{19}$$

We will define pumping speed, S, as the ratio of the net mass flow to a surface to the density adjacent to that surface.

The net mass flow to surface A_2 can be shown to be W_1A_1. Thus,

$$S = \frac{W_1 A_1/A_2}{\rho} = \frac{W_1 F_{21}}{\rho} \tag{20}$$

Substituting the expression for ρ, given in (19), into (20)

$$S = \left\{\frac{2F_{21}}{\left[1 + \frac{F_{21}}{f_{c2}} - F_{21} + \frac{W_2}{f_{c2}W_1}\right]\left[1 - \sqrt{1-F_{21}}\right] + \sqrt{\frac{T_1}{T_2}}\left[F_{21}\left(\frac{1-f_{c2}}{f_{c2}}\right) + \frac{W_2}{f_{c2}W_1}\right]\left[1 + \sqrt{1-F_{21}}\right]}\right\}\frac{v_1}{4} \tag{21}$$

Special situations are of particular interest. Suppose $A_1 \ll A_2$; then F_{21} is very small. Also, because the total vaporization will be less than the total introduced load, $W_1A_1 > W_2A_2$ which requires $W_1 \gg W_2$.

Then, expanding $\sqrt{1-F_{21}}$ by the binomial theorem, we have $1-\sqrt{1-F_{21}} = (1/2)F_{21} + \ldots$, and taking the limit $F_{21} \to 0$ as $A_1 \to 0$.

$$\lim_{A_1 \to 0} \frac{S}{A_2} = \frac{4}{1 + 4\left(\frac{1-f_{c2}}{f_{c2}}\right)\sqrt{T_1/T_2}} \cdot \frac{v_1}{4} \tag{22}$$

If complete capture occurs, i.e., if $f_{c2} = 1$, the pumping speed per unit area is four times the so-called orifice speed.

The ratio of "observed" pumping speed to orifice speed i.e., $(S/A_2)/(v_1/4)$, is shown in Figure 2 as a function of the capture fraction of the cryopumping array. Aribitrary assumptions are: the vehicle diameter is slightly greater than a third of the shroud diameter, the vehicle temperature is 300°K, and the shields on the shroud are 80°K, or 100°K, or 200°K. The difference in the curves for $F_{21} = 0$ and $F_{21} = 0.1$ is insignificant. The ratio of "observed" pumping speed to orifice speed is shown in Figure 3 as a function of the capture fraction for different test vehicle sizes.

It is important to note that the density of molecules adjacent to a surface A_1 is quite different from the density adjacent to A_2. The mass flow rate to surface A_1 per unit area is

$$\frac{J_2 A_2 F_{21}}{A_1} = \frac{m_{21}}{A_1} = \frac{\rho_{21}}{2\pi} \int_{\theta=0}^{\pi/2} (2\pi \sin\theta \, d\theta) \, v_2 \cos\theta = \frac{\rho_{21} v_2}{2} \tag{23}$$

The mass flow away from surface A_1 per unit area is

$$J_1 = \frac{m_{12}}{A_1} = \frac{\rho_1 v_1}{2} \tag{24}$$

The total density adjacent to A_1 is therefore

$$\rho = (\rho_{21} + \rho_1) = \frac{2J_2}{v_2} + \frac{2J_1}{v_1} \tag{25}$$

Because of the fact that a nude ionization gauge actually measures density rather than pressure, the value of "pressure" determined by such a gauge is proportional to

$$P \propto \frac{2J_1}{v_1}\left[1-\sqrt{1-F_{21}}\right] + \frac{2J_2}{v_2}\left[1+\sqrt{1-F_{21}}\right] \tag{26}$$

at the cryopumping shroud, and is proportional to

$$P \propto \frac{2J_2}{v_2} + \frac{2J_1}{v_1} \tag{27}$$

at the vehicle.

The observed cryopumping speed of the shroud is therefore dependent not only on the shield temperature, the capture fraction, and the relative vehicle size, but also on whether the ionization gauge is at the shroud, or elsewhere.

3.2 ULTIMATE CHAMBER PRESSURE

The lowest pressure that can be reached in a chamber occurs when the mass capture rate exactly equals the mass vaporization rate from the heat sink; equivalently, when $W_1 = 0$.

$$W_2 A_2 = \left[J_2 (1-F_{21}) + J_1 F_{21}\right] A_2 f_{c2} \tag{28}$$

or

$$\frac{W_2}{f_{c2}} = J_2 + (J_1 - J_2) F_{21} \tag{29}$$

Because $J_1 - J_2 = W_1 = 0$,

$J_1 = J_2 = \frac{W_2}{f_{c2}}$, and the density at A_2 is

$$\rho = \left[\sqrt{T_2/T_1}\ .\ (1-\sqrt{1-F_{21}}) + (1+\sqrt{1-F_{21}})\right] \frac{2W_2}{f_{c2}\ v_2} \tag{30}$$

based on all gas leaving surface A_2 having the temperature T_2 and all gas leaving surface A_1 having the temperature T_1.

However, the mass flow of vapor from the cryopanels back into the chamber is determined by the cryopanel temperature, the cryopanel and shield frontal area, and the capture fraction i.e., the cryopump geometry.

The rate of condensate evaporation from any surface is the same as the condensation onto that surface from equilibrium gas in contact with the condensate. Assuming the ideal gas law,

$$W_2 = f_{c2} \cdot \left(\frac{v_4}{4} \right) \cdot \frac{P' M}{R T_4} \tag{31}$$

where

P' = equilibrium vapor pressure at T_4

T_4 = cryoplate (and condensate) temperature

R = universal gas constant

M = molecular weight of the gas

The factor f_{c2} occurs because that fraction of the molecules vaporized from the cryoplate which find their way into the interior of the chamber must equal the fraction of incident molecules (onto the cryopumping array) which find their way through the shields and to the cryoplates, for equilibrium conditions.

Combining equations (30) and (31) yields:

$$\rho = \left[\sqrt{T_2/T_1} \cdot (1 - \sqrt{1-F_{21}}) + (1 + \sqrt{1-F_{21}}) \right] \frac{v_4}{2v_2} \cdot \frac{P' M}{R T_4} \tag{32}$$

An ionization gauge actually reads density, but it is calibrated to give the correct value for pressure in an equilibrium gas at some calibration temperature T_3. That is, the pressure reading is given by

$$P'' \propto \rho \tag{33}$$

where the proportionality factor is $R T_3/M$.

That is,

$$P'' = \left(\frac{R T_3}{M} \right) \rho \tag{33a}$$

Therefore an expression for the reading on a nude ionization gauge at the ultimate low pressure in a system (no outgassing from the test object) is obtained by combining equations (32) and (33a) and substituting $v_4/v_2 = \sqrt{T_4/T_2}$.

That is

$$P'' = \left[\frac{(1-\sqrt{1-F_{21}})}{\sqrt{T_4\,T_1}} + \frac{(1+\sqrt{1-F_{21}})}{\sqrt{T_4\,T_2}} \right] \cdot \frac{T_3}{2} \cdot P' \qquad (34)$$

For an empty chamber ($F_{21} = 0$) the gauge reads

$$P'' = \frac{T_3\,P'}{\sqrt{T_4\,T_2}} \qquad (35)$$

If $T_3 = 300°K$, $T_4 = 20°K$, and $T_2 = 100°K$, then

$$P'' = 6.71\,P' \qquad (36)$$

and the ultimate pressure as indicated by a nude ionization gauge is significantly different from the vapor pressure of the condensate.

Figure 4 shows the ratio of the ultimate pressure in the chamber as measured with an ionization gauge, to the vapor pressure of the condensate. This is done for T_1 and $T_3 = 300°K$, $T_4 = 20°K$, and T_2 = various temperatures.

It may be noted that for $T_2 = T_3 = T_1$, and $F_{21} = 0$,

$$P'' = \sqrt{T_2/T_4}\;P' \qquad (37)$$

which is the familiar expression for the pressure difference caused by the thermal transpiration effect.

If $T_4 = T_2 \neq T_3 = T_1$ as would occur for a "room temperature" vehicle inside a uniform temperature shroud, and if again $F_{21} = 0$, then

$$P'' = \frac{T_3}{T_2} \cdot P' \qquad (38)$$

as would be expected on the basis of direct application of the ideal gas law.

3.3 UNDESIRABLE SURFACE TEMPERATURES

Aside from pumping speed considerations, it may be noted from Figure 5, which shows vapor pressures as a function of temperature for several common chamber constituents, that under certain circumstances there are temperature ranges which should be avoided for the cryopanel shields. This is because temperature variation through these ranges will alternately cause condensation or evaporation depending on the chamber pressure, the shield temperature, and the gas being pumped. For example, the vapor pressure of water (ice) varies from 10^{-10} torr to 10^{-4} torr as the temperature varies from 125°K to 185°K. Below 125°K, the amount of evaporation is negligible. Above 185°K, (and below 10^{-4} torr) condensation will not occur. For temperatures within the range, variation of temperature usually causes uncertainty in the resulting chamber pressure (for a given pumping speed).

A similar undesirable temperature range occurs between 66°K and 100°K if a substantial amount of carbon dioxide is introduced into the system. Various undesirable bands between 21°K and 44°K occur depending on the amounts of N_2, O_2, CO, and CH_4 in the system.

4.0 SIMULATION ERROR

4.1 DEFINITION OF SIMULATION ERROR

The temperature of a vehicle or other test object in a space simulation chamber is usually higher than it would be if actually in space for two reasons. First, a small part of the simulated solar thermal radiation is reflected from the "black" heat sink so there is more total thermal load reaching the vehicle than there would be in space. Second, the heat sink radiates heat to the vehicle because it is warmer than the "equivalent" temperature of space (which is about 4°K). The temperature error caused by reflection of radiation from the thermal shroud is reduced by using a chamber large as compared with the test object. The error caused by the thermal shroud temperature being greater than 4°K is minimized by using a low heat sink temperature as compared to the test object temperature. The total increase in test object temperature when in the chamber rather than in space, is defined as the simulation error.

4.2 DERIVATION OF EXPRESSION FOR SIMULATION ERROR

4.2.1 Heat Balance By The Net Radiation Method

The temperature of a vehicle receiving thermal radiation inside a cold and evacuated "black" cavity is probably best obtained by the electrical network analogy of net radiation. The correspondence is set-up as follows. The net radiation leaving a surface, Q_{net}, is

$$Q_{net} = (H-G)\,A \tag{39}$$

where

G = total radiation per unit area incident on the surface

H = total radiation per unit area leaving the surface

A = area of the grey surface

Defining I as the emission of radiation per unit area for a black body, it follows that

$$I = \sigma T^4 \tag{40}$$

where

σ = Stefan-Boltzmann constant

T = absolute temperature of the body

Then H can be written as

$$H = e_s I + (1-e_s) G \tag{41}$$

where e_s = surface emissivity

This is equivalent to

$$(1-e_s)(H-G) = e_s (I-H) \tag{42}$$

Therefore

$$Q_{net} = \frac{(I-H)}{(1-e_s)/(e_s A)} \tag{43}$$

An electrical analogy exists in which

Q_{net} corresponds to current,

(I-H) corresponds to potential difference,

and $\frac{1-e}{eA}$ corresponds to electrical resistance.

If two grey surfaces A_1 and A_2 interchange radiant energy, the net radiation from A_1 to A_2 is

$$(Q_{net})_{12} = A_1 F_{12} H_1 - A_2 F_{21} H_2 = A_1 F_{12} (H_1 - H_2)$$

where F_{12} is the view factor of surface 1 to surface 2, and where A_2F_{21} equals A_1F_{12}. That is, if a black body of area A_1 is at a uniform temperature T_1 and emitting thermal radiation according to the cosine distribution law,* then F_{12} is the fraction of this radiation which strikes surface A_2. F_{12} depends only on the mutual geometry of two surfaces, and it is a geometrical fact that for any two surfaces A_1 and A_2, $A_1F_{12} = A_2F_{21}$.

Consequently, in addition to the expression for net radiation to a surface, depending on surface properties, there is also an expression for the net radiation interchange between two surfaces, depending on the total radiation leaving each surface and the sizes, shapes, and relative orientation of the surfaces. In this latter expression, H_1-H_2 corresponds to potential difference, and $(A_1F_{12})^{-1} = (A_2F_{21})^{-1}$ corresponds to electrical resistance.

4.2.2 Equivalent Network for Space Simulation

Consider a source of thermal radiation (a solar simulator) to be irradiating a test object enclosed inside, but not in physical contact with, an evacuated grey wall enclosure. This enclosure is nearly always maintained at a substantially lower temperature than that of the test object, and therefore is sometimes called a thermal shroud or heat sink. The source of thermal radiation is at a very much higher temperature than that of either the test object or the heat sink.

For purposes of calculation, it will be assumed that both the heat sink and the test object are spherical, and also that the incident thermal radiation is uniformly distributed around the test object. Such a solar simulator might consist of electrical resistance heaters distributed around the test object. Typically, these heaters would have reflectors between the resistance elements and the thermal shroud in order to increase the efficiency of irradiation. However, for most practical designs, some radiant heat will bypass the test object and this bypass radiation will strike the heat sink wall. A schematic cross section of the configuration is shown on Figure 6.

* The cosine distribution assumes that the amount of radiation per unit area of A_1 going in any given direction (per unit solid angle) varies as the cosine of the angle between this given direction and the normal to the surface.

In addition to the solar simulation, there may also be a source of heat inside the test object. In actual space vehicles, this may be heating from the various types of electronic equipment, from auxiliary power sources, or from the central power plant of space propulsion engines. Regardless of the source, this heating is independent of whether the test object is in the space simulation chamber or in space.

The thermal network for a vehicle in the space simulator is shown in Figure 7. The thermal network for a vehicle in space is shown in Figure 8. The actual values of thermal potentials and resistances are replaced by the symbols E and R respectively.

The following equations hold for the circuit shown in Figure 7:

$$E_s - E_w = Q_1 R_1 + (Q_1 + Q_2) R_3 + (Q_1 + Q_2 + Q_3) R_4 \quad (44)$$

$$E_v - E_w = Q_2 R_2 + (Q_1 + Q_2) R_3 + (Q_1 + Q_2 + Q_3) R_4 \quad (45)$$

$$E_s - E_w = Q_3 R_5 + (Q_1 + Q_2 + Q_3) R_4 \quad (46)$$

where E_s = thermal "potential" of the emitting surfaces of the solar simulator,

E_v = thermal "potential" of the test object or "vehicle",

E_w = thermal "potential" of the cold wall, or heat sink.

A similar set of equations exists for the circuit of Figure 8, corresponding to conditions in space.

In principle, these sets of equations may be used directly to determine the difference between E_v, the thermal "potential" of a vehicle in a space simulator, and E_v', the thermal "potential" of a vehicle in space. This will then give the difference between T_v, the temperature of the vehicle in the simulator, and T_v', the temperature of the vehicle in space.

However, as shown in the following analysis, since $Q_1 = Q_1'$ and $Q_2 = Q_2'$, the increase of E_v' to E_v is caused by the increase of E_w' to E_w, which tends to increase H_w', as well as by the presence of Q_3, which increases the "potential drop" from H_w' to E_w' and thereby also tends to increase H_w' (see Figures 7 and 8). The increase of H_w' to H_w has the effect of increasing H_v' to H_v, therefore increasing E_v to E_v';

from this the difference $T_v - T_v'$ is obtained. To obtain an explicit simplified solution, the sums of resistances (and potentials) is approximated by omitting those which are negligible as compared with others in a sum. This is done by calculating order of magnitude values. First, evaluate R_1'. The diameter of the sun is approximately 860,000 miles, and the distance from the earth to the sun averages about 93,000,000 miles. The cross section of a spherical test object five feet in diameter is 19.6 sq ft. So, for an actual earth orbit, the fraction of total emitted solar radiation which strikes the exposed side (actually the cross section) of the test object is

$$F_{sv}' = \frac{19.6}{4\pi (93 \times 10^6 \times 5280)^2} = 6.5 \times 10^{-24},$$

$$A_s' = \pi (8.6 \times 10^5 \times 5280)^2 = 6.5 \times 10^{19} \text{ sq ft, and}$$

$$R_1' = \frac{1}{A_s' F_{sv}'} \quad \frac{1}{4.2 \times 10^{-4} \text{ sq ft}} = 2380 \text{ sq ft}^{-1}$$

In a simulator, T_s might typically be 3800°K. The surface of the sun has a temperature (based on the type of thermal radiation emitted) of 6000°K. Therefore, using $A_s \sigma T_s^4 F_{sv} = A_s' \sigma (T_s')^4 F_{sv}'$, which predicates that the radiation incident on the test object is the same in the space simulator as it is in space,

$$R_1 = \frac{1}{A_s F_{sv}} = \left(\frac{T_s}{T_s'}\right)^4 \cdot \frac{1}{A_s' F_{sv}'} = \left(\frac{3800}{6000}\right)^4 \times 2380 = 390 \text{ sq ft}^{-1}$$

The surface area of the test object (a five foot diameter sphere) is taken to be 78.5 sq ft. Then $A_v \gg A_s F_{sv}$, $A_v \gg A_s' F_{sv}'$, and

$$R_3 \doteq 1/A_v \ll R_1$$

$$R_3' \doteq 1/A_v \ll R_1'$$

Also, $R_4 = \frac{1-e_w}{e_w A_w} < \frac{1-e_w}{e_w A_v} < \frac{1}{A_v}$ for $e_w > 0.5$,

so that for any reasonably "black" thermal shroud, $R_4 \ll R_1$. Also if $e_w \doteq 0.9$, as is usual, then $R_4 \ll R_3$.

Finally, F_{sv} will always exceed 2/3 for any well designed system, so that

$$A_s (1-F_{sv}) \leq 1.28 \times 10^{-3} \text{ sq ft, and } R_5 \gg R_3 \text{ as well as } R_5 \gg R_4.$$

Similarly, comparing potentials,

$$E_s \gg E_v \text{ and } E_w, \quad E_s' \gg E_v' \text{ and } E_w'.$$

It will also be true in most cases that $E_v \gg E_w$, $E_v' \gg E_w'$, and $E_w \gg E_w'$.

It is therefore an excellent approximation that, from equations 44, 45, and 46,

$$Q_1 R_1 + Q_2 (R_3 + R_4) + Q_3 R_4 = E_s \tag{47}$$

$$Q_1 (R_3 + R_4) + Q_2 (R_2 + R_3 + R_4) + Q_3 R_4 = E_v - E_w \tag{48}$$

$$Q_1 R_4 + Q_2 R_4 + Q_3 R_5 = E_s \tag{49}$$

These equations are used to compare thermal "currents." Solving for Q_1,

$$Q_1 = \frac{E_s}{R_1} \left[\frac{(R_2 + R_3 + R_4) R_5 - R_4^2 - R_2 R_4}{(R_2 + R_3 + R_4) R_5 - R_4^2} \right] \tag{50}$$

For any reasonable values of the thermal resistances

$$R_2 R_4 \ll (R_2 + R_3 + R_4) R_5 - R_4^2$$

and

$$Q_1 \doteq \frac{E_s}{R_1}$$

Similarly, $Q_1' = E_s'/R_1'$; and because $E_s'/R_1' = E_s/R_1$, then $Q_1 \doteq Q_1'$.

For any given orbit, there will be a definite fixed value of Q_1, and for any given vehicle there will be given a definite fixed value of Q_2. Therefore for any given situation, Q_2 has a constant ratio K to Q_1. These relationships can be written as:

$$Q_2 = KQ_1 \tag{51}$$

and

$$Q_2' \doteq KQ_1' \tag{52}$$

Any adjustment in K will therefore cause a corresponding adjustment in E_v.

Solving for Q_3,

$$Q_3 = \frac{E_s \left[R_1 (R_2 + R_3 + R_4) - (R_3 + R_4)^2 - R_2 R_4\right] - (E_v - E_w) R_1 R_4}{R_1 \left[(R_2 + R_3 + R_4) R_5 - R_4^2\right]} \tag{53}$$

and for situations of practical interest, where

$$R_2 R_4 + (R_3 + R_4)^2 \ll R_1 (R_2 + R_3 + R_4), \text{ and}$$

$$(E_v - E_w) R_4 \ll E_s (R_2 + R_3 + R_4), \text{ also:}$$

$$R_4^2 \ll (R_2 + R_3 + R_4) R_5$$

$$Q_3 \doteq E_s/R_5 = (E_s/R_1)(R_1/R_5) \doteq Q_1 (R_1/R_5) \tag{54}$$

(Evaluation of Q_3' is of no interest in the analysis).

Combining equations (48), (51) and (54) yields:

$$E_v = E_w + Q_1 \left[(1 + K + R_1/R_5) R_4 + (1 + K) R_3 + K R_2\right] \tag{55}$$

and since $R_2 \equiv R_2'$ and $R_3 \doteq R_3'$,

$$E_v - E_v' = (E_w - E_w') + Q_1 (1 + K + R_1/R_5) R_4 \tag{56}$$

There remains only to evaluate $E_v - E_v'$, $E_w - E_w'$ and Q_1.

$$\begin{aligned} E_v - E_v' &= \sigma \left[T_v^4 - (T_v')^4\right] \\ &= \sigma (T_v - T_v') \left[T_v^3 + T_v^2 (T_v') + T_v (T_v')^2 + (T_v')^3\right] \\ &\doteq \sigma (T_v - T_v') 4 T_v^3, \end{aligned} \tag{57}$$

where the evaluations have been restricted to situations in which

$E_v - E_v' \ll E_v$, i.e. $T_v \doteq T_v'$.

$E_w - E_w' = \sigma \left[T_w^4 - (T_w')^4 \right]$, and if $T_w \geq 20°K$,

then $T_w^4 \geq 160,000°K^4$,

$(T_w')^4 = (4°K)^4 = 256°K^4$, and

$$E_w - E_w' \doteq E_w \tag{58}$$

Q_1 is evaluated from $(Q_1 + Q_2) R_3 = H_2 - H_4$, where

$$H_4 = E_w + (Q_1 + Q_2 + Q_3)R_4$$

$$= E_w + Q_1 (1 + K + R_1/R_5)R_4, \text{ and} \tag{59}$$

$$H_2 = E_v - Q_2 R_2$$

$$= E_v - KQ_1 R_2. \tag{60}$$

[illegible],

$$Q_1 = \frac{E_v - E_w}{(1+K)R_3 + (1 + K + R_1/R_5)R_4 + KR_2}, \tag{61}$$

where usually E_w may be neglected as compared with E_v.

The equation for $E_v - E_v'$ then becomes

$$T_v - T_v') \, 4T_v^3 \doteq T_w^4 + T_v^4 \left[\frac{(1 + K + R_1/R_5) R_4}{(1 + K)R_3 + (1 + K + R_1/R_5)R_4 + KR_2} \right] \tag{62}$$

Substituting values for resistances and dividing by $4 T_v^3$ gives the thermal simulation error.

$$T_v - T_v' \doteq \frac{T_w^4}{4\,T_v^3} + \left(\frac{T_v}{4}\right)\left(\frac{1-e_w}{e_w}\right)\left(\frac{A_v}{A_w}\right)\left[\frac{K + F_{sv}^{-1}}{\left(\frac{e_v+K}{e_v}\right) + (K + F_{sv}^{-1}).\left(\frac{1-e_w}{e_w}\right)\left(\frac{A_v}{A_w}\right)}\right] \quad (63)$$

For a sufficiently cold thermal shroud, $T_w^4/4\,T_v^3$ is replaced by $(T_w^4/4\,T_v^3) - ((T_w')^4/4T_v^3)$ in this expression, and for a vehicle temperature comparable to the shroud temperature, $T_v/4$ is replaced by $(T_v/4) - (T_w^4/4\,T_v^3)$.

4.2.3 Specific Applications

The temperature of a spherical vehicle in space can be obtained from the equation for E_v' (space) corresponding to equation (55) for E_v. It is

$$E_v' = E_w' + Q_1' \left[(1 + K)R_3 + KR_2\right] \quad (64)$$

where, as before, $R_4' = 0$.

Explicitly,

$$(T_v')^4 \doteq (T_w')^4 + (T_s')^4\, A_s'\, F_{sv'} \cdot \left(\frac{e_v + K}{e_v}\right) \cdot \frac{1}{A_v},$$

and neglecting T_w' as compared to T_v'

$$T_v' = T_s' \left[\frac{A_s'\, F_{sv'}}{A_v} \cdot \frac{e_v + K}{e_v}\right]^{1/4} \quad (65)$$

$$= 6000°K \times 0.048 \times \left(\frac{e_v + K}{e_v}\right)^{1/4}$$

$$= \left[\frac{e_v + K}{e_v}\right]^{1/4} \times 288°K \quad (66)$$

Taking $e_v = 0.1$ and $K = 0.025$, we get $T_v' = 304°K$, and it is true that most metallic vehicles subjected to solar irradiation in an earth orbit achieve a temperature of $T_v' \doteq 300°K$. Using $T_v' = 300°K$, $e_w = 0.9$, $e_v = 0.1$, $F_{sv} = 2/3$, and $K = 0.025$, the equation for simulation error becomes

$$T_v - T_v' \doteq \left[\frac{12.70}{1.25 + 0.17\,(A_v/A_w)}\right] \cdot \frac{A_v}{A_w} + \frac{T_w^4}{1.08 \times 10^8} \qquad (67)$$

which is plotted in Figure 9, for various ratios of A_v/A_w.

The value taken for K is arbitrary, but it corresponds to an internal heat generation of 110 watts in an earth orbit vehicle two meters in diameter, and is therefore considered reasonable. For most tests, it is doubtful that the expense of cooling a thermal shroud below liquid nitrogen temperature can be justified on the basis of temperature simulation alone. As can be seen from the equation, there will remain a temperature error even for $T_w = 4°K$.

Although attention is generally focused on systems in which solar simulation is of primary importance, it is interesting to consider the simulation error when the internal heating exceeds the external (solar) heating. This situation might occur, for example, with a nuclear powered vehicle in the earth's shadow. For such a case K is large, and the simulation error becomes

$$T_v - T_v' = \frac{T_w^4}{4\,T_v^3} + \left[\frac{T_v}{4}\right]\left[\frac{1-e_w}{e_w}\right]\left[\frac{A_v}{A_w}\right] \cdot \left[\frac{1}{e_v} + \frac{1-e_w}{e_w} \cdot \frac{A_v}{A_w}\right]^{-1} \qquad (68)$$

If a great amount of internal heating is present, then T_v is large and the importance of T_w in the simulation error is considerably reduced. For many situations of this type, temperatures from -50° to -100°F may be quite adequate.

Indeed, it is particularly important during design of a space simulation chamber, to carefully weigh the benefits obtained by maintaining the heat sink at various temperature levels against the costs of generating the necessary refrigeration effect. Therefore, it is important to reduce T_w only if this reduction will reduce $T_v - T_v'$ to an acceptable level. The expense and reduced reliability of using liquid helium, for example, rather than liquid nitrogen for cooling a space environmental temperature shroud is almost never justified.

The preceding analysis is limited by the assumption of complete spherical symmetry as well as ideal physical isolation. The assumption of a spherical test chamber and test object is not too serious, but the assumption of a spherical distribution of solar simulation does limit the accuracy of the method. Nevertheless, the results are indicative of actual temperature simulation errors, and show that it is economically beneficial to focus attention on the vehicle temperature rather than the heat sink temperature. For more complicated geometrical configurations than the one presented here, the network technique would still be used. Reference may be made to the original thermal network presentation: A. K. Oppenheim, Trans. A.S.M.E., 78, 725 (1956).

5.0 SURFACE TEMPERATURE VARIATION

5.1 EFFECT OF HEAT SINK TEMPERATURE VARIATION ON VEHICLE TEMPERATURES

Consider a heat sink which is exposed to a heat source within the chamber. Control of the heat sink temperature is provided by circulating a fluid through flow areas which are attached to the heat sink. An expression relating the heat load, and the heat sink temperature difference is

$$Q = w\bar{c}_p (T_{f2} - T_{f1}) \tag{69}$$

where

Q = heat load

w = fluid flow rate

$\bar{c}_p$ = mean fluid specific heat

T_{f2} = fluid temperature leaving the heat sink

T_{f1} = fluid temperature entering the heat sink

The actual heat sink and fluid temperature differences are closely related as the convection heat transfer temperature difference is relatively small.

Since the heat sink flow areas are limited by practical design considerations, the fluid mass flow rates are also limited. For a given heat load and fluid, the temperature difference of the heat sink can become substantial. The effect of this temperature difference on the equilibrium temperature of a test vehicle will be examined.

Consider the radiant heat exchange between a spherical vehicle and a spherical thermal heat sink. If both are at uniform temperatures, the net heat transfer between them can be written as

$$Q = F_e A_v \sigma (T_v^4 - T_s^4) \tag{70}$$

where T_v = uniform temperature of the vehicle

T_s = uniform temperature of the heat sink

F_e = emissivity factor

A_v = Area of the vehicle

σ = Stefan-Boltzmann constant

If the heat sink is not at uniform temperature then some fraction f_1 is at a slightly higher temperature, T_1, where

$$T_1 = T_o + \eta \Delta T \tag{71}$$

where

ΔT = over-all variation in heat sink temperature

η = function between 0 and 1

T_o = coldest temperature of heat sink

There is an nth fraction, f_n, of the heat sink at a temperature T_n where

$$T_n = T_o + \eta_n \Delta T \tag{72}$$

Thus each of these fractions of heat sink area are transferring heat at a different rate and

$$Q = Q_1 + Q_2 + - - - - Q_n \tag{73}$$

Or

$$Q = \sum_{i=1}^{n} Q_i \tag{74}$$

where $$Q_i = f_1 F_e A_v \sigma \left[T_v^4 - (T_o + \Delta T)^4 \right] \tag{75}$$

for e_s, the heat sink emissivity ≈ 1 and $o \leq \eta \geq 1$

A linear temperature distribution will be assumed across any particular

cooling zone in the sink for simplification. The fractions f_i can be related to η_i by

$$f_i = d\eta_i \tag{76}$$

Therefore,

$$Q = \int_{\eta=o}^{1} \sigma F_e A_v \left[T_v^4 - (T_o + \eta \Delta T)^4\right] d\eta \tag{77}$$

integrating and solving for T_v^4

$$T_v^4 = \frac{Q}{F_e A_v \sigma} + T_o^4 + 2T_o^3 \Delta T + 2 T_o^2 (\Delta T)^2 + T_o (\Delta T)^3 + \frac{\Delta T^4}{5} \tag{78}$$

for no variation in heat sink temperature, $\Delta T = 0$ and the ideal vehicle temperature (T_v') is given by

$$(T_v')^4 = \left(\frac{Q}{\sigma F_e A_v}\right) + T_o^4 \tag{79}$$

Therefore, the error in vehicle temperature due to variation in heat sink temperature is

$$(T_v^4) - (T_v')^4 = 2T_o^3 \Delta T + 2T_o^2(\Delta T)^2 + T_o(\Delta T)^3 + \frac{(\Delta T)^4}{5} \tag{80}$$

If $(T_v)^4 - (T_v')^4$ is assumed to be approximately equal to $(T_v - T_v')\, 4T_v^3$ for small differences in vehicle temperature, then

$$T_v - T_v' = \frac{2T_o^3 \Delta T}{4T_v^3} + \frac{2T_o^2 \Delta T^2}{4T_v^3} + \frac{T_o(\Delta T)^3}{4T_v^3} + \frac{\Delta T^4}{20\, T_v^3} \tag{81}$$

or

$$T_v - T_v' = \frac{T_o^3 \Delta T}{2T_v^3} + \frac{T_o^2 \Delta T^2}{2\, T_v^3} + \frac{T_o \Delta T^3}{4T_v^3} + \frac{\Delta T^4}{20\, T_v^3} \tag{82}$$

Figure 10 shows the effect of the variation of heat sink temperature on the vehicle temperature for a vehicle temperature T_v of 300°K and for various heat sink temperatures, T_o. It is important to note that the coldest heat sink temperature is taken as equivalent to the "uniform" heat sink temperature for a 0 ΔT system. From this figure it is evident that accuracy of the simulation is largely dependent upon the magnitude of the design heat sink temperature T_o, rather than the magnitude of the heat sink temperature difference. Thus the value of $T_v - T_v'$ is only 1.44 °K for a heat sink ΔT of 20°K at T_o of 150°K when T_v = 300°K.

The second phase of this development considers the question of variation in vehicle temperature due to a variation of heat sink temperature when the average heat sink temperature is compared with a uniform but equal temperature.

Thus, for linear temperature distribution,

$$T_{ave} = T_o + \Delta T/2 \tag{83}$$

$$(T_v')^4 = \frac{Q}{\sigma F_e A_v} + (T_o + 1/2\,\Delta T)^4 \tag{84}$$

Subtracting equation (84) from equation (78) and solving for $T_v - T_v'$ as in equation (80) thru (82), we have

$$T_v - T_v' = \frac{T_o^2 \Delta T^2}{8T_v^3} + \frac{T_o \Delta T^3}{8T_v^3} + \frac{11\Delta T^4}{320T_v^3} \tag{85}$$

This difference is again plotted as Figure 11 for various values of ΔT at the same typical values of T_o used for Figure 10. It is clearly evident that the error in vehicle temperature due to variation in heat sink temperature is insignificant if the average value of the heat sink temperature is equal to the uniform temperature.

This investigation indicates that low temperature differences on heat sinks are not necessary for reasonably accurate heat balance tests. In fact the error associated with the difference in heat sink temperature and actual temperatures in space could be greater than the error due to heat sink temperature variations. Thus, the use of a fluid such as gaseous nitrogen or helium instead of liquids could be considered for reasonable heat loads without excessive gas flow rates.

5.2 RELATIONSHIP BETWEEN FLUID PROPERTIES AND HEAT SINK TEMPERATURE DIFFERENCE

A general relationship between fluid properties and the flow areas required in the heat sink can be established. Assume that a given heat transfer rate between fluid and heat sink must be provided with a given temperature difference of the fluid during its passage through the heat sink. Further assume that the pressure drop of the fluid is equal and fixed regardless of the fluid and that the temperature difference due to convection heat transfer between the fluid and heat sink is constant.

As stated earlier

$$Q = w\bar{c}_p\Delta T \tag{86}$$

where

Q = heat transferred from fluid to heat sink per path

w = flow rate of fluid, lb/hr - path

$\bar{c}_p$ = mean specific heat of fluid

ΔT = temperature difference of fluid across sink

The pressure drop of the fluid flowing through the circular channels in the heat sink is given by the Darcy relationship

$$\Delta P = C\,\frac{f_r w^2}{D^5 \bar{\rho}} \tag{87}$$

Where

ΔP = pressure drop across sink per unit length

C = constant of proportionality

f_r = friction factor and a function of roughness and Reynolds number

D = diameter of flow area

$\bar{\rho}$ = mean density of fluid

Solving for w and combining equation (86) and (87) then

$$Q = \bar{c}_p \Delta T \sqrt{\frac{\Delta p D^5 \bar{\rho}}{C f_r}} \tag{88}$$

With ΔT, ΔP, Q, f_r, all assumed constant, and comparing two different fluids, then

$$\frac{D_1}{D_2} = \left[\frac{(\bar{c}_p \ \bar{\rho}^{1/2})_2}{(\bar{c}_p \ \bar{\rho}^{1/2})_1} \right]^{2/5} \tag{89}$$

If liquid nitrogen is used as one fluid, the required diameter for any other fluid can be determined as some multiple of the diameter required for LN_2. (The same length of tubing for both fluids is implied.) A graph relating Q, and D_2 for LN_2, with the specific heat and the density is included as Figure 12.

6.0 THERMODYNAMIC SYSTEMS

6.1 GENERAL SYSTEMS CLASSIFICATION

The thermodynamic systems which could be employed to control heat sink temperatures can be categorized as follows:

1. Those systems which utilize a single fluid which is lost from the system; such as LN_2 boil-off systems;

2. Those closed cycle systems which completely regenerate the refrigerant such as LN_2 reliquefiers and helium refrigerators.

3. Those systems utilizing two or more fluids - one fluid circulates through the heat sink and appropriate heat exchangers, while a second fluid provides the heating or cooling faction.

An example of the third category is a gaseous nitrogen circulation system in which steam, LN_2, or a freon system is used to effect the necessary heating or cooling. An LN_2 subcooler is a second example of this type system.

These three general classifications are arranged in order of their increasing control flexibility while also reflecting an increase in complexity. The need for a wide temperature control range in a simulation facility, however, often requires a multiple fluid system. The fluids best suited for circulation through the heat sink in such systems, are gaseous nitrogen, and gaseous helium. A flow schematic of a system utilizing gaseous helium which will provide temperature control over a range from 20° to 373°K is shown on Figure 13. As shown, the gas would be circulated by a compressor through heating or cooling exchangers and through the heat sink or load. A schematic of a similar system which could provide temperature control at two temperature levels simultaneously is shown on Figure 14.

An alternate approach to the systems shown on Figures 13 and 14 is one in which individual control systems are utilized independently for control at specific temperatures. Since different fluids are utilized, however, it is necessary to provide the heat sink venting or draining provisions to facilitate changing from one system to another. Or, separate flow areas through the heat sink can be provided for each fluid. The latter approach complicates the heat sink piping and design but it is often preferable.

6.2 SYSTEM CYCLE ANALYSIS

The performance of several closed cycle systems is of particular interest where temperature control is required at unique levels. In particular, the following systems will be examined in some detail in the following sections:

1. Sub-atmospheric nitrogen reliquefier,
2. Atmospheric nitrogen reliquefier,
3. Neon reliquefier,
4. Hydrogen reliquefier,
5. Helium dense gas refrigerator.

6.2.1 Sub-atmospheric Nitrogen Reliquefier

The high heat loads associated with large simulation facilities coupled with long term continuous operating periods has markedly increased the desirability to recover and re-use the nitrogen vapor. A cycle analysis of atmospheric return pressure nitrogen reliquefier systems was conducted as part of an earlier study, See Section 4.7 of report number AEDC-TDR-63-71. The results of this analysis are also included here for comparison with the other systems.

An important reduction in heat sink temperature can be realized, while retaining the advantages of using nitrogen as the refrigerant, by decreasing the pressure above liquid nitrogen thereby depressing the boiling point. As shown in Figure 5, reductions in heat sink temperatures below 100°K markedly improve the cryopumping capabilities of carbon dioxide. A system low pressure of 2.94 psia was considered which corresponds to a vapor equilibrium temperature of 118.5°R. These systems therefore provide refrigeration below 140°R while retaining the advantages of closed cycle operation. The vapor pressure curve for nitrogen is shown on Figure 15.

Utilizing the analysis procedure developed in the referenced report, the performance of a reliquefier operating at a sub-atmospheric low pressure was determined for two sets of operating conditions. The applicable flow schematic is shown on Figure 16. Evaluation of the cycle performance is made by calculation of RE, the refrigeration

effect provided by a given system per pound of gas circulated through the low pressure compressor. The cycle efficiency, ξ, is then determined by

$$\xi = \frac{W_k}{RE} \tag{90}$$

where W_k = net input work, BTU/lb.

A general comparison of cycles was made by evaluating the ratio of the efficiency, ξ, and the theoretical, Carnot efficiency ξ_c.

The following general assumptions were made for these calculations:

1. Expander adiabatic expansion efficiency = 85%
2. Compressor over-all efficiency = 70%
3. Expander output work is 90% recovered
4. Gas at expander exhaust is saturated.

An important parameter in these calculations is x_e, the by-pass fraction, defined as the ratio of mass flow through the expander to the total system mass flow. The cycle performance increases as x_e increases since a greater percentage of the gas is expanded in a high efficiency expander. However, the maxiumum value of x_e is limited and is dependent upon operating pressures. This limitation is imposed because a temperature "reversal" of warm and cold streams is indicated (by heat balance) when the by-pass fraction is excessive and there is condensation in the cold heat exchanger. (See section 4.73 of report number AEDC-TDR-63-71.)

The analysis was made for a maximum and intermediate system pressures of 35 and 9 atmospheres respectively and again for pressures of 9 and 2.5 atm. The by-pass fraction for the first case was 0.7 and, for the second case, 0.45. The results are summarized on Table 1. As shown, the high pressure system is much superior from a performance standpoint while the cycle pressures are still within limitations of heat exchangers and other equipment.

6.2.2 Neon Reliquefier

A liquid neon system could be utilized for temperature control of heat sink surfaces in the range between 26°K and 45°K. Due to the high cost of neon, a reliquefier would be especially attractive. Both the Claude cycle, shown schematically on Figure 17, and the split-stream cycle examined for the nitrogen systems were investigated.

For these calculations, the maximum and the intermediate pressure (for the split-stream cycle) were taken as 500 psia and 130 psia. The basic purpose of the expander in the Claude cycle is to make-up for component inefficiencies and consequently, the value of the x_e was taken at only 0.1. Other assumptions were made the same as for the nitrogen cycles. A liquid neon temperature of 50°R was considered. Under these conditions, the Claude cycle produces a RE = 3.01 BTU/lb. In the split-stream cycle and operating between the pressures indicated and with an x_e = 0.75, a value for RE = 4.9 BTU/lb is obtained. These results are also summarized on Table 1. The particular choice of 130 psia for the neon intermediate pressure was chosen primarily to obtain a direct comparison with the nitrogen and hydrogen systems.

6.2.3 Hydrogen Reliquefier

Hydrogen reliquefiers are of particular interest because the liquefaction temperature of 36.7°R makes a hydrogen reliquefier competitive with nominal 20°K (36°R) cold gas helium refrigerators. Although explosion hazards exist, a well operated hydrogen plant is no more dangerous than many other chemical plants. Considering a split-stream cycle with a maximum pressure of 35 atm., an intermediate pressure of 9 atm., a liquid temperature of 36.7°R, and the compressor and expander efficiencies as before, a calculated value of RE = 30.76 BTU/lb was obtained. The value of x_e was 0.8.

6.2.4 Helium Refrigerator

The helium dense gas refrigerator has been extensively used for cooling surfaces in simulation chambers to below 20°K. Again an extensive cycle analysis was presented in detail in report number AECD-TDR-63-71. A schematic of the most commonly used cycle is shown in Figure 18. Considering a compressor efficiency of the 70%, a 75% expander efficiency, a system pressure ratio of 8, and a cold end heat exchanger ΔT = 4°R, then RE= 22.4 BTU/lb.

The evaluation of ξ/ξ_c must take into account that the load is not isothermal. This matter has been discussed in some detail by Robert Jacobs* who has analyzed the case of constant "high" temperature environmental sink with an infinite number of Carnot cycles each transferring an infinitesimal amount of heat to this sink from its appropriate part of the non-uniform low temperature source. He concludes that the efficiency of an "ideal" cycle with such a non-uniform cold source can be based on a Carnot cycle having its low temperature source (sink) at the log mean temperature of the actual cold source. For the helium cycle considered, the refrigeration occurs between 19.2°R and 36°R. Thus, the log mean temperature is 26.8°R and $\xi/\xi_c = .4$.

6.2.5 Summary

A comparison of the various cycles examined is shown on Table 1. Of special interest is the ratio of actual to ideal refrigeration effect per lb. of fluid circulated. These values reflect the operating temperature of the cycle in question but also indicate the relative efficiencies of the process. For example, although the hydrogen and helium systems operate at approximately the same temperature levels, the helium system is more efficient.

The primary reason for this better performance is that the helium system uses the expander for cooling the entire helium flow. The hydrogen reliquefier, on the other hand, cools only a fraction of the total flow. The remainder of the hydrogen is cooled on passing through the Joule-Thompson valve, which is not as efficient as an expander.

6.3 AIR SEPARATION PLANT VS. NITROGEN RELIQUEFIER

Refrigeration effect at nitrogen temperatures could be provided by an air separation plant or a nitrogen reliquefier. The two systems are similar in design and both liquefy nitrogen. However, the systems differ in that the air separation plant is basically an open system while the nitrogen reliquefier is a recirculating or closed system. A flow schematic of the air plant is shown on Figure 19.

* R. B. Jacobs, the Efficiency of an Ideal Refrigerator, P. 567 Advances in Cryogenic Engineering Vol. 7, Plenum Press, New York, 1962.

BLANK PAGE

TABLE 1

SUMMARY OF CALCULATIONS

Working Fluid	Actual RE BTU/lb	$\frac{\xi \text{ (Actual)}}{\xi_c \text{ (Ideal)}}$	$\frac{\text{Work}}{\text{Ref. Effect}}$	By-Pass Fraction x_e	High Pressure psia	Intermediate Pressure psia	Low Pressure psia	Ref. Temp. °R	Mass Flow lb/hr 1000 KW
Nitrogen	12.58	0.446	6.45	0.85	500	130	15	139	271,000
Nitrogen	25.18	0.380	9.35	0.7	514.5	132.3	2.94	118.5	136,000
Nitrogen	7.97	0.151	23.58	0.45	132	35	2.94	118.5	428,300
Neon-Split Strm.	4.9	0.230	42.7	0.75	500	130	15	50	696,000
Neon-Claude	3.01	0.094	104	0.1	500	-	15	50	1,133,000
Hydrogen	30.76	0.208	66	0.8	500	130	14.7	36.7	111,000
Helium	22.4	0.404	47.4	-	360	-	45	19.2 to 36.0	152,000

In the air plant, air is cooled from ambient temperatures, liquefied, fractionated, and the nitrogen is pumped to the load or storage. The oxygen is warmed and vented. The heat removal from the nitrogen is the sum of the latent heat plus the sensible heat. In the reliquefier, only the latent heat and the driving potential of the counterflow heat exchangers must be removed. Thus, more input energy is required for the air plant than for the reliquefier for equal outputs. Also, since the reliquefier operates on a closed cycle, the return stream from the load is larger for the reliquefier than for the air plant. Thus the flow rate through the reliquefier expander is greater without encountering theoretical temperature "reversals" in the heat exchanger. This higher mass flow in the expander circuit provides improved performance of the reliquefier. The over-all performance comparison is shown in detail in Table 2.

TABLE 2. PERFORMANCE COMPARISON OF AIR SEPARATION PLANT AND RELIQUEFIER - 1000 KW CAPACITY

Item	Air Plant	Reliquefier
Min. Pressure	15 psia	15 psia
Int. Pressure	130 psia	130 psia
Max. Pressure	600 psia	500 psia
Total Mass Flow	300,000 lb/hr	271,000 lb_m/hr
Expander Mass Ratio	0.60	0.85
Net work required	15,200 KW	6,450 KW
Work/Ref. Effect	15.2	6.45

A comparison of the two systems includes other important considerations. Start-up of the reliquefier would require an estimated 1000 gallons of LN_2 and leakage from the system would total an additional 3 GPM. Thus, operation of the reliquefier would be dependent upon this LN_2 supply. It would be possible to cool-down the reliquefier without pre-cooling liquid, but the necessary gas supply required to charge the system would be considerably more expensive than an equal

amount of liquid. The air plant input would require only air and electric power. A comparison of first costs for a reliquefier and an air plant each providing 1,000 KW capacities are shown in Tables 3 and 4 respectively. The first cost of the air plant is 9% greater and the operating costs, 37% greater than the reliquefier.

With the relatively small quantity of additional LN_2 needed for make-up and because of the demonstrated performance superiority of the reliquefier, a combination of some merit would be a smaller capacity air plant, approximately 30 tons/day for 2 - 1000 KW units with adequate storage and a reliquefier system sized to absorb the heat load in the chamber.

A second technique for introducing additional flexibility is to combine the air plant and reliquefier capabilities into a single system. The compressors and heat exchangers required for a reliquefier or air plant are sufficiently similar so that a combined system functioning as an air plant or a reliquefier could be feasible. The purifiers for removal of carbon dioxide and water vapor, the freon refrigerator for pre-cooling, and the separation column would be unique to the air plant but the remainder of the system could, after purging, be utilized as a reliquefier.

TABLE 3. FIRST COST COMPARISON OF AIR SEPARATION PLANT AND NITROGEN RELIQUEFIER - 1000 KW CAPACITY

Item	Air Plant	Reliquefier
Compressors	$ 562,000.00	$ 426,000.00
Expander	67,000.00	60,000.00
Heat Exchangers	100,000.00	177,000.00
Air Column & Purifier	35,000.00	-0-
Piping & Installation	369,000.00	369,000.00
Valves & Controls	44,300.00	44,300.00
Storage	52,600.00	52,600.00
Pumps	4,400.00	4,400.00
Equipment Cost	$1,234,300.00	$1,133,300.00

TABLE 4. YEARLY OPERATING COST COMPARISON OF AIR SEPARATION PLANT AND NITROGEN RELIQUEFIERS 1000 KW CAPACITY

Item	Air Plant	Reliquefier
Power required	15,200 KW	10,700 KW
Power rate	$.001/KW-Hr	$.001/KW-Hr
Yearly use	4300 Hr	4300 Hr
Yearly power cost	$65,500.00	$46,000.00
No. of Op. Personnel	4.5	3.5
Annual Personnel Cost	$54,000.00	$42,000.00
Maintenance	$15,000.00	$10,000.00
Total Annual Operating Cost	$134,500.00	$98,000.00

6.4 SUBCOOLED NITROGEN SYSTEM VS. NITROGEN RELIQUEFIER

The refrigeration effect necessary to maintain the temperature of heat sinks below 100°K is usually supplied by vaporizing liquid nitrogen. Several systems of varying complexities have been utilized for circulating the LN_2 and cooling the shrouds. The subcooled nitrogen system or subcooler is one such system. In this system, shown schematically on Figure 20, the LN_2 is used as the refrigerant and the heat transfer fluid. A closed loop of LN_2 is pressurized and circulated to the heat sink where it is warmed without exceeding the boiling point. The liquid is then returned to a heat exchanger where the heat is transferred to an open stream of boiling LN_2. This system limits the boil-off rate of LN_2 to the sum of the heat added in the thermal shroud plus the pump work. The temperature difference between the atmospheric nitrogen and the pressurized loop however, raises the minimum temperature available for cooling the load. By flashing the liquid returning from the load into a separation tank and providing a make-up supply for the vented vapor, a slightly lower temperature LN_2 can be introduced to the heat sink,

but this technique suffers by the absence of NPSH for the pumps. With either variation of the subcooler system, the opportunity to utilize the sensible heat of the gaseous vaporized nitrogen between 100°K and ambient is absent. Also, the extremely pure and dry gas is lost necessitating constant replacement. The continuous operation of a total loss system at high heat loads requires large storage capacities and a ready supply of LN_2. (A 500 KW heat load would vaporize in excess of 77,000 gallons of LN_2 in a 24 hour period).

The reliquefier system consists of a subcooled circuit for cooling the shroud as shown on Figure 21, and a system for removal of the latent heat of vaporization of the nitrogen, thereby reliquefying it. Thus, the loss of the cooling potential available as the sensible heat is prevented. The primary operating cost for cooling with a liquefier circuit together with the subcooled system as opposed to the subcooler alone, is thus changed from LN_2 make-up to electrical energy.

An economic comparison of these alternate systems includes consideration of the following:

1. Cost of LN_2
2. Cost of electrical energy
3. Additional operation and maintenance costs required for the more complex reliquefier
4. Total number of operating hours in question for the facility
5. First cost of both systems

Due to the marked difference in first cost, the subcooler is considerably more economical to operate on a short term basis. A derivation of an expression to determine the operating period after which the reliquefier system becomes more economical is included.

Consider the following definitions

C_r = reliquefier first costs -installed $

C_s = subcooler first costs - installed $

P_c = power costs, $/KW-Hr

N_c = LN_2 costs, \$/gal

W_r = reliquefier power requirements, KW

W_s = subcooler power requirements, KW

V = LN_2 requirements, gal/hr

t = time, hrs.

Z_r = reliquefier maintenance and operating costs, \$/hr

Z_s = subcooler maintenance and operating costs, \$/hr

The cost of installing and operating a reliquefier system is thus given by

$$C_{total} = C_r + W_r P_c t + Z_r t \tag{91}$$

The comparable cost for the subcooler is given by

$$C_{total} = C_s + W_s P_c t + Z_s t + V N_c t \tag{92}$$

The break even point, B, exists when these costs are equal, then

$$C_r + W_r P_c t + Z_r t = C_s + W_s P_c t + Z_s t + V N_c t \tag{93}$$

or

$$B = t = \frac{C_r - C_s}{V N_c - (W_r - W_s) P_c - (Z_r - Z_s)} \tag{94}$$

The following simplifying assumptions can be made:

1. The installed first cost of a 1000 KW reliquefier is \$1,758,000 (on the basis of two required).
2. The installed first cost of a 1000 KW subcooler is \$200,000 (on the basis of two required).
3. The power requirements differential, $(W_r - W_s)$ is 10,700 KW.

BLANK PAGE

4. The operating cost difference ($Z_r - Z_s$) is $15.00 per operating hour.

5. LN_2 consumption is 6530 gal/hr

Thus

$$B = \frac{1,558,000}{6530\ N_c - 10,700\ P_c - 15} \tag{95}$$

The break-even point B is plotted versus LN_2 costs for various power costs on Figure 22. The total costs of both systems are plotted versus operating hours on Figure 23 for various LN_2 and power costs.

6.5 MODULAR SIZE OF SYSTEMS

The first cost of refrigeration systems shows a marked decrease per unit capacity as the total capacity is increased. Thus, for minimum first costs, the maximum capacity systems for which equipment is available are indicated. However, to insure that refrigeration effect was available when needed despite maintenance down-time, several units, each providing a fraction of total capacity, would be provided. Also, the smaller systems are considerably more flexible to start, operate, and shutdown and are adequate for the tests during which less than full capacities are required.

For a 2,000 KW reliquefier system providing refrigeration in the 80-90°K range, the use of 4 units each of 500 KW design capacity are considered to be a desirable compromise. These four separate systems could be connected to the same separation tank but it would be advantageous to use one tank with each pair of systems. One such assembly, providing 1000 KW of refrigeration, is shown schematically on Figure 21. With these four units, capacities of 500, 1000, 1500 or 2000 KW would be available while operating each system at its rated and most efficient capacity.

Considering systems providing refrigeration effect in the 20-30°K range, the maximum modular capacity from an equipment availability standpoint would be 20 KW. However, for a total capacity of 40 KW, the use of 4 units each supplying 10 KW would be preferable.

7.0 HEAT SINK AND CRYOPANEL WARM-UP SYSTEMS

7.1 WARM-UP SYSTEMS - GENERAL

In the previous sections of this report, several systems were evaluated which were useful for cooling the heat sink surfaces and maintaining them at cryogenic temperatures while absorbing heat from various sources. In this section, the alternatives available for rapidly returning the test chamber to a condition where access is possible will be examined.

The most used technique for warm-up of the heat sinks in space simulation chambers is to remove the cooling source and wait until the cold surfaces are warmed by radiation heat transfer with the chamber walls. When the heat sink temperature is sufficiently warm, the chamber vacuum is broken with air. This procedure has been shown to require approximately twenty-seven (27) hours. A considerable reduction in the warm-up time is possible by accelerating the heat transfer to the heat sink. If the chamber vacuum is broken with dry gas such as nitrogen, convection heat transfer is available for augmenting radiation heat transfer. This technique has several undesirable features, however, and is usually employed on an emergency basis only. For a heat sink operating with liquid nitrogen as the coolant, the heat transfer between the chamber walls and the heat sink can reduce the temperature of the chamber walls to below the dew point of the surrounding air, and moisture condenses on the surfaces. This moisture contaminates instrumentation, rusts chamber structural members, and is a general nuisance. A second undesirable feature is that due to the absence of oxygen, suitable precautions must be taken before personnel can safely enter the chamber. Breaking the chamber vacuum with dry air does preclude the safety hazard; however, equipment for cleaning, drying and storing the air previous to demand, must be available. Also the heat sink will usually condense some of this air during the initial period of warm-up, thereby further tending to cool the lower section of the chamber.

It is therefore desirable, if accelerated warm-up is required, to provide a heat source and a heat transfer media for adding heat to the heat sinks. In practice, this source has been provided with either electrical heating elements utilizing radiation heat transfer, or by circulating a fluid, which has been warmed in systems external to the chamber, through the heat sinks. The electrical warm-up system usually provides quicker response times; however, the problems of element life

and arcing at certain chamber pressures severely limits its applications. Of particular interest in this study are the thermodynamic systems for providing the necessary heat for warm-up.

The application of specific warm-up systems to the facility depends upon what type of cooling is provided. With heat sinks cooled by liquid nitrogen, it is convenient to utilize nitrogen gas as the heat transfer media during warm-up. A circulation system forces warm gas through the same heat sink flow areas used for the liquid nitrogen. It could, of course, be possible to utilize the same fluid for warm-up and for cold operation. Thus nitrogen gas or helium gas could be circulated and either warm or cool the heat sink as required as discussed in other sections of this report. The use of liquid for both applications is limited by the high vapor pressures at elevated temperatures of those liquids with low freezing points, and the high freezing points of those with moderate vapor pressures at elevated temperatures. The higher specific heat values and/or greater densities of liquids make them the natural selection for the heat transfer media if the operating temperature range is small.

The flow schematic of one system which as been utilized for warm-up is shown on Figure 24. In this system, a booster compressor provides the pressure necessary for the recirculation of the gas through the heat sink and system heat exchangers. The heat of compression is removed in an after cooler; the gas then passes through a counter-flow heat exchanger. This counter-flow exchanger provides thermal isolation between the cold heat sink and the ambient compressor. The gas is then heated in a heat exchanger by electrical resistance heaters or steam, and circulated through the heat sink. The cooled return gas passes through the counter-flow heat exchanger before entering the compressor suction. By operating this system at an elevated suction pressure, the gas density is increased so that reasonable pressure drops are experienced with maximum flow-rates.

The time necessary to warm a given heat sink is considerably less with the gas circulation system than by natural warm-up, and is dependant upon the rate of heat input, the flow rate of gas, and the amount of overshoot permissible. However, a total elapsed time of 2 to 5 hours is considered normal.

Other systems have been utilized for accelerated warm-up of heat sinks. In one system, shown schematically on Figure 25-a, the counter-flow heat exchanger is omitted by mixing a part of the heated high pressure stream with the cold return stream. This technique also has the

advantage of utilizing the heat of compression for the warm-up effort. The disadvantages of this approach include the complex control and valving system necessary to provide the compressor suction with warm gas at uniform pressures, and the inefficiency of compressing a part of the gas flow which is used for warming the return stream. Also, this system could not be utilized for warming the heat sink above ambient temperatures.

A third system, shown schematically on Figure 25-b, utilizes a blower operating at low temperatures to force gas through a heater and the heat sink before it is returned to the blower. Since this approach utilizes low pressure gas at high volume flow rates, the flow areas through the heat sink must be necessarily quite large. However, when combined with a boiling LN_2 cooling system, which also requires large flow area, the system has some merit.

The systems considered above are all closed, recirculation type systems. It is possible of course, to accelerate warm-up to some degree with a total loss, flow through system. This approach represents a minimum of equipment investment. A substantial warm gas supply is required which could be provided by a vaporizer and sufficient heat input capacity to warm the gas stream to approximately 250°F.

7.2 CRYOPANEL WARM-UP

In a simulation chamber in which helium-cooled cryopanels are provided together with the nitrogen-cooled heat sink and shields, the warm-up system usually circulates nitrogen gas through the liquid flow areas only. Warm-up of the cryopanels is a special problem. By design, the heat transfer between the shields and the cryopanel surfaces is quite small. Therefore, the heat sink surfaces are often warmed to ambient temperature, while the cryopanel surfaces are still near nitrogen temperatures. To warm the cryopanels at a higher rate, helium from the refrigerator can be circulated through these panels and through a thaw heater with by-pass provisions so that the refrigerator heat exchangers would not be warmed. This technique would insure a cryopanel warm-up period matching the heat sink warm-up.

7.3 HEAT SINK WARM-UP WITH CONSTANT HEAT INPUT

Consider a warm-up gas cycle with constant heat input as shown on Figure 26, Applying the First Law to the system

$$Q = M_s(h_2 - h_1)/\Delta t \qquad (96)$$

where

Q = rate of heat added, BTU/hr

M_s = mass of heat sink to be warmed, lb_m

h = heat sink material enthalpy, BTU/lb_m: subscript 1 initial condition, subscript 2, final condition

Δt = finite time interval

Let the specific heat addition, q, be defined as:

$$q = Q\Delta t / m_g \Delta t = Q/m_g \tag{97}$$

where

m_g = mass flow rate of gas = $M_g/\Delta t$

M_g = total mass of gas circulated during warm-up of the heat sink through the temperature range in question, lb_g

Therefore, the specific mass of gas required is:

$$M_g/M_s = \Delta t\, m_g/M_s = \frac{\Delta t Q/q}{\Delta t Q/(h_2 - h_1)} = (h_2 - h_1)/q \tag{98}$$

Values of the specific gas requirements for copper, aluminum, and stainless steel are plotted on Figure 27 for initial temperatures of 20°K and on Figure 28, for 77°K. Both figures are for a constant value of the specific heat addition, $q = 1$ BTU/lb_m. For different values of q, the specific mass requirement would be inversely proportional to the specific heat addition as shown by equation (98). Values for the specific heat of the metals were taken from "A Compendum of Properties of Materials at Low Temperatures."

7.4 HEAT SINK WARM-UP WITH CONSTANT HEAT SINK INLET GAS TEMPERATURE

Consider a second warm-up cycle with constant load inlet gas temperature. Applying the First Law to the heat sink for a differential time, dt,

$$m_g \bar{c}_p (T_{g,o} - T_{g,f})\, dt = M_s dh \tag{99}$$

where

$\bar{c}_p$ = mean specific heat at constant pressure for the heating gas, $BTU/lb_g - °R$

$T_{g,o}$ = inlet temperature of the heating gas and considered constant, °R.

$T_{g,f}$ = exit temperature of the gas, °R.

The heat exchange effectiveness between the gas and the heat sink is defined as the amount of heat exchange divided by the maximum amount which could be exchanged. For this development, the effectiveness is taken as 100%. Thus, $T_{g,f}$ is equal to the heat sink temperature, T_p.

$$\text{Also, let } m_g dt = dM_g \tag{100}$$

Making these substitutions in equation (99), the following relationship is obtained.

$$\bar{c}_p (T_{g,o} - T_p)\, dM_g = M_s dh \tag{101}$$

$$\int dM_g/M_s = M_g/M_s = \int_{T_{p1}}^{T_{p2}} dh/\bar{c}_p (T_{g,o} - T_p) \tag{102}$$

where T_p = temperature of heat sink.

Thus, the specific gas requirement can be determined by numerically integrating equation (102). However, if small temperature increments are considered, the enthalpy of the heat sink can be written as

$$dh = \bar{c}_s\, dT_p \tag{103}$$

where $\bar{c}_s$ = mean specific heat of the heat sink material at at temperature, T_s, BTU/lb_m - °R

Making this approximation,

$$\frac{M_g}{M_s} = \int_{T_{p1}}^{T_{p2}} \frac{\bar{c}_s \, dT_p}{\bar{c}_p(T_{g',o} - T_p)} = \int_{(T_{p1} - T_{g',o})}^{(T_{p2} - T_{g',o})} \frac{\bar{c}_s d(T_p - T_{g',o})}{\bar{c}_p(T_{g',o} - T_p)}$$

then

$$\frac{M_g}{M_s} = \frac{\bar{c}_s}{\bar{c}_p} \ln \frac{T_{g',o} - T_{p1}}{T_{g',o} - T_{p2}} \tag{104}$$

In the first development with Q = a constant, the specific gas requirement was independent of the gas used in the cycle; however, in this development with $T_{g',o}$ = a constant, the specific gas requirement is a function of the specific heat of the gas. A graph relating M_g/M_s and the final temperature T_{p2} for T_{p1} = 20°K is shown on Figure 29, for helium gas, and on Figure 30, for nitrogen gas. The heat sink materials shown are copper, aluminum, and stainless steel. Similar graphs are included as Figures 31, and 32, for T_1 = 77°K. The value of $T_{g',o}$ for these figures was taken as 350°K. (170°F.)

7.5 HEAT SINK WARM-UP TIME

The warm-up time of the heat sink panels will be examined for the condition of constant gas inlet temperature to the heat sink, a gas mass flow rate of m_g, and a gas exit temperature at a time-wise varying temperature of $T_{g,e}$. The exit temperature is not necessarily the same as the heat sink temperature in this development. Consider a section of a heat sink panel as shown below.

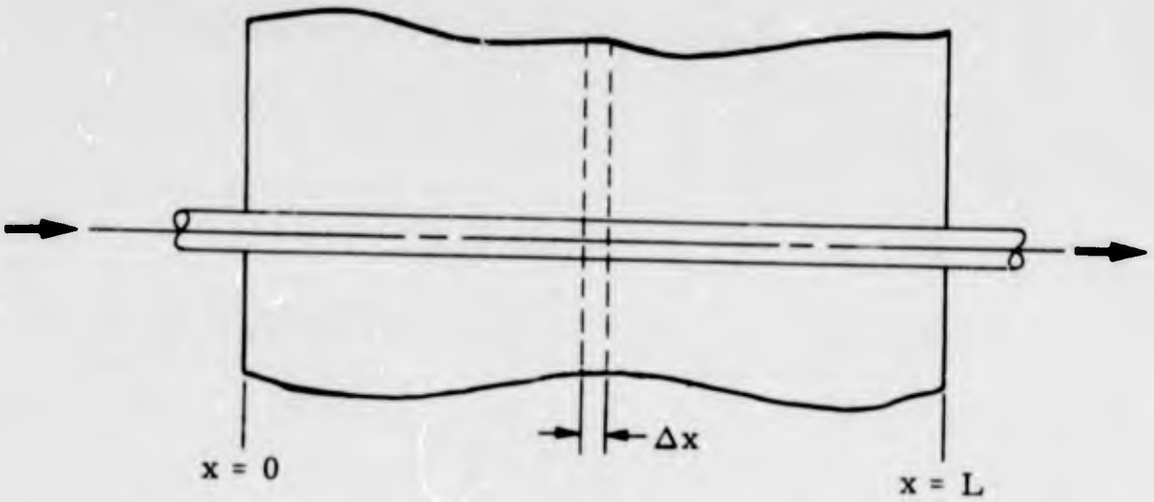

The position coordinate x = 0 corresponds to the point where the gas enters the panel, and at x = L, the gas exits the panel. The temperature of the panel, $T_p = T_p(x, t)$ is a function of coordinate x and time t. If the panel material is aluminum with a high thermal conductivity, the temperature will be considered constant in the panel in a plane normal to the direction of gas flow. Applying the First Law to a differential element of the panel, and considering that the radiation heat transfer is negligible, then,

$$Q_{in} = Q_{out} + Q_{retained}$$

or

$$Q \text{ convection in} + Q \text{ conduction in} = Q \text{ conduction out} + Q \text{ retained} \quad (105)$$

where

$$Q \text{ convection in} = h_c A_h (T_g - T_p) \frac{dx}{L} \quad (106)$$

$$Q \text{ conduction in} = -k_s A_p \frac{\partial T_p}{\partial x} \quad (107)$$

$$Q \text{ conduction out} = Q \text{ cond. in} + \frac{\partial (Q \text{ cond. in})}{\partial x} dx = -k_s A_p \frac{\partial T_p}{\partial x} - k_s A_p \frac{\partial^2 T_p}{\partial x^2} dx \quad (108)$$

$$Q \text{ retained} = \bar{c}_s \cdot M_s \cdot \frac{dx}{L} \frac{\partial T_p}{\partial t} \quad (109)$$

where

T_p = temperature of the panel at position x and at time t, °R

hc = heat transfer coefficient between the gas and the panel, BTU/hr - ft^2°R

A_h = heat transfer area between the gas and the panel, ft^2

M_s = mass of panel, lb_m

$\bar{c}_s$ = mean specific heat of panel, BTU/lb_m°R

T_g = temperature of the gas at position x at time t, °R

k_s = thermal conductivity of the panel, BTU/hr - ft - °R

A_p = cross sectional area of the panel, ft^2

L = total length of panel in the direction of flow of gas, ft.

t = time, hr.

Substituting equations (106), (107), (108), and (109) in (105)

$$h_c A_h (T_g - T_p) \frac{dx}{L} - k_s A_p \frac{\partial T_p}{\partial x} =$$

$$-k_s A_p \frac{\partial T_p}{\partial x} - k_s A_p \frac{\partial^2 T_p}{\partial x^2} \cdot dx + \bar{c}_s M_s \frac{dx}{L} \cdot \frac{\partial T_p}{\partial t} \qquad (110)$$

Simplifying,

$$\frac{\partial T_p}{\partial t} = \frac{h_c A_h}{M_s \bar{c}_s} \cdot (T_g - T_p) + \frac{k_s A_p L}{M_s \bar{c}_s} \cdot \frac{\partial^2 T_p}{\partial x^2} \qquad (111)$$

If the thermal conductivity is high, the temperature gradients in the panel are small, and the term including $\frac{\partial^2 T_p}{\partial x^2}$ can be considered negligible and equation (111) written as

$$\frac{\partial T_p}{\partial t} = \frac{h_c A_h}{M_s \bar{c}_s} \cdot (T_g - T_p) \tag{112}$$

Repeating the First Law analysis to a differential element of gas,

$$Q \text{ convection} = Q \text{ internal energy} + Q \text{ enthalpy} \tag{113}$$

$$Q \text{ convection} = h_c (A_h/L) (T_p - T_g)\, dx \tag{114}$$

$$Q \text{ internal energy} = \rho c_p (V_g/L)\, dx \frac{\partial T_g}{\partial t} \tag{115}$$

$$Q \text{ enthalpy} = m_g c_p \frac{\partial T_g}{\partial x}\, dx \tag{116}$$

where

V_g = volume of gas within the panel, ft^3

ρ = density of gas at position x and at time t, lb_g/ft^3

For gases, the change in internal energy is much smaller than the enthalpy transport and heat transfer terms, therefore the internal energy term will be neglected.

Substituting equations (114) and (116) in (113) and simplifying,

$$\frac{\partial T_g}{\partial x} = \frac{h_c A_h}{m_g c_p L} \cdot (T_p - T_g) \tag{117}$$

The boundary conditions for equations (112) and (117) are

(1) at $x = 0$, $T_g = T_{g,o}$ = constant

(2) at $t = 0$, $T_p = T_{p1}$ = constant (initial temperature of the panel).

For convenience, the variables β and γ will be defined as follows

$$\gamma = ax = \frac{h_c A_h}{m_g c_p L} \cdot x \tag{118}$$

$$\beta = bt = \frac{h_c A_h}{M_s \bar{c}_s} \cdot t \tag{119}$$

$$\theta' = \frac{T_{g,o} - T_p}{T_{g,o} - T_{p1}} \tag{120}$$

$$\theta'_g = \frac{T_{g,o} - T_g}{T_{g,o} - T_{p1}} \tag{121}$$

Thus, by differentiating and rewriting

$$\frac{\partial \theta'}{\partial \beta} = - \frac{\partial T_p}{\partial \beta} \left[\frac{1}{(T_{g,o} - T_{p,1})} \right] \tag{122}$$

and

$$\partial \beta = b \, \partial t \tag{123}$$

Also,

$$\theta' - \theta'_g = (T_g - T_p) \tag{124}$$

Combining these expressions and equation (112)

$$\frac{\partial \theta'}{\partial \beta} = \frac{-b(T_g - T_p) \quad \partial t}{\partial \beta} = - \frac{\partial \beta \ (T_g - T_p)}{\partial \beta}$$

or

$$\frac{\partial \theta'}{\partial \beta} = T_p - T_g \tag{125}$$

then

$$\frac{\partial \theta'}{\partial \beta} = (\theta'_g - \theta') \tag{126}$$

Applying a similar technique to equation (117)

$$\frac{\partial \theta'_g}{\partial \gamma} = (\theta' - \theta'_g) \tag{127}$$

The boundary equations for equations (126) & (127) became

(1) at $\gamma = 0$, $\theta'_g = 0$

(2) at $\beta = 0$, $\theta' = 1$

Differentiating equation (126) with respect to γ

$$\frac{\partial \theta'^2}{\partial \beta \, \partial \gamma} = \frac{\partial \theta'_g}{\partial \gamma} - \frac{\partial \theta'}{\partial \gamma} \tag{128}$$

From equations (126) & (127)

$$\frac{\partial \theta'_g}{\partial \gamma} = (\theta' - \theta'_g) = - \frac{\partial \theta'}{\partial \beta} \tag{129}$$

Making this substitution, the differential equation for the temperature of the panel can be written as

$$\frac{\partial^2 \theta'}{\partial \beta \, \partial \gamma} + \frac{\partial \theta'}{\partial \beta} + \frac{\partial \theta'}{\partial \gamma} = 0 \tag{130}$$

This equation was solved by H. Hausen, Tech. Mech. Thermodynamics, Vol. 1, pg. 219, (1930). (See also: H. Hausen, Warmeubertragung im Gegenstrom, Gleichstrom, und Kreuzstrom, Springer Verlag, Berlin, (1950) and E. R. G. Eckert and R. M. Drake, Jr., Heat and Mass Transfer, Book Co., Inc., New York (1959) pg. 487; and Max Jacob, Heat Transfer, Vol. 2, John Wiley and Sons, Inc. New York, (1957), pp. 284 - 289). The results are tabulated on Table 5 in terms of the dimensionless variables, and included in graph form on Figure 33.

$\beta = \frac{h_c A_h t}{M_s \bar{c}_s}$	$100\ E = 100\ (Q_{total}/Q_{max}) = 100\ (Q_{total})/M_s \bar{c}_s (T_{g'o} - T_{pl})$									
	$NTU = \frac{h_c A_h}{m_g C_p} = a\ L$									
	1	2	3	4	5	6	7	8	9	10
0	0.0	0.0	0.0	0.0	0.0	0.0	0.0	0.0	0.0	0.0
1	49.0	37.8	29.9	24.3	20.2	17.3	15.1	13.2	11.8	10.6
2	74.0	62.2	52.1	44.0	37.6	32.5	28.4	25.2	22.5	20.3
3	86.5	78.0	67.9	60.0	52.5	46.8	41.4	37.3	33.6	30.5
4	92.8	87.1	79.6	72.6	65.8	59.4	53.6	48.5	44.0	40.0
5	96.4	93.0	87.7	81.3	74.7	68.7	62.8	57.6	52.8	48.6
6	98.6	96.4	93.0	88.3	83.3	77.7	72.0	66.8	61.9	57.3
7	99.2	97.6	95.3	92.0	88.4	83.6	78.6	73.9	69.1	64.8
8	99.6	98.7	97.0	94.6	91.7	88.4	84.5	80.3	76.1	71.8
9	99.8	99.4	98.4	97.0	94.8	92.0	88.9	85.2	81.3	77.4
10	100	99.7	99.2	98.4	96.9	95.0	92.9	89.7	86.3	82.7
15	100	100	99.9	99.8	99.6	99.2	98.8	98.1	97.3	95.8
20	100	100	100	100	99.9	99.8	99.7	99.5	99.4	99.2

TABLE 5

Effectiveness of the heating process as a function of the number of transfer units, NTU, with the time variable β as a parameter.

7.6 HEAT SINK WARM-UP TIME CONSIDERING HEAT EXCHANGE EFFECTIVENESS

The total energy added to the heat sink can be written as

$$Q_{total} = \int_0^L (M_s \bar{c}_s / L)(T_p - T_{p1})\, dx \qquad (131)$$

In terms of the dimensionless parameters,

$$(T_p - T_{p1}) = (T_{g,o} - T_{p1}) - (T_{g,o} - T_p) \qquad (132)$$

From equation (120),

$$(T_p - T_{p1}) = (1 - \theta')(T_{g,o} - T_{p1}) \qquad (133)$$

Aso, $dx = \frac{d\gamma}{a}$ from equation (118).

Therefore, equation (131) can be written as

$$Q_{total} = \frac{(M_s \bar{c}_s)(T_{g,o} - T_{p1})}{aL} \cdot \int_0^L (1-\theta')\, d\gamma \qquad (134)$$

The maximum possible energy addition for a constant inlet temperature of $T_{g,o}$ for the heating gas is given by,

$$Q_{max} = M_s \bar{c}_s (T_{g,o} - T_{p1}) \qquad (135)$$

i.e. The heat sink cannot be heated to a temperature higher than $T_{g,o}$ by the heating gas.

The effectiveness of the heating process is defined as

$$E = Q_{total}/Q_{max} = \frac{1}{aL} \cdot \int_0^{aL} (1 - \theta')\, d\gamma \qquad (136)$$

The integration of this expression can be carried out graphically using the values of θ' vs. γ with β as a parameter as given in Table 5. These results are shown in Table 6 and Figure 34.

The quantity

$$aL = h_c A_h / m_g c_p \tag{137}$$

where (a) is defined by equation (118) is similar to the "number of heat transfer units: and is denoted as (NTU). Further, it is noted that the time parameter

$$\beta = \frac{h_c A_h \cdot t}{M_s \bar{c}_s}$$

can be written as the product of two quantities as follows:

$$\beta = \frac{h_c A_h}{m_g c_p} \cdot \frac{m_g c_p t}{M_s \bar{c}_s} = (NTU)\ (X_r) \tag{138}$$

where

$$(X_r) = \frac{m_g c_p t}{M_s \bar{c}_s} = \text{heat capacity ratio}$$

and is the heat capacity of the gas/heat capacity of the solid. The heat capacity ratio is directly related to the specific gas requirements as follows

$$\frac{M_g}{M_s} = \frac{m_g t}{M_s} = \frac{\bar{c}_s}{c_p} \cdot (X_r) \tag{139}$$

The relationship shown as equation (104) can be written in terms of the effectiveness of the heating process and the heat capacity ratio as follows,

$$X_r = \ln \left[\frac{T_{g,o} - T_{p1}}{T_{g,o} - T_{p2}} \right] \tag{140}$$

$$100\,E = \frac{Q_{total} \times 100}{Q_{max}} = \frac{Q_{total} \times 100}{M_s \bar{c}_s (T_{g,o} - T_{p1})} \; ; \; NTU = \frac{h_c A_h}{m_g c_p}$$

NTU											
1	E	49.0	74.0	86.5	92.8	96.4	98.6	99.2	99.6	99.8	100
	X_r	1	2	3	4	5	6	7	8	9	10
2	E	37.8	62.2	78.0	87.1	93.0	96.4	97.6	98.7	99.4	99.7
	X_r	0.5	1.0	1.5	2.0	2.5	3.0	3.5	4.0	4.5	5.0
3	E	29.9	52.1	67.9	79.6	87.7	93.0	95.3	97.0	98.4	99.2
	X_r	0.33	0.67	1.00	1.33	1.67	2.00	2.33	2.67	3.00	3.33
4	E	24.3	44.0	60.0	72.6	81.3	88.3	92.0	94.6	97.0	98.4
	X_r	0.25	0.50	0.75	1.00	1.25	1.50	1.75	2.00	2.25	2.50
5	E	20.2	37.6	52.5	65.8	74.7	83.3	88.4	91.7	94.8	96.9
	X_r	0.20	0.40	0.60	0.80	1.00	1.20	1.40	1.60	1.80	2.00
6	E	17.3	32.5	46.8	59.4	68.7	77.7	83.6	88.4	92.0	95.0
	X_r	0.17	0.33	0.50	0.67	0.83	1.00	1.17	1.33	1.50	1.67
7	E	15.1	28.4	41.4	53.6	62.8	72.0	78.6	84.5	88.9	92.9
	X_r	0.14	0.29	0.43	0.57	0.71	0.86	1.00	1.14	1.29	1.43
8	E	13.2	25.2	37.3	48.5	57.6	66.8	73.9	80.3	85.2	89.7
	X_r	0.13	0.25	0.38	0.50	0.63	0.75	0.88	1.00	1.13	1.25
9	E	11.8	22.5	33.6	44.0	52.8	61.9	69.1	76.1	81.3	86.3
	X_r	0.11	0.22	0.33	0.44	0.56	0.67	0.78	0.89	1.00	1.11
10	E	10.6	20.3	30.5	40.0	48.6	57.3	64.8	71.8	77.4	82.7
	X_r	0.10	0.20	0.30	0.40	0.50	0.60	0.70	0.80	0.90	1.00
10	E	95.8	99.2								
	X_r	1.50	2.00								
9	E	97.3	99.4								
	X_r	1.67	2.22								
8	E	98.1	99.5								
	X_r	1.88	2.50								
7	E	98.8	99.7								
	X_r	2.14	2.86								
6	E	99.2	99.8								
	X_r	2.50	3.33								
5	E	99.6	99.9								
	X_r	3.00	4.00								

TABLE 6

Effectiveness of the heating process as a function of NTU with X_r as a parameter.

since

$$\frac{Q_{total}}{M_s \bar{c}_s (T_{g',o} - T_{p1})} = E = \frac{M_s \bar{c}_s (T_{p2} - T_{p1})}{M_s \bar{c}_s (T_{g',o} - T_{p1})} =$$

$$= \frac{(T_{g',o} - T_{p1}) - (T_{g',o} - T_{p2})}{(T_{g',o} - T_{p1})} \tag{141}$$

Therefore equation (138) can be written as

$$X_r = \ln \frac{1}{1 - E} \tag{142}$$

Solving equation (142) for E

$$E = 1 - e^{(-X_r)} \tag{143}$$

The effectiveness, E, is plotted versus the heat capacity ratio, X_r for various values of the number of heat transfer units, (NTU) on Figure 35. Also, Figure 36 is a graph of X_r versus (NTU) for various values of the effectiveness, E. By knowing or assuming the value of certain variables which are included in the expression for X_r, (NTU), the warm-up time, or some other dependent variable can be evaluated. Sample calculations of this procedure are included in Appendix A of this report.

8.0 HEAT SINK DESIGN

8.1 EFFECT OF TEMPERATURE CONTROL SYSTEM ON HEAT SINK DESIGN

The relationship between the heat sink design and the thermodynamic system providing the heating or cooling action is an important consideration. To examine this relationship, some of the requirements of a heat sink are tabulated below.

1. Minimum number of weld joints in the fluid line.
2. Good heat transfer between the fluid line and the heat sink surface; therefore, material with good thermal conductivity is required.
3. Minimum heat sink mass consistent with good rigid mechanical stability.
4. Readily prefabricated in sections for ease of installation.
5. Proper emissivities.
6. Low cost on an over-all installed basis.
7. Provide adequate flow areas for the heat transfer fluid.
8. Fabricated of a material suited for use over the required temperature range.

Consider first the requirement for adequate flow-areas for the fluid lines. The thermal load, the design temperature difference, and the specific heat of the fluid determine the quantity of fluid necessary in a given path. This flow rate, combined with the density of the fluid, determines the flow area requirements. For example, use of a subcooled LN_2 system would require relatively small flow areas, while a boiling nitrogen system would have areas considerably larger for the same cooling effect. Similarly, circulating gas through the heat sink would require larger flow areas than for the liquid for the same heat load. In each case, it is important to provide, (1) sufficient flow area to maintain pressure drops at a minimum, and (2) the same pressure drop through various parallel passages for which no flow control is available.

A second area in which the temperature control system and the heat sink design are closely related is the material strength. Operation of a gas circulation system at elevated pressures would be desirable to provide further reduction in the required flow areas. However, the stress level produced at these higher pressures would require increased wall thicknesses of the tube which could limit the fabrication technique, as well as the cost.

Assuming that the temperature difference allowable on the heat sink surfaces and the heat load are specified, the spacing between adjacent tubes is a function of the sheet thickness as well as the type and quantity of fluid circulated. If a narrow tube spacing is required, the manifolding complications, number of weld joints, and therefore cost is affected. Also a variable in this regard is the heat sink thickness, since the heavier wall would permit use of larger tube spacings than does the thinner wall thickness.

The intended temperature level of various systems have an additional effect on heat sink design. Due to the tremendous increase in power required to generate a given amount of refrigeration as the temperature of the refrigerant is decreased, it is very important to prevent unwarranted heat leaks. Special precautions are therefore taken, by shielding or similar techniques, to prevent or minimize heat leaks. A second consideration in regard to the operating temperature level is the design expansion and contraction allowance of the heat sink sections. It is necessary to provide adequate clearance for contraction of the heat sink panel during cool-down from the ambient to the operating temperature. This design clearance and the means for supplying it would depend on the expected change in temperature.

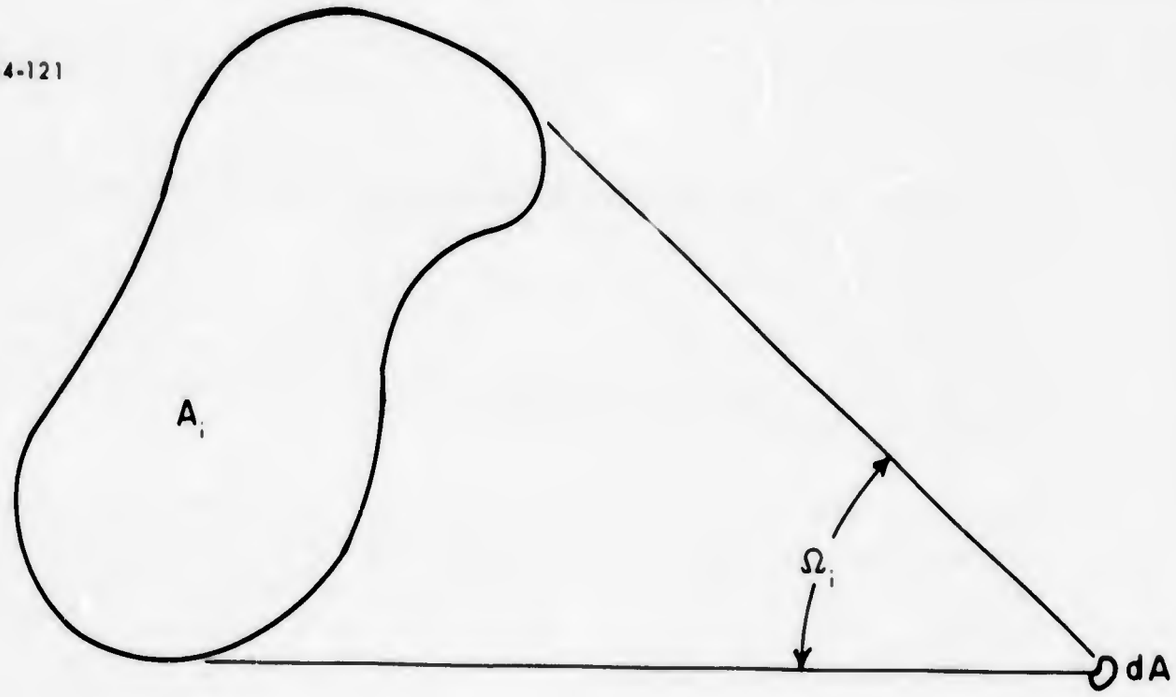

FIGURE 1 - a. DEFINITION OF SOLID ANGLE Ω

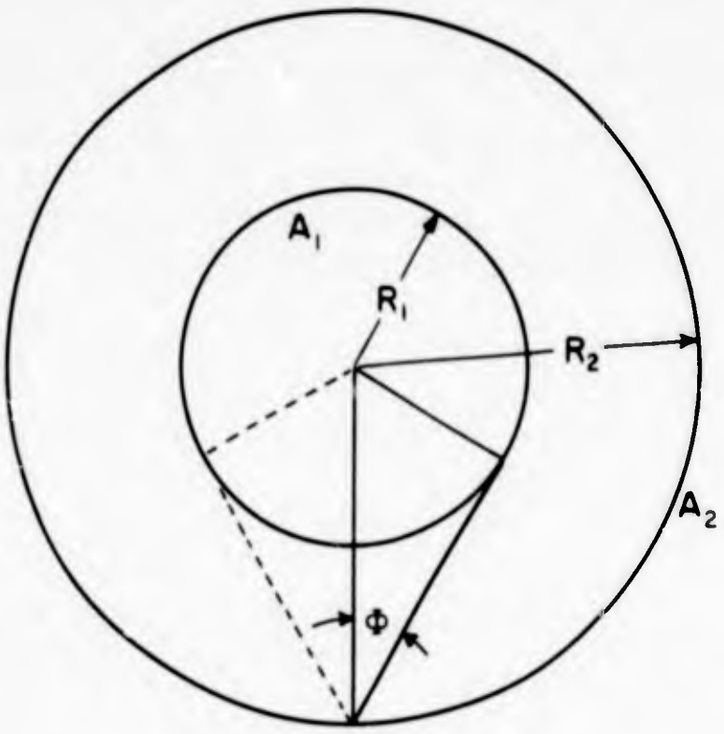

FIGURE 1 - b. DEFINITION OF ANGLE Φ

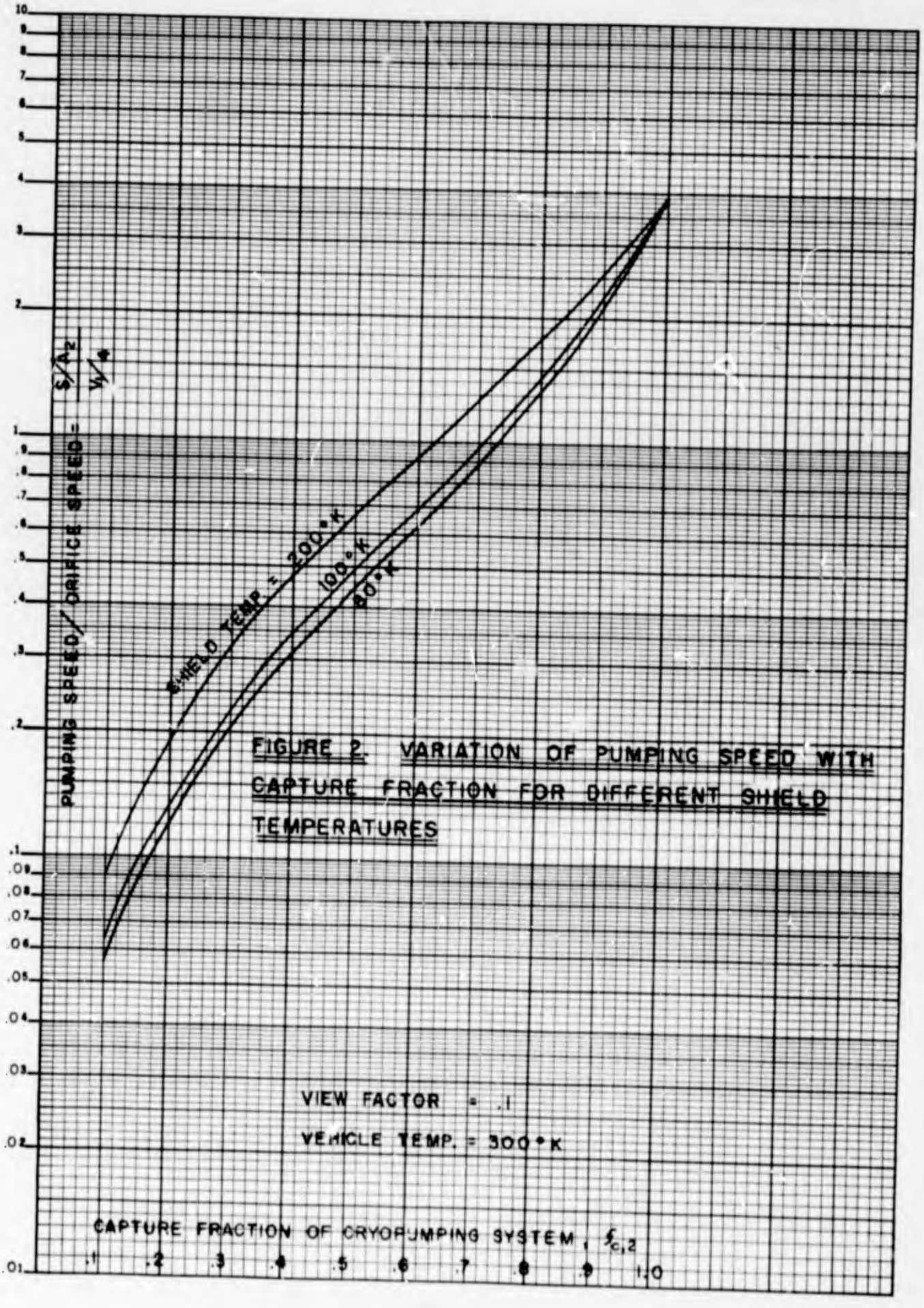

FIGURE 2. VARIATION OF PUMPING SPEED WITH CAPTURE FRACTION FOR DIFFERENT SHIELD TEMPERATURES

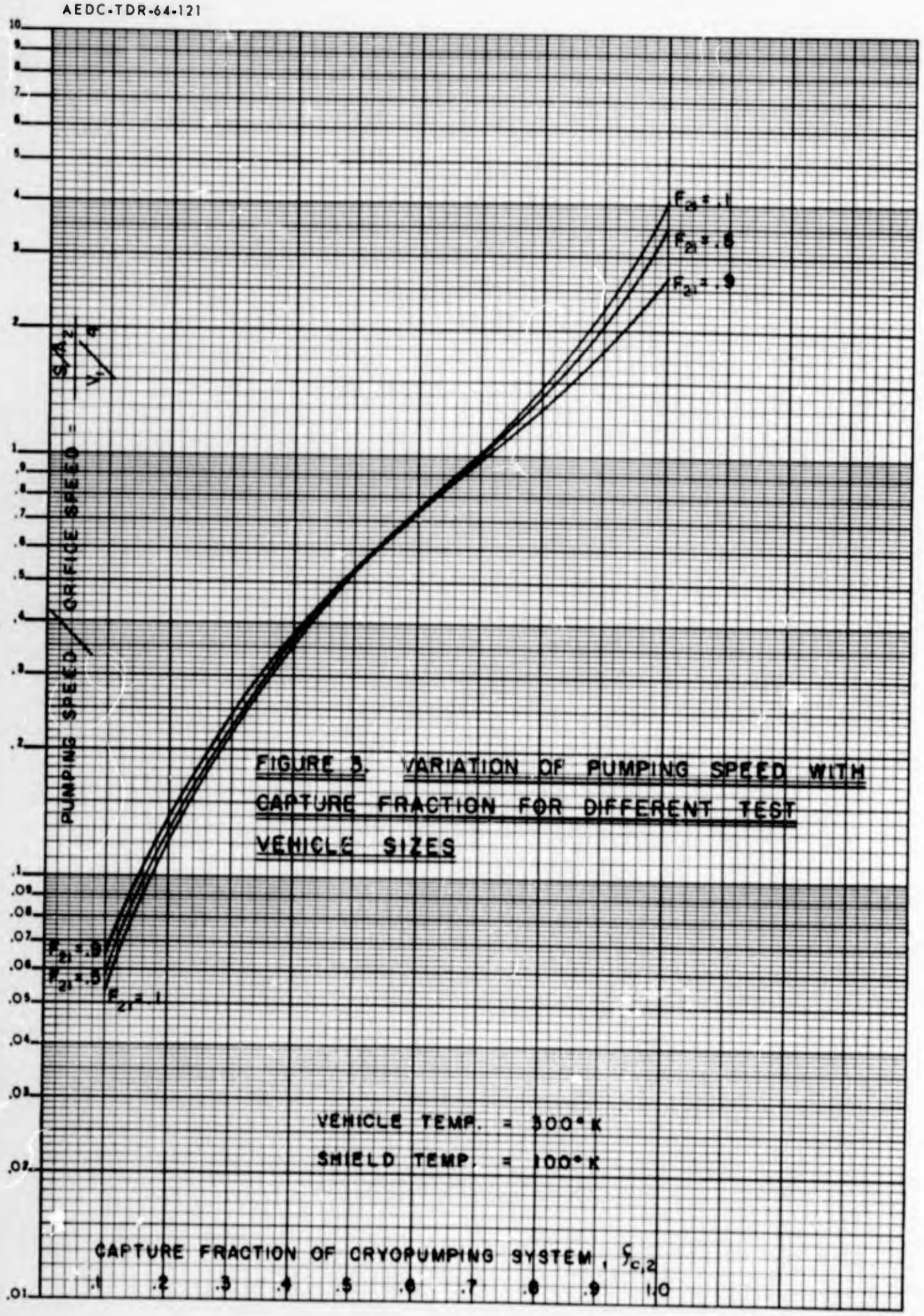

FIGURE 8. VARIATION OF PUMPING SPEED WITH CAPTURE FRACTION FOR DIFFERENT TEST VEHICLE SIZES

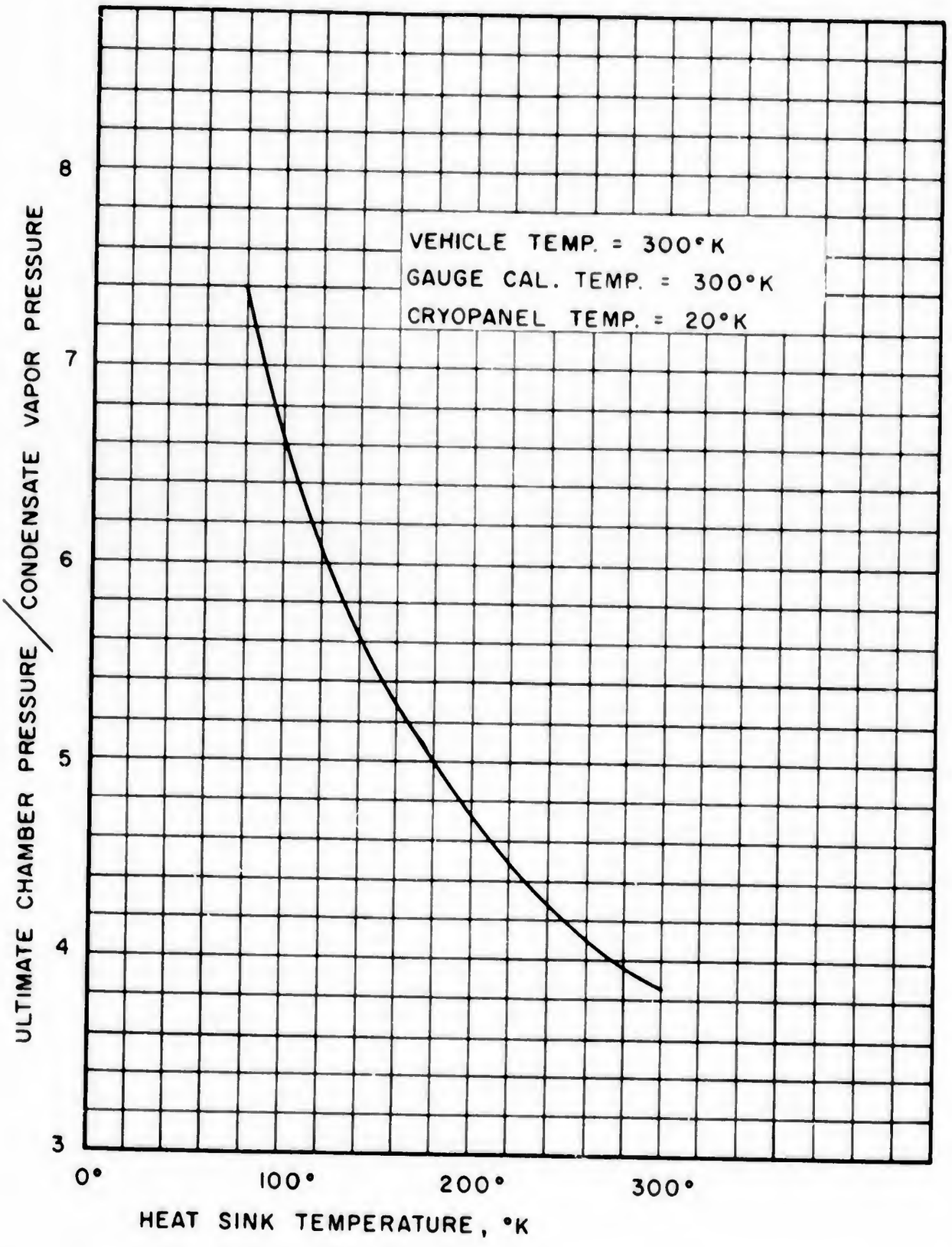

FIGURE 4. ULTIMATE CHAMBER PRESSURE / CONDENSATE VAPOR PRESSURE VS. HEAT SINK TEMPERATURE

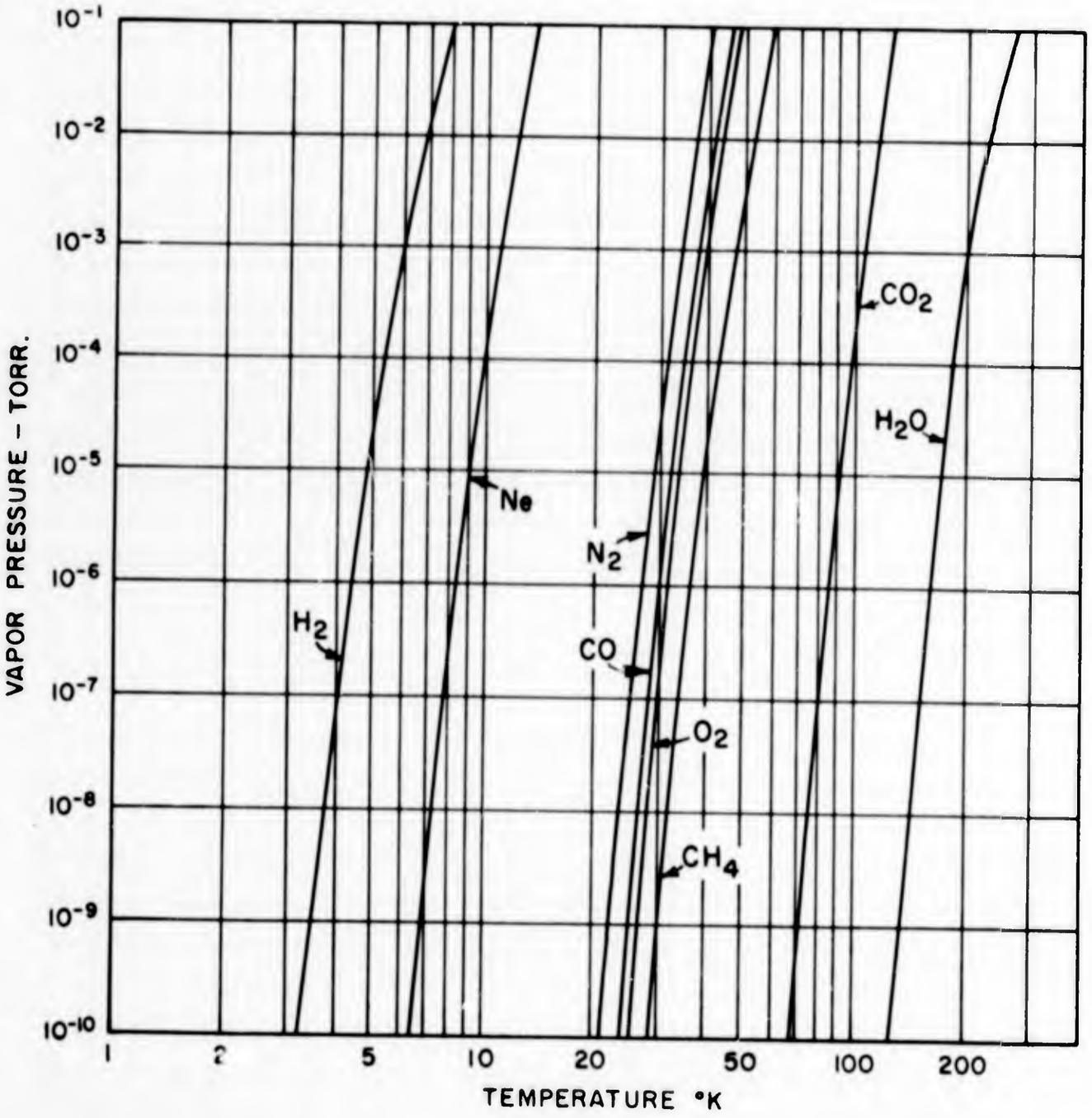

FIGURE 5. VAPOR PRESSURE OF COMMON GASES VS. TEMPERATURE OF CONDENSATE

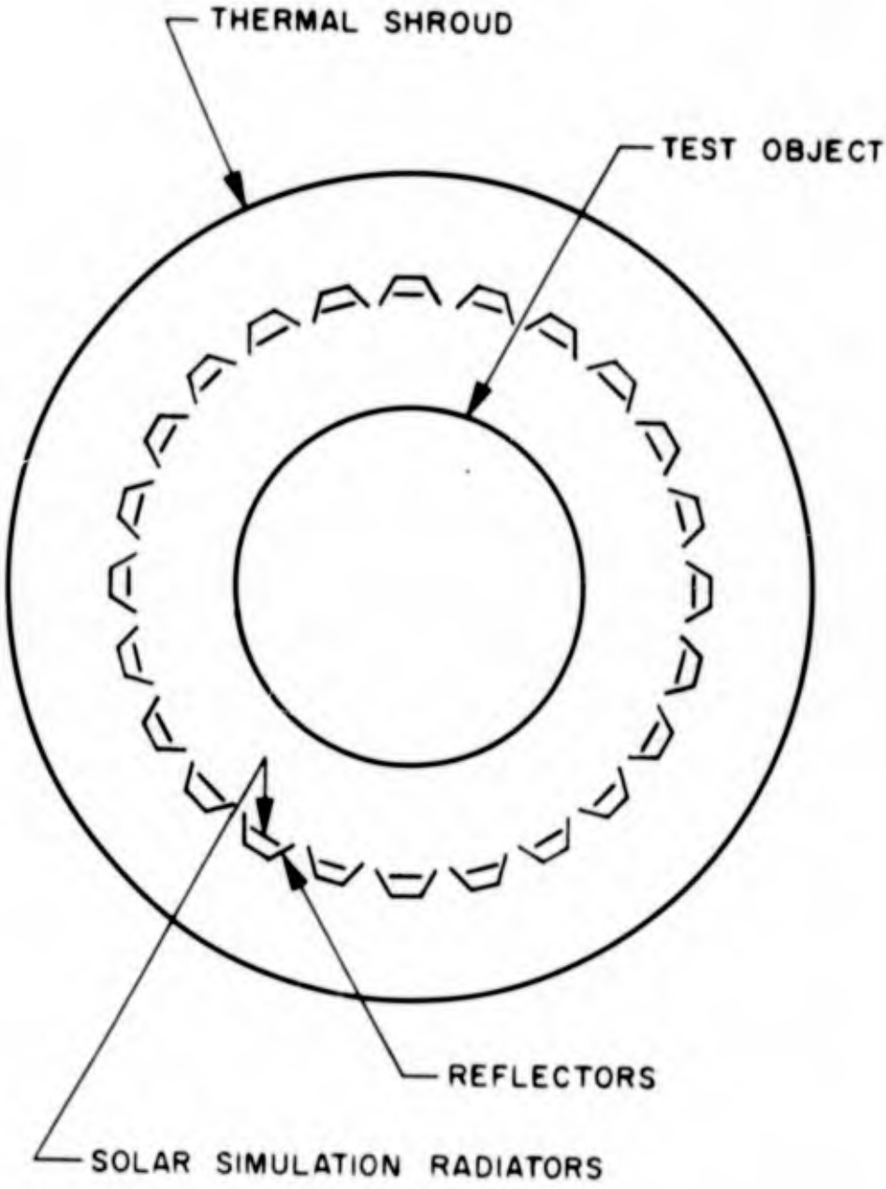

FIGURE 6. SCHEMATIC OF SOLAR RADIATION CONFIGURATION

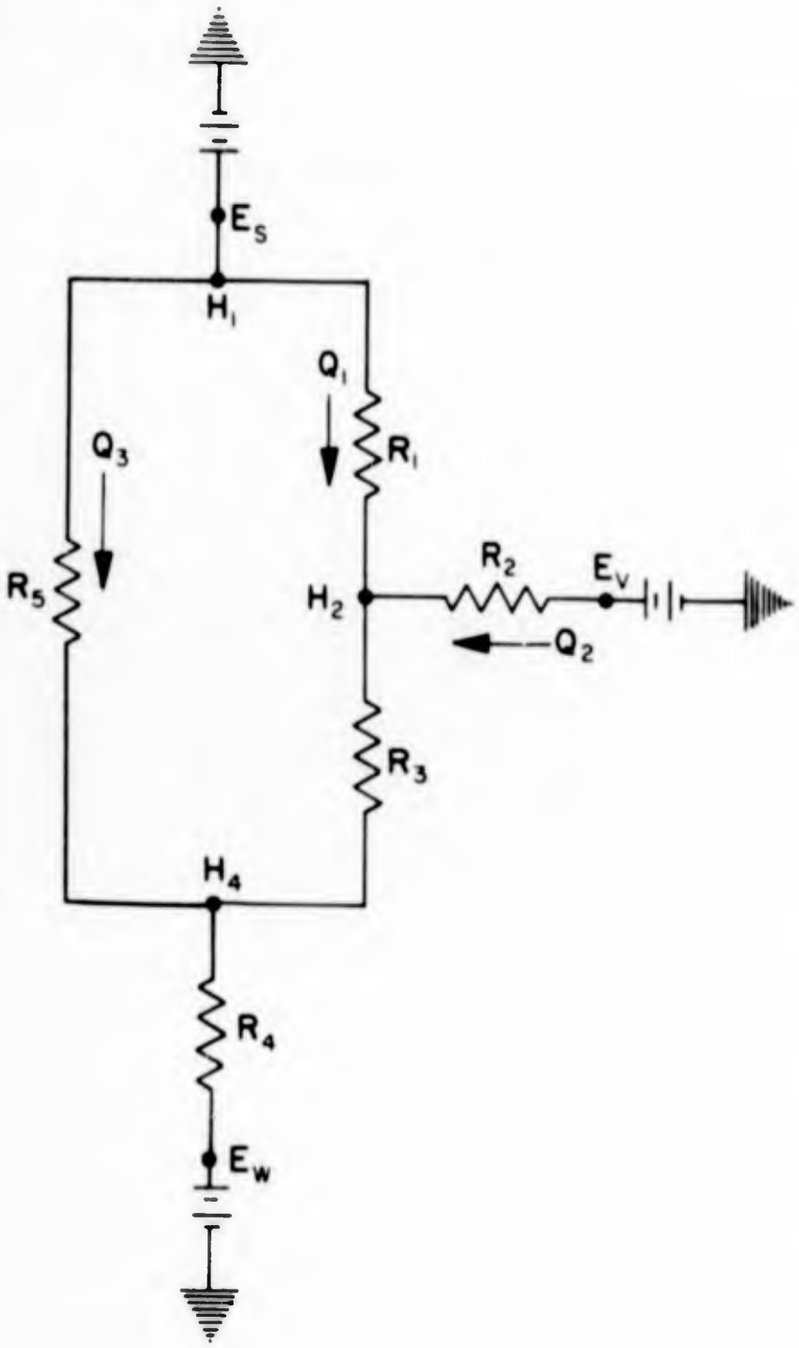

$$R_1 = \frac{1}{A_S F_{SV}}$$

$$R_2 = \frac{1 - e_V}{e_V A_V}$$

$$R_3 = \frac{1}{A_V - A_S F_{SV}}$$

$$R_4 = \frac{1 - e_W}{e_W A_W}$$

$$R_5 = \frac{1}{A_S - A_S F_{SV}}$$

$$E_S = \sigma (T_S)^4$$

$$E_V = \sigma (T_V)^4$$

$$E_W = \sigma (T_W)^4$$

FIGURE 7. THERMAL NETWORK FOR VEHICLE IN SPACE SIMULATOR

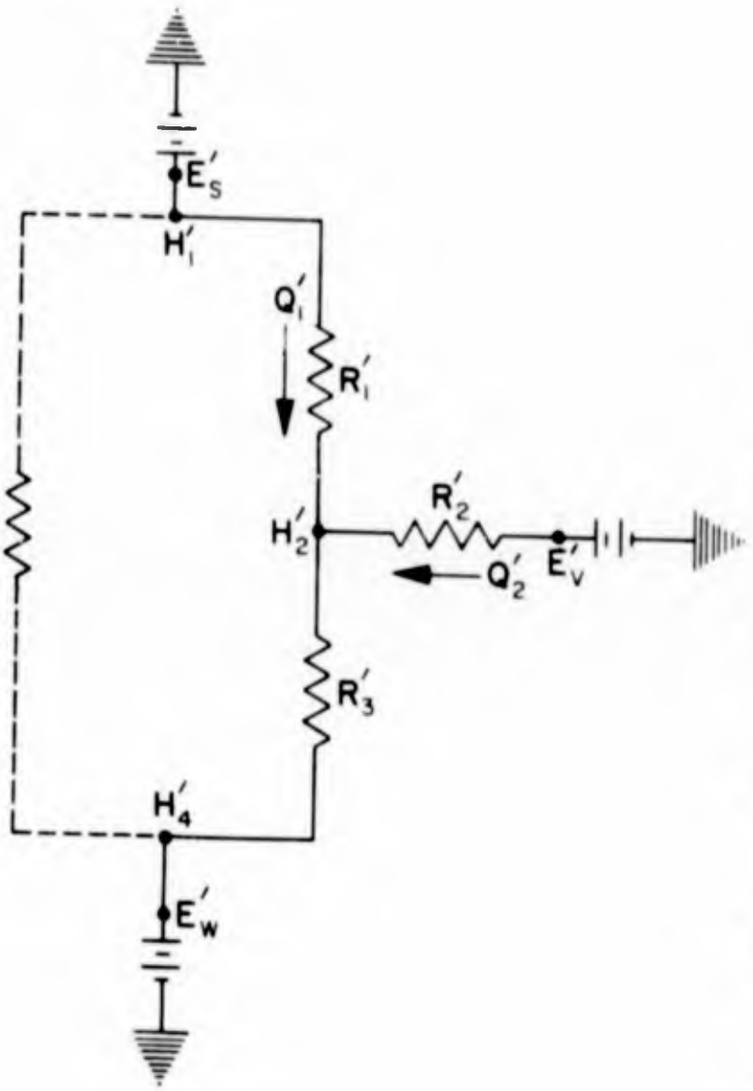

$$R_1' = \frac{1}{A_S' F_{SV}'} = \frac{(T_S'/T_S)^4}{A_S F_{SV}}$$

$$R_2' = R_2 = \frac{1 - e_V}{e_V A_V}$$

$$R_3' = \frac{1}{A_V - A_S' F_{SV}'}$$

$$E_S' = \sigma (T_S')^4$$

$$E_V' = \sigma (T_V')^4$$

$$E_W' = \sigma (T_W')^4$$

FIGURE 8. THERMAL NETWORK FOR VEHICLE IN SPACE

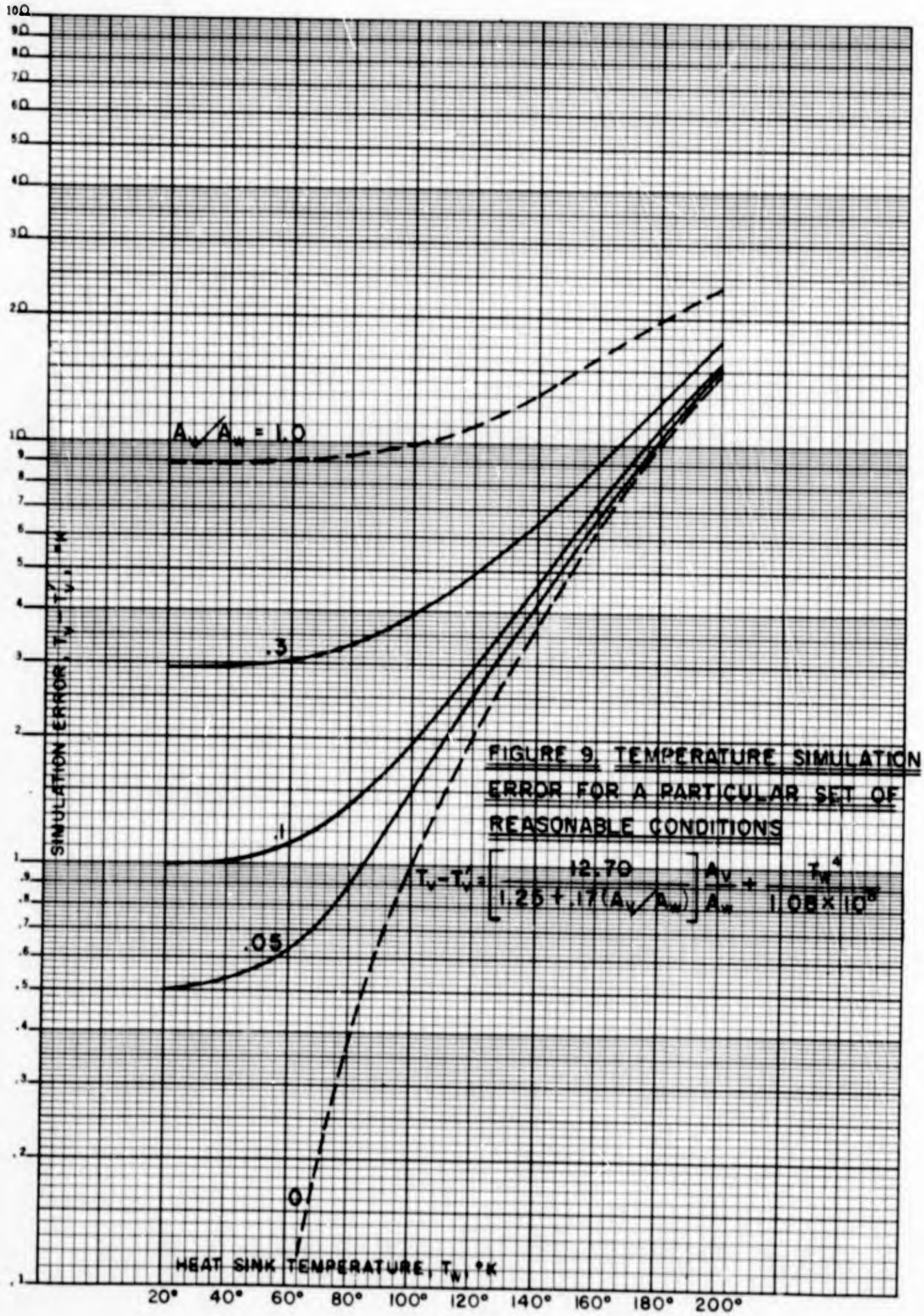

FIGURE 9. TEMPERATURE SIMULATION ERROR FOR A PARTICULAR SET OF REASONABLE CONDITIONS

BLANK PAGE

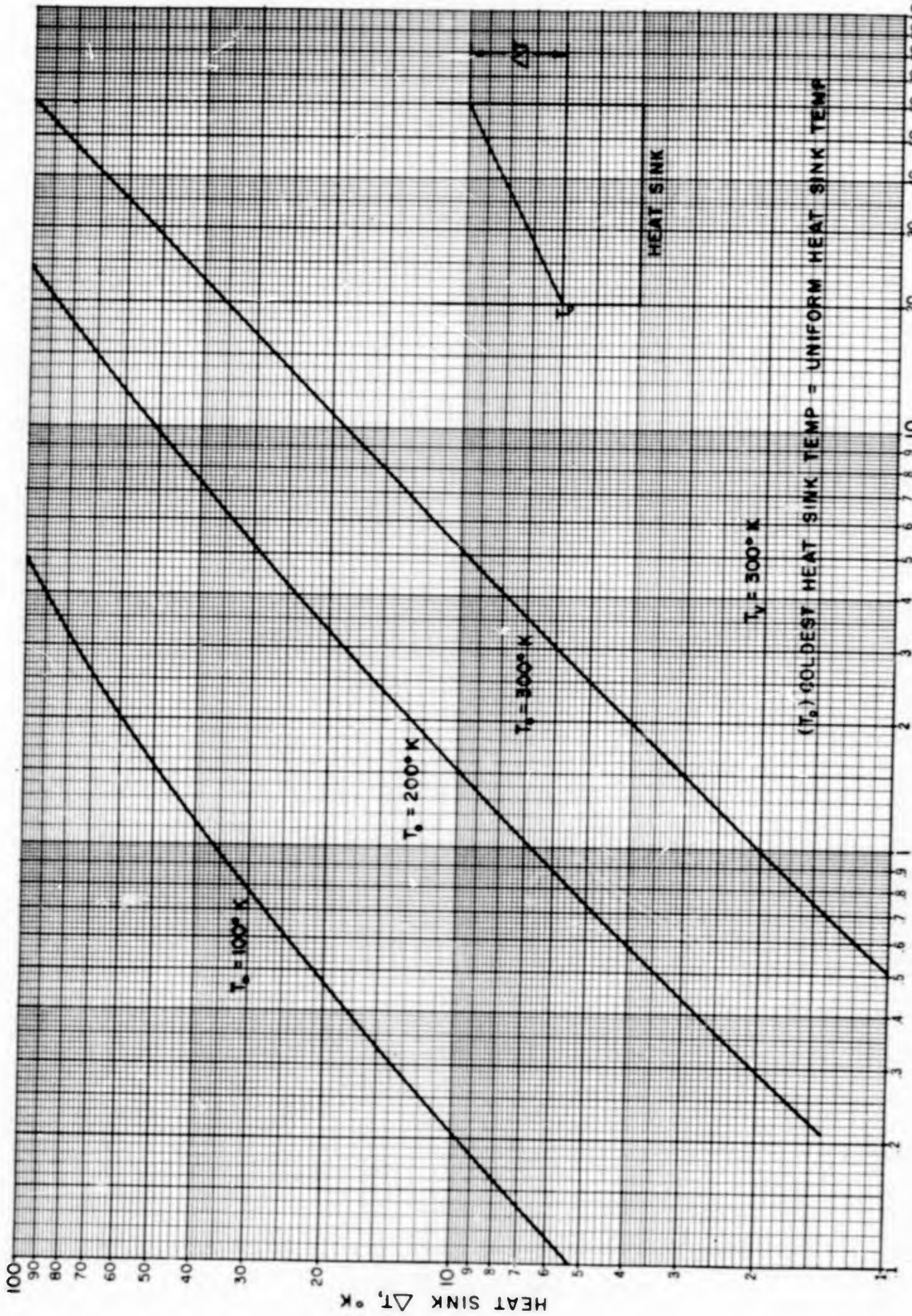

FIGURE 10. VARIATION IN VEHICLE TEMPERATURE DUE TO HEAT SINK ΔT

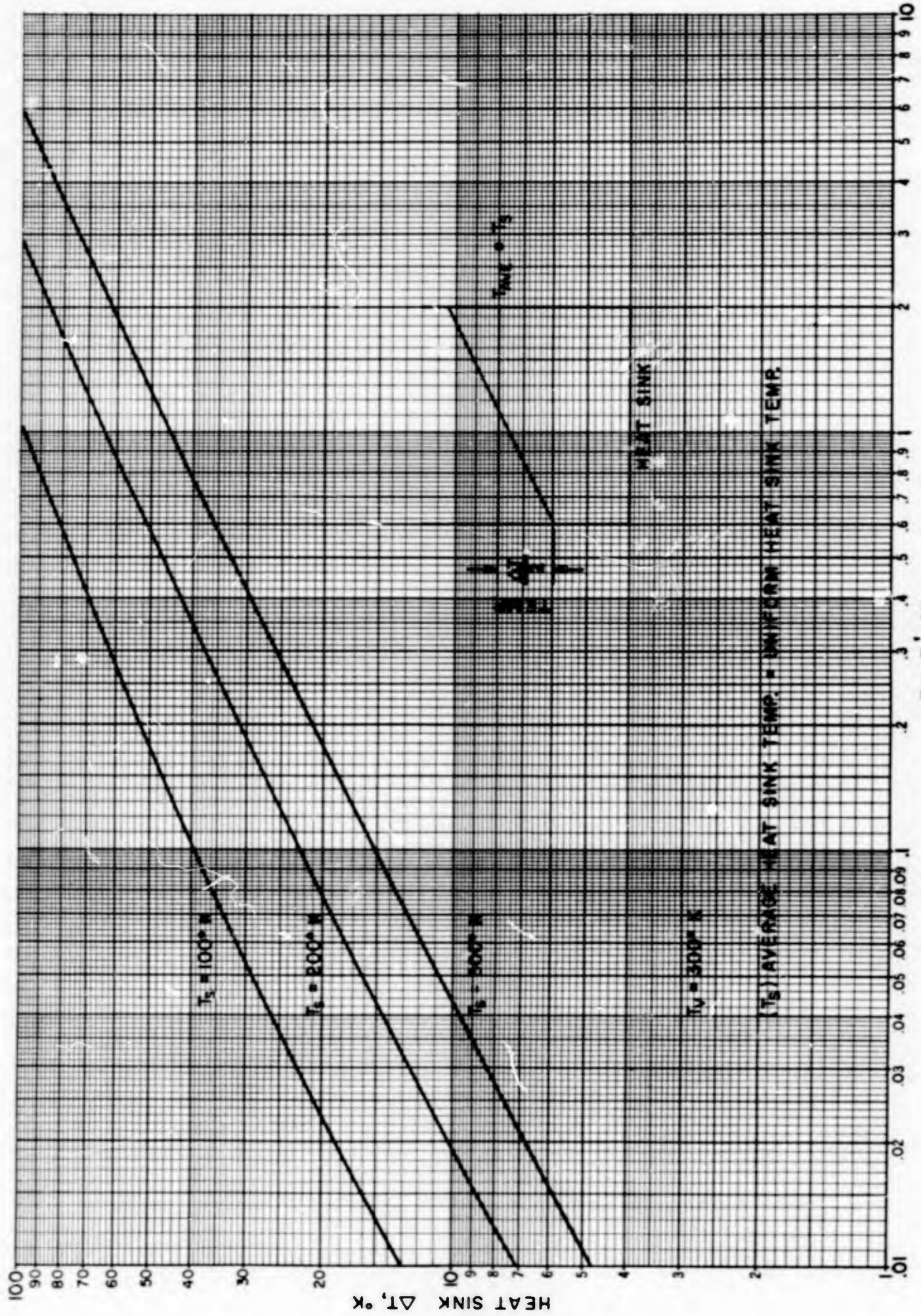

FIGURE 11. VARIATION IN VEHICLE TEMPERATURE DUE TO HEAT SINK ΔT

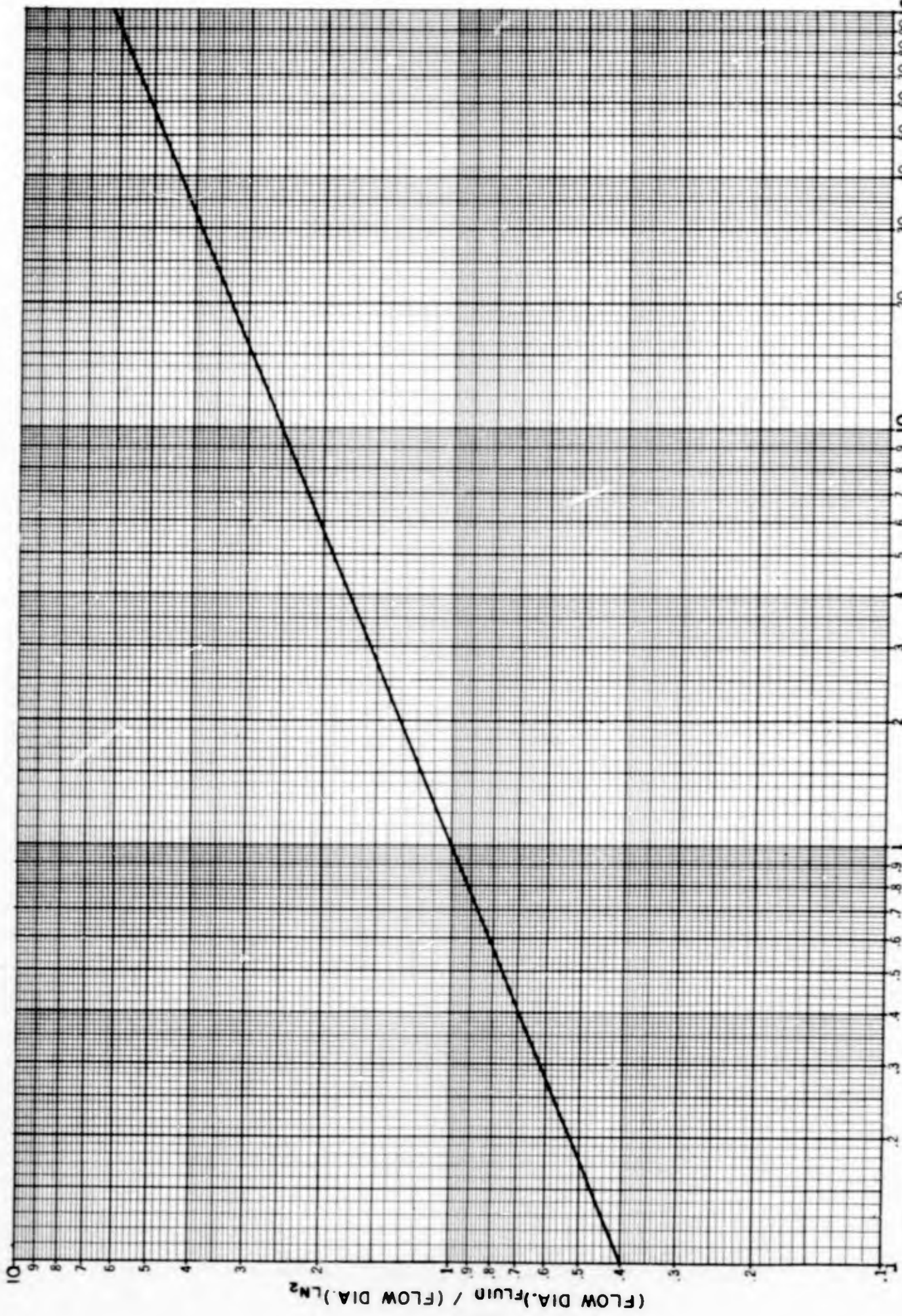

FIGURE 12. HEAT SINK FLOW DIA. FOR FLUIDS COMPARED WITH LN_2

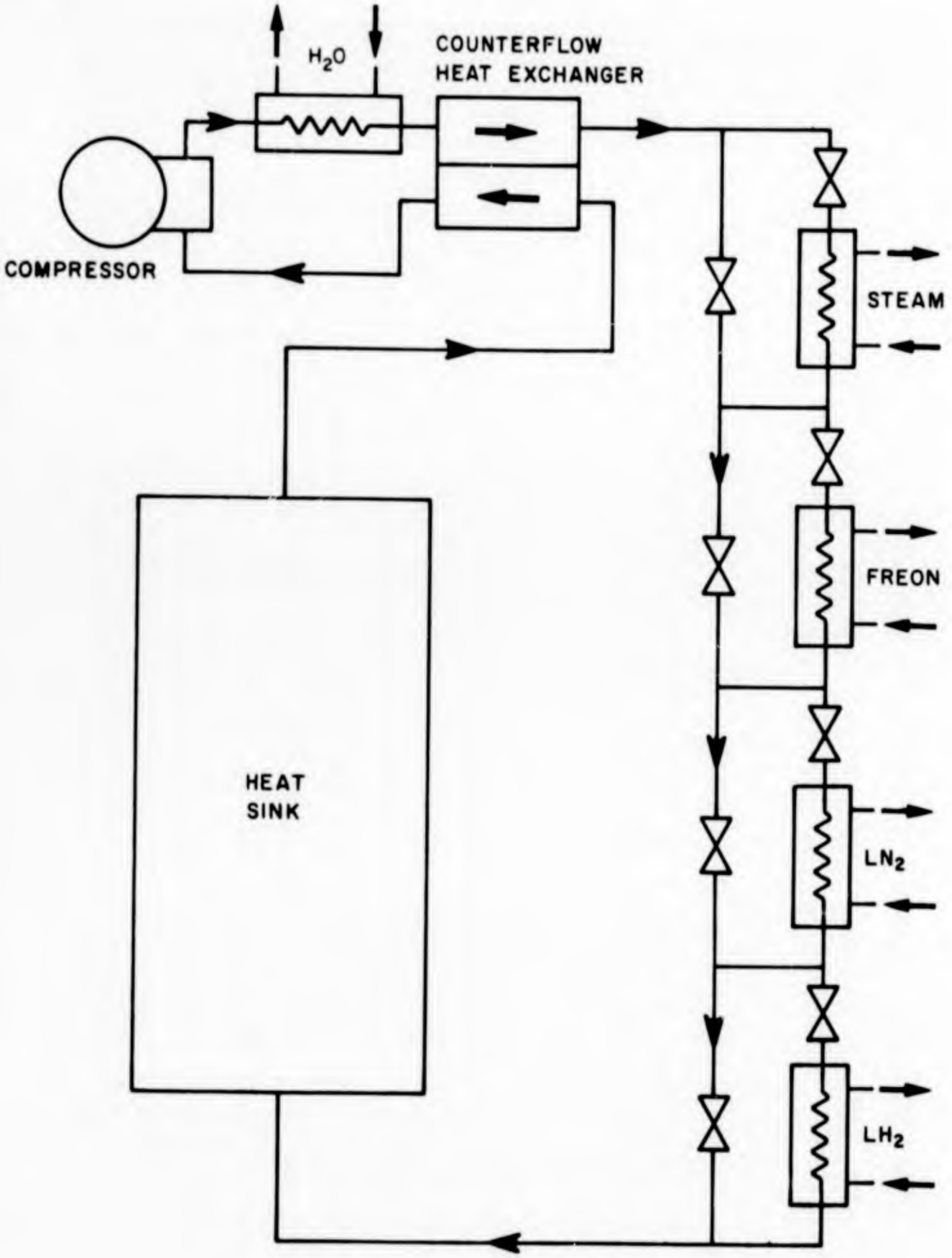

FIGURE 13. GAS CIRCULATION SYSTEM

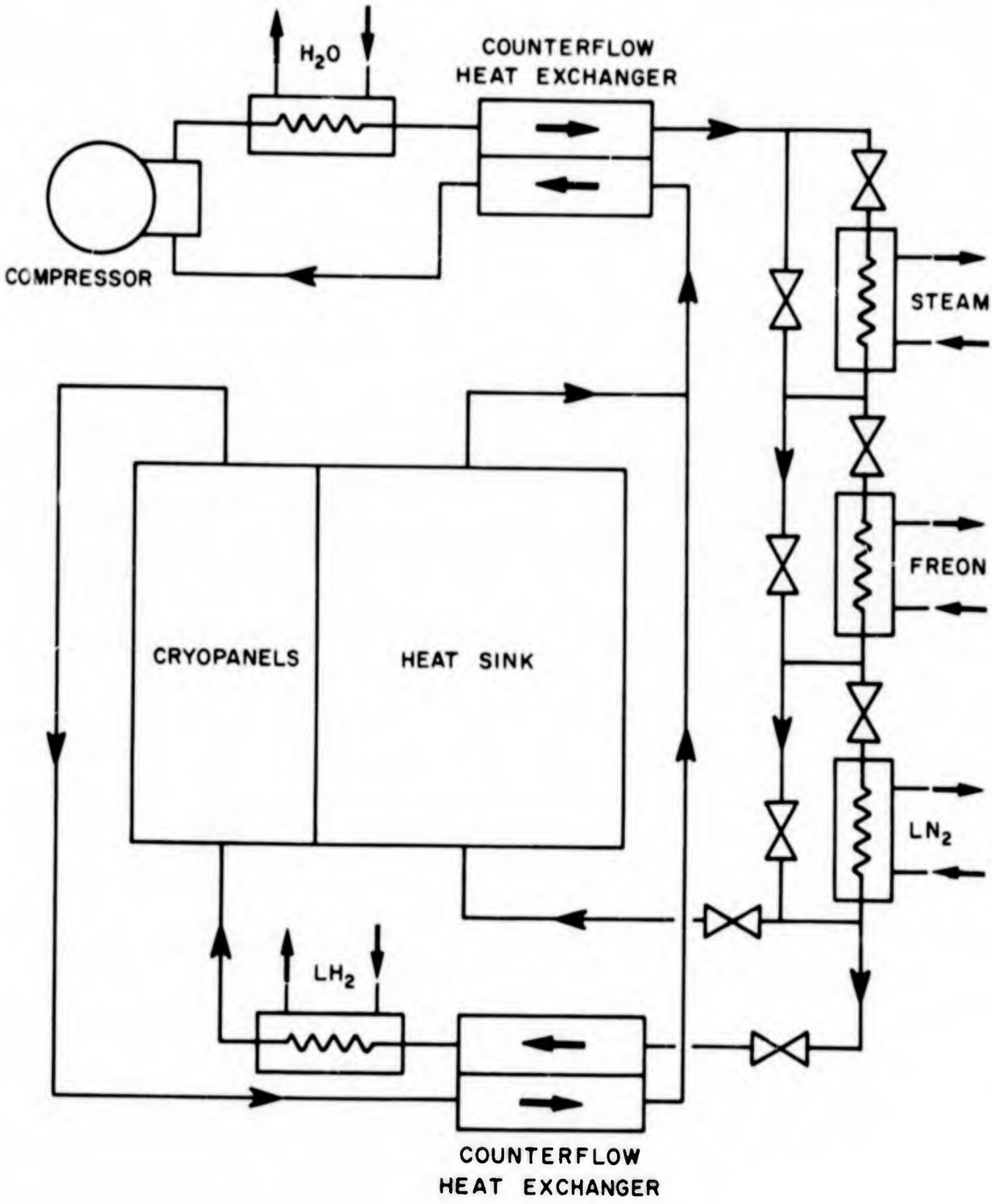

FIGURE 14. TWO TEMPERATURE CONTROL WITH GAS CIRCULATION SYSTEM

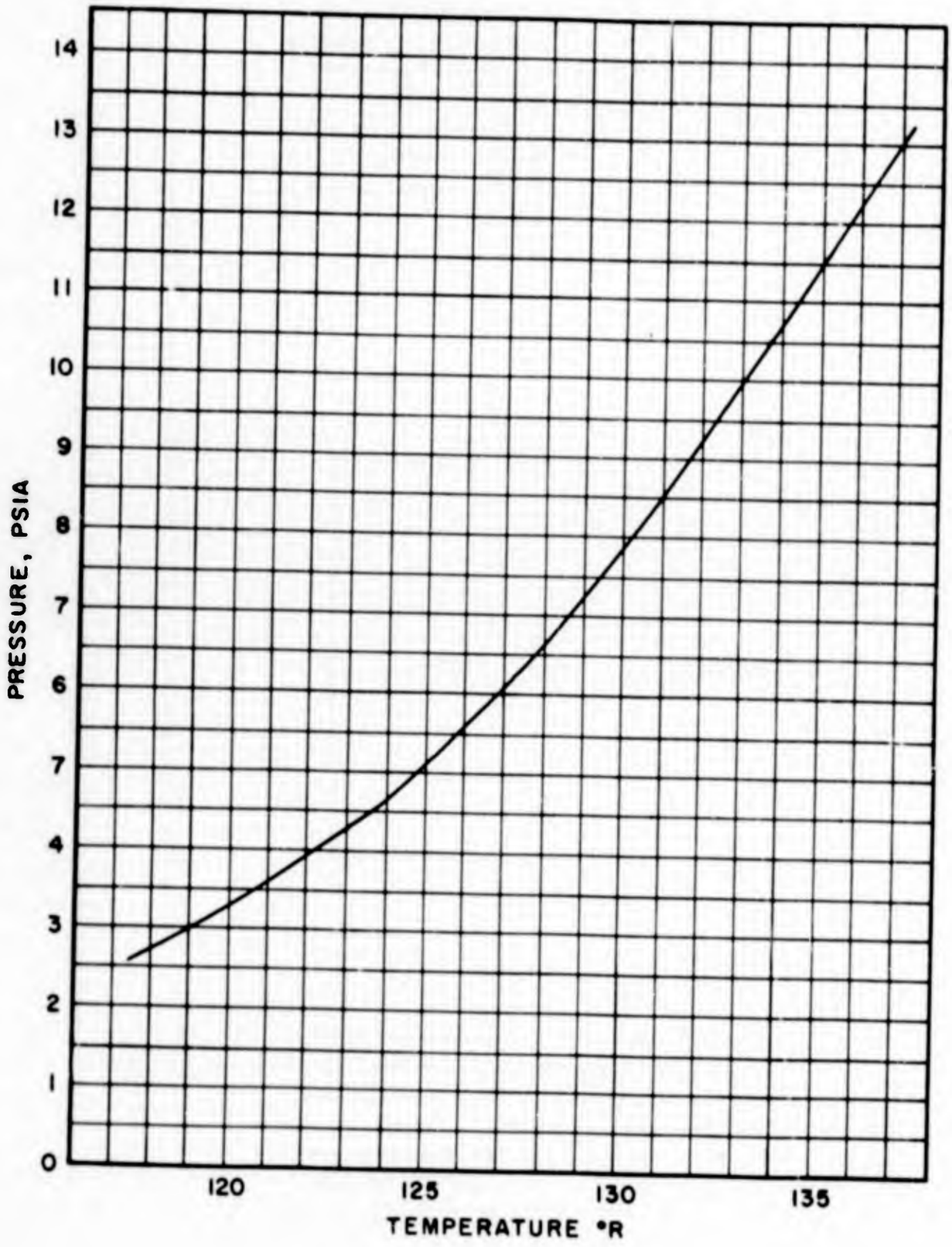

FIGURE 15. VAPOR PRESSURE OF NITROGEN

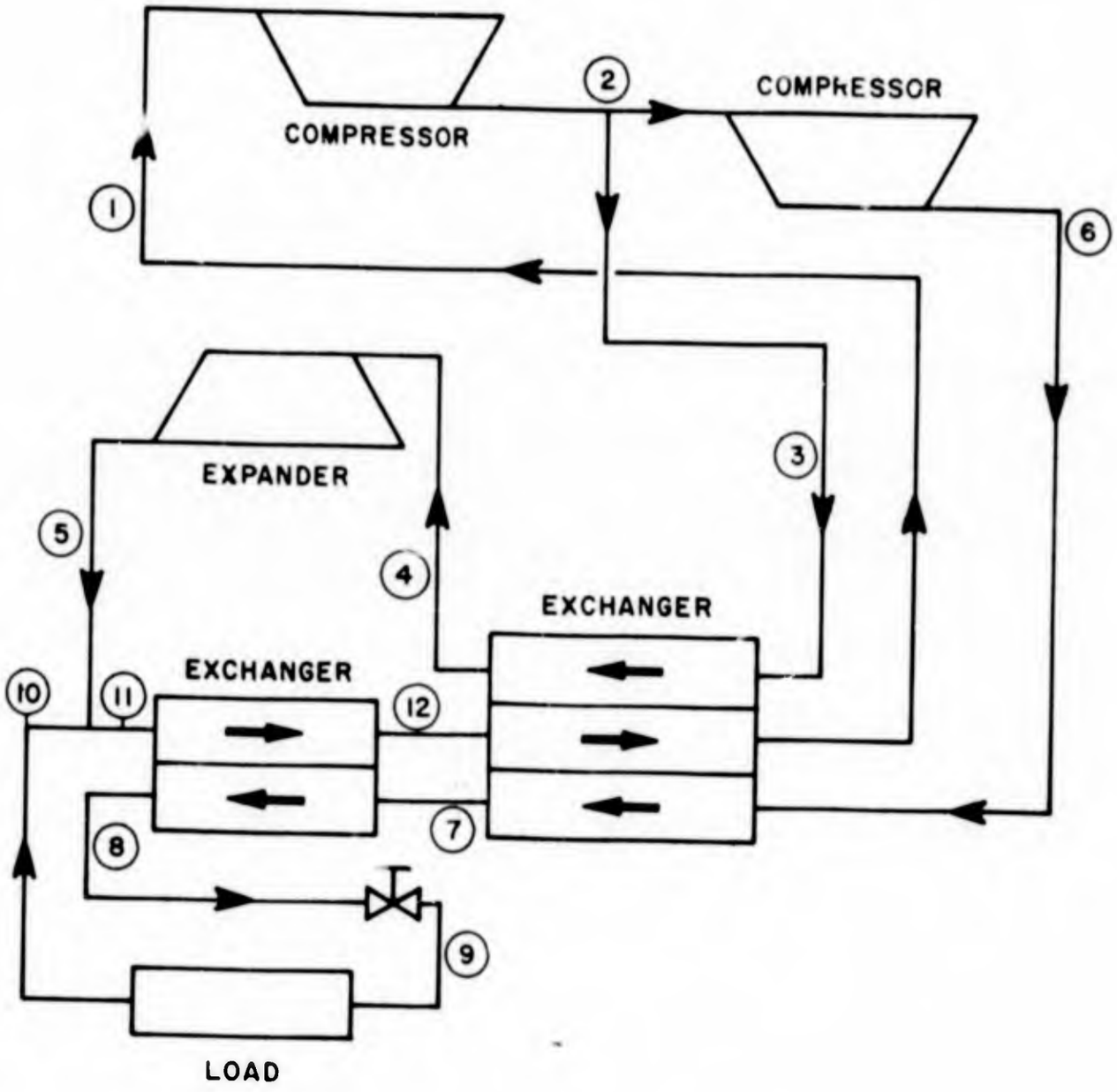

FIGURE 16. SPLIT STREAM RELIQUEFIER WITHOUT SUBCOOLER

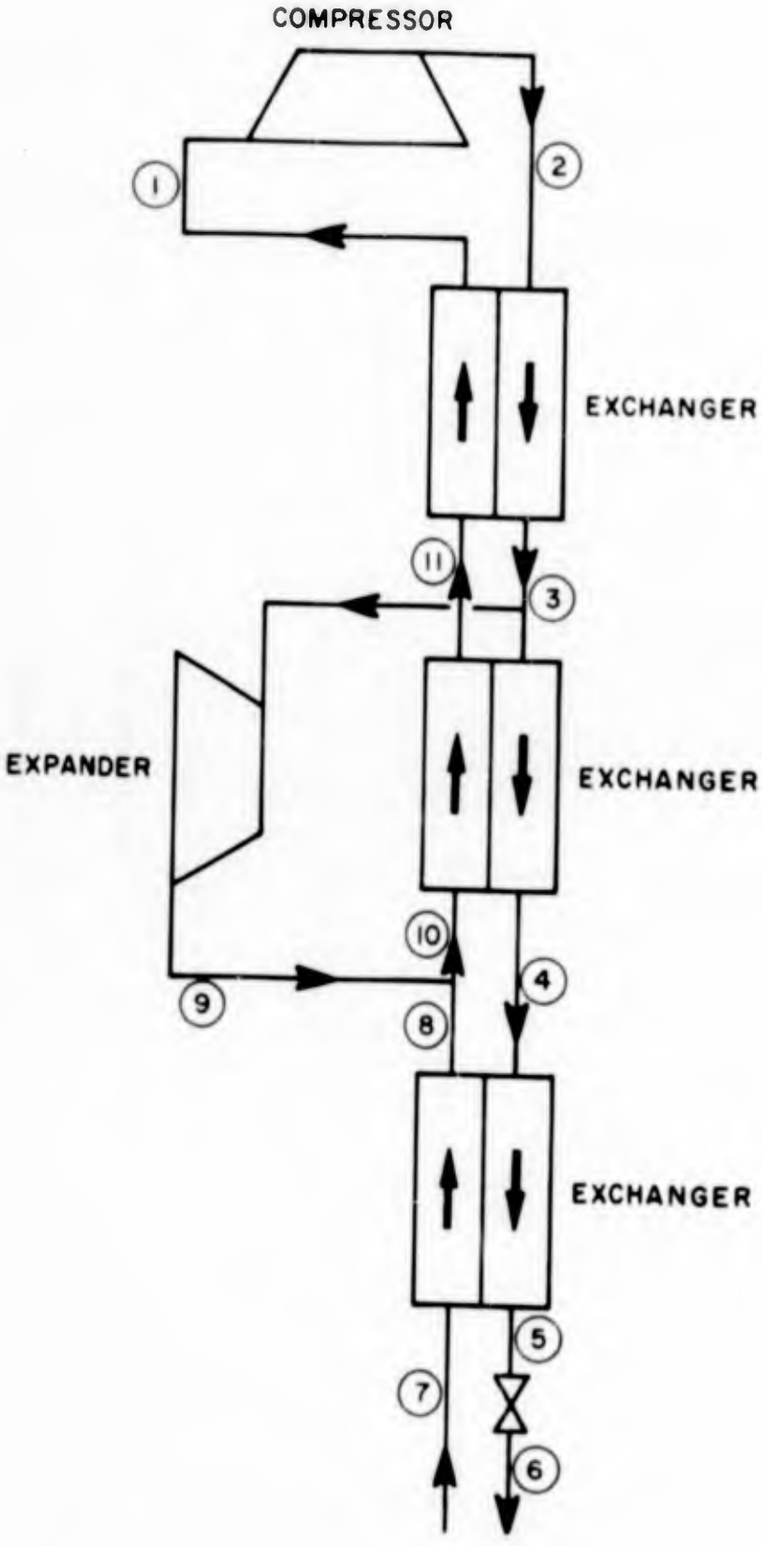

FIGURE 17. FLOW SCHEMATIC OF CLAUDE CYCLE FOR NEON RELIQUEFIER

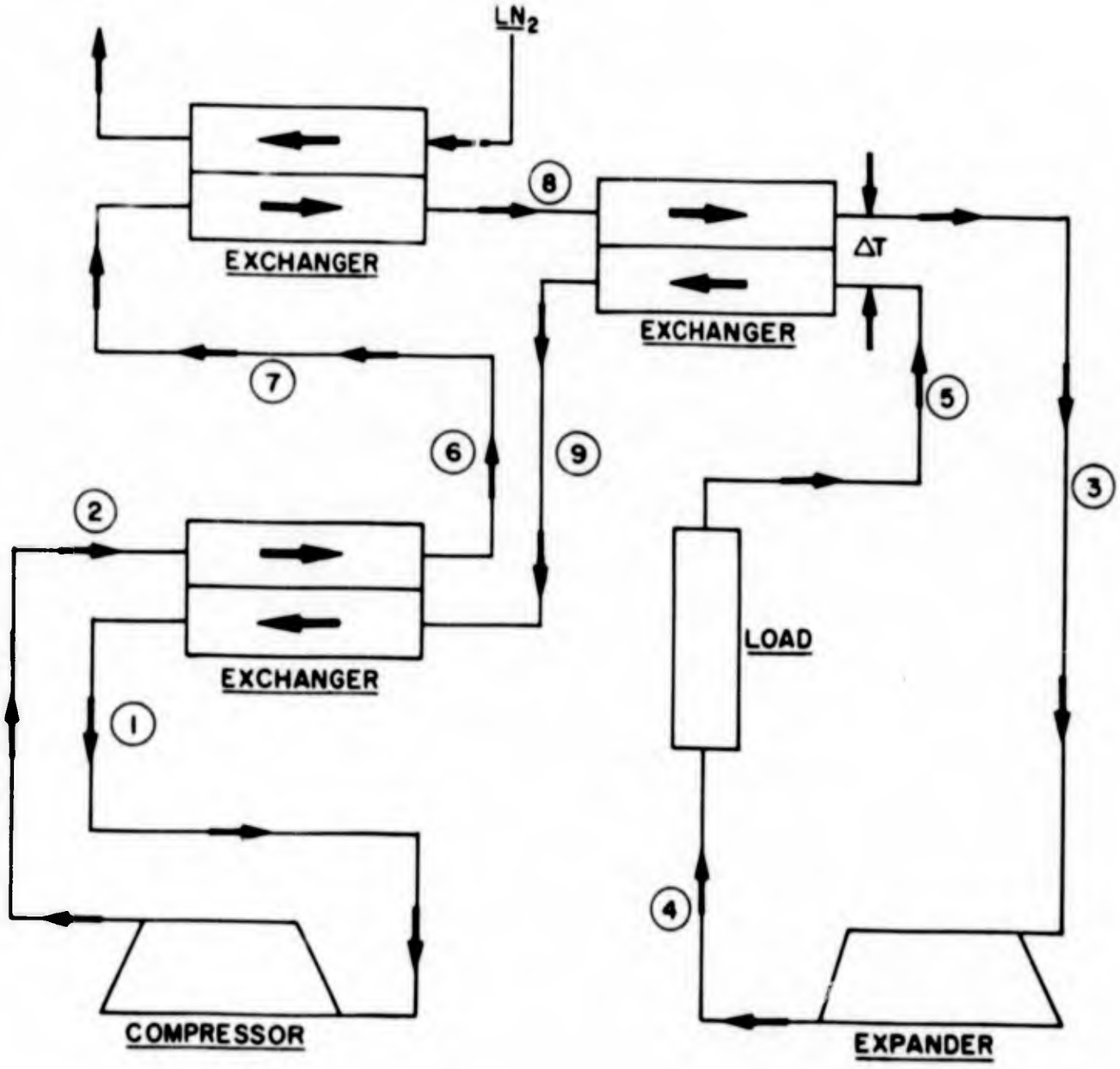

FIGURE 18. HELIUM REFRIGERATION CYCLE

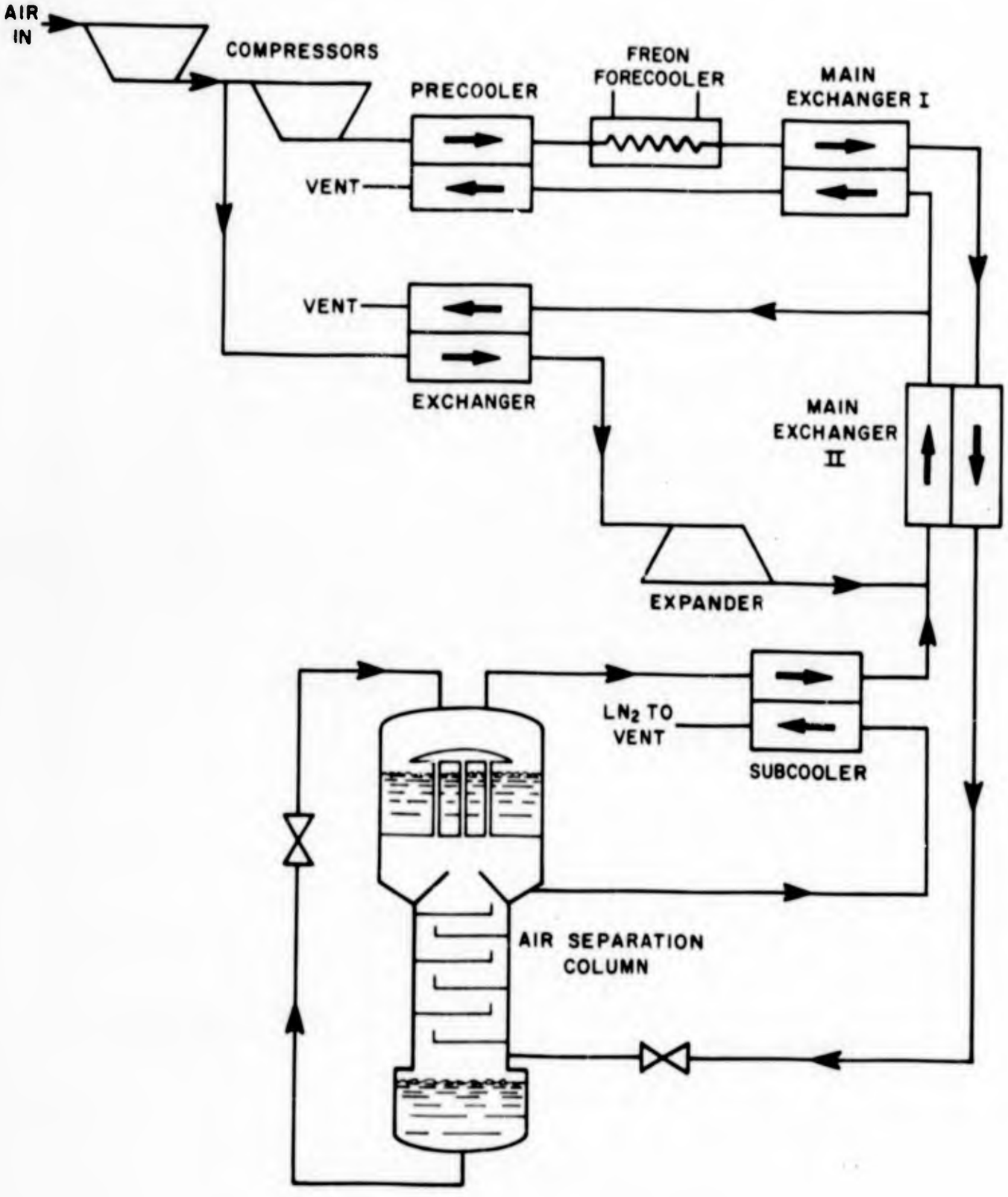

FIGURE 19. AIR SEPARATION PLANT

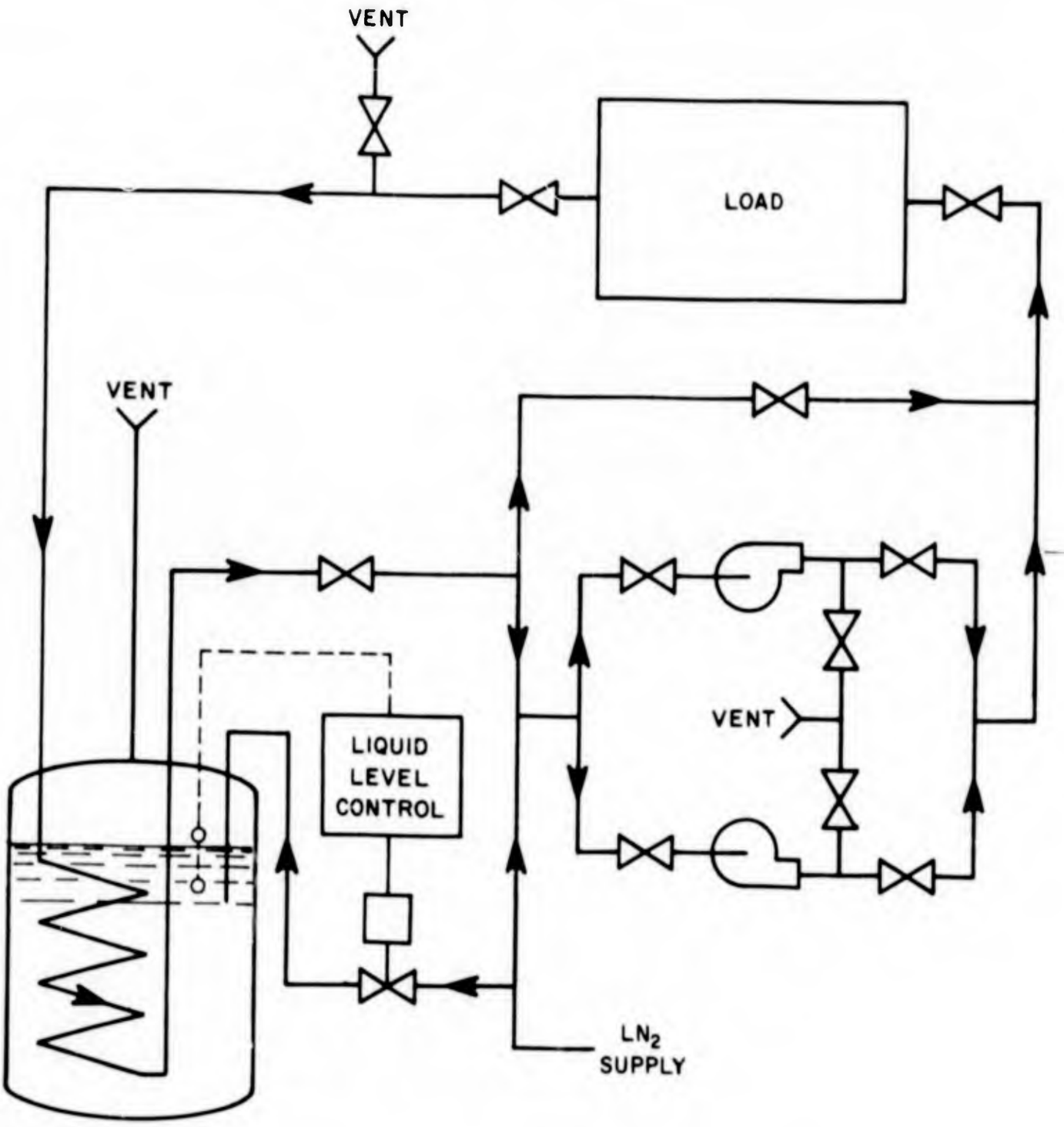

FIGURE 20. SUBCOOLER TYPE NITROGEN CIRCULATION SYSTEM

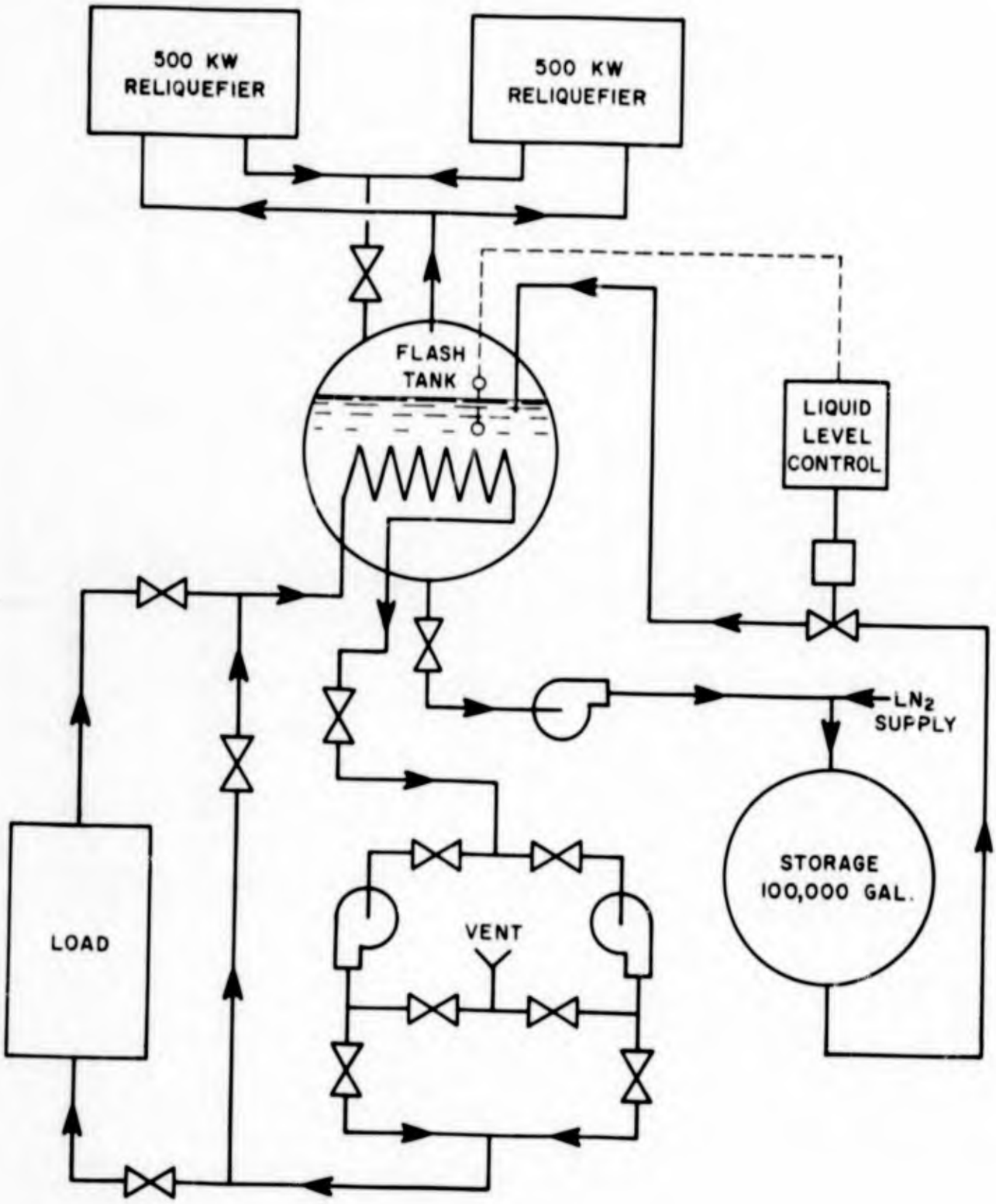

FIGURE 21. PUMPING SYSTEM FOR 1000 KW NITROGEN RELIQUEFIER

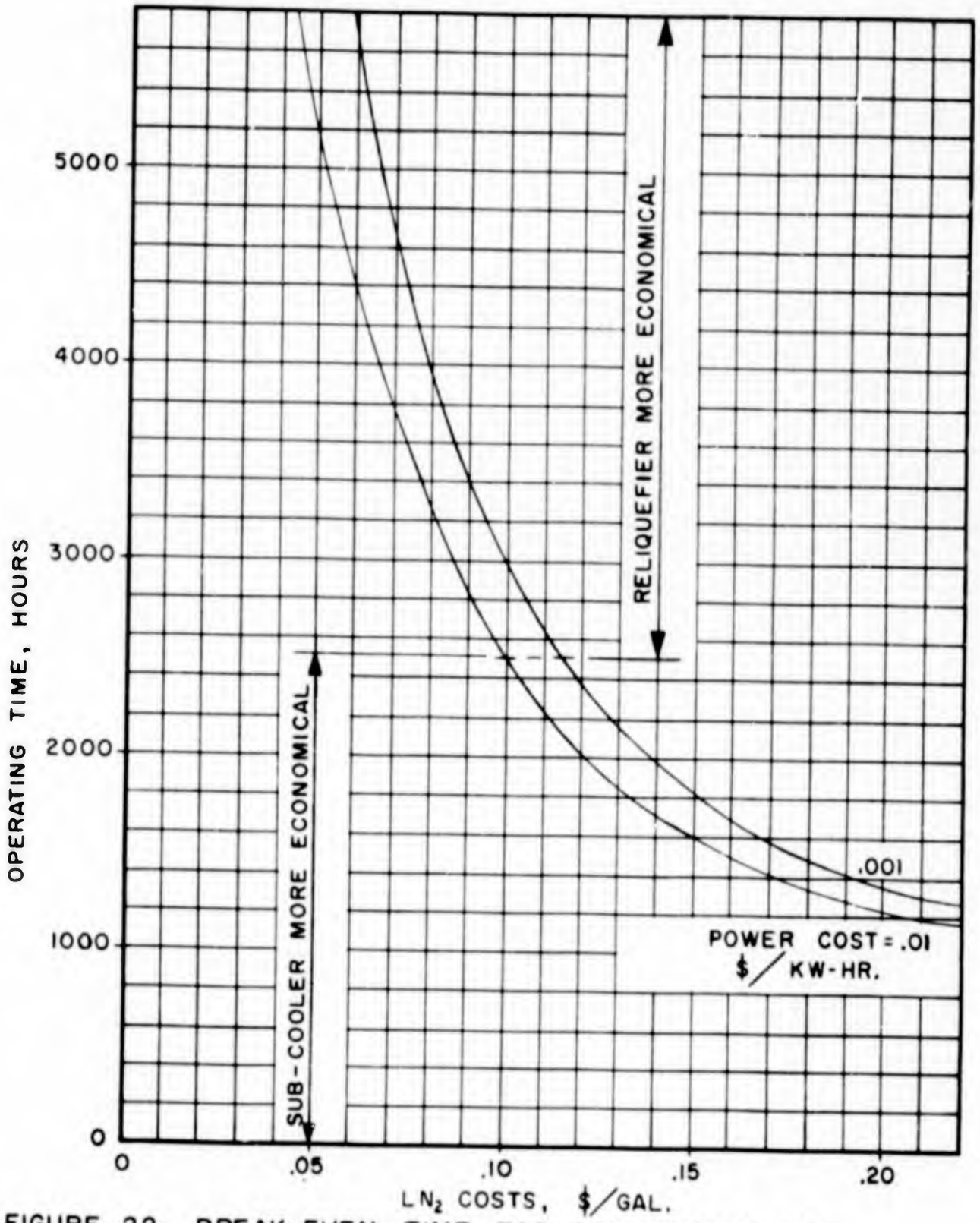

FIGURE 22. BREAK-EVEN TIME FOR SUB-COOLER VS. RELIQUEFIER

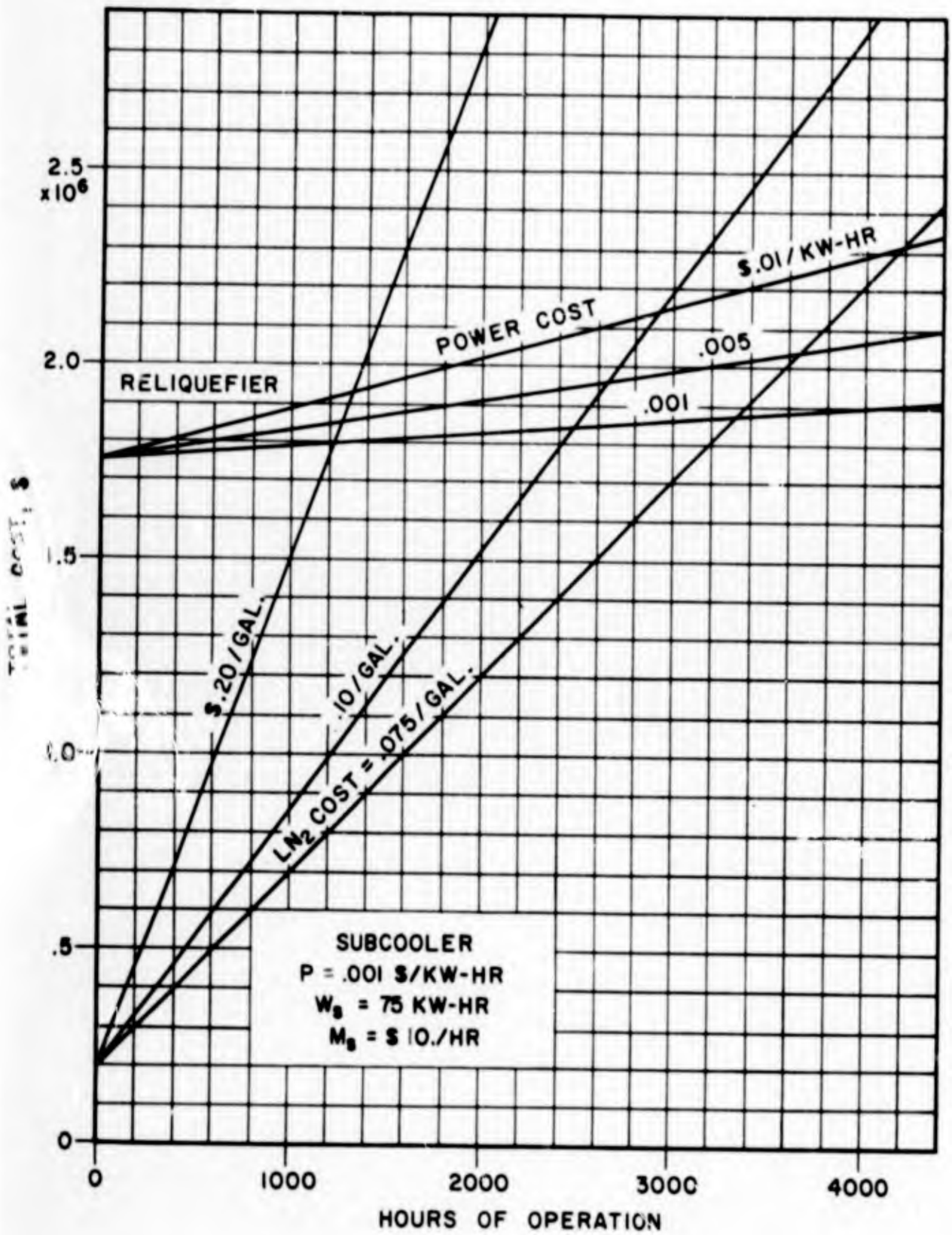

FIGURE 23. TOTAL COST OF 1000 KW SUBCOOLER AND RELIQUEFIER VS. HOURS OF OPERATION

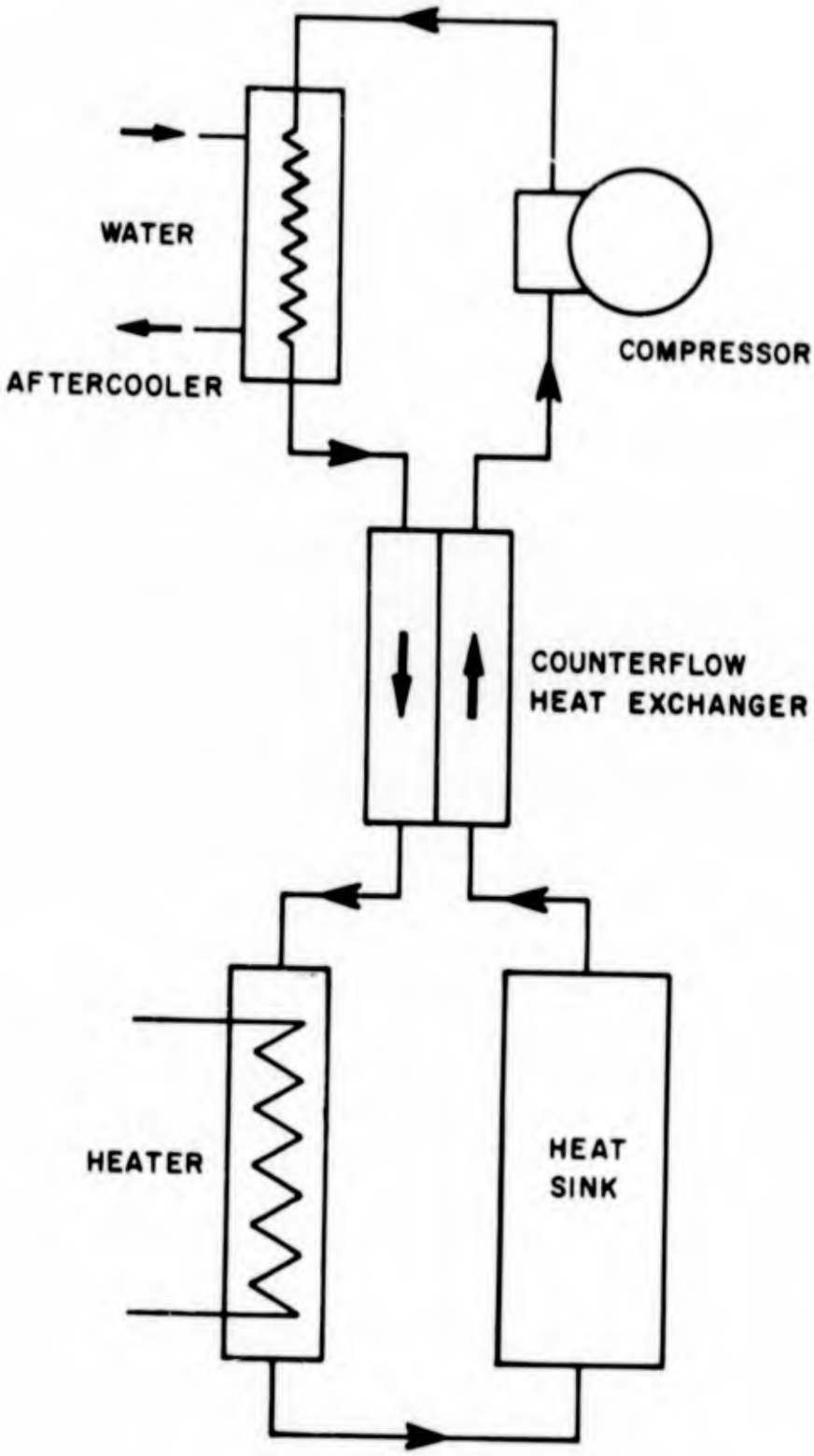

FIGURE 24. SCHEMATIC OF WARM-UP SYSTEM

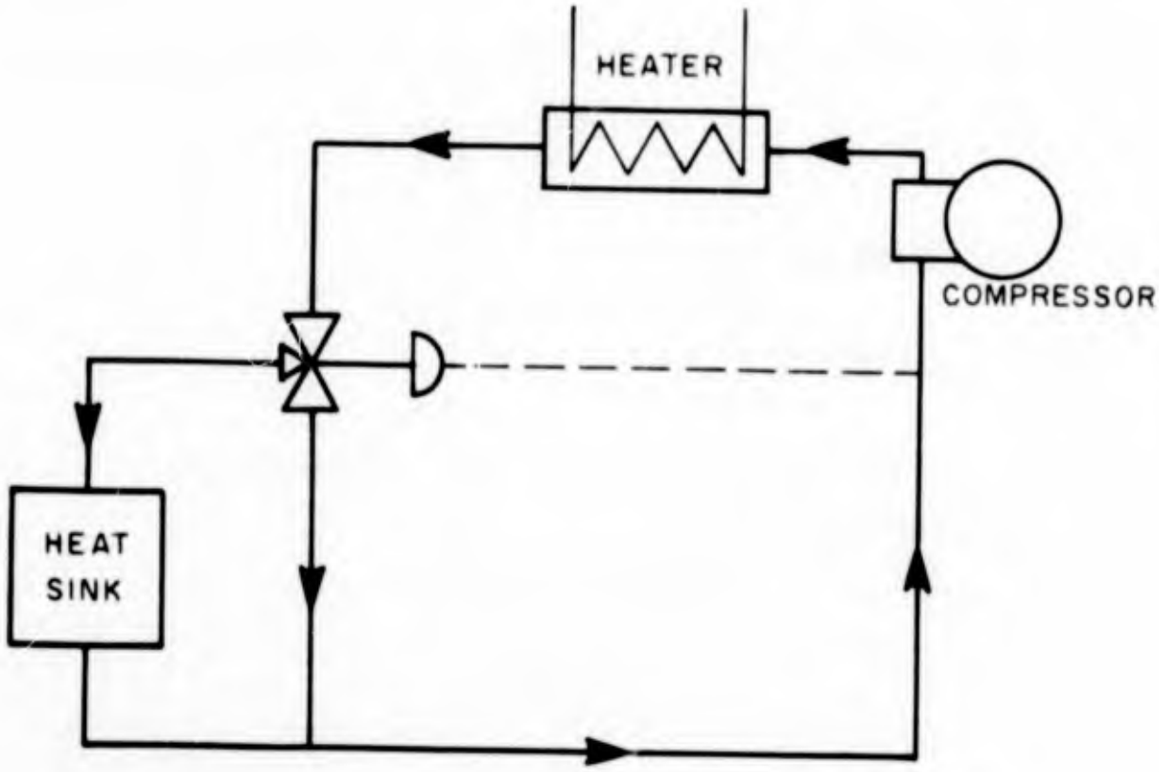

FIGURE 25-a. SCHEMATIC OF SIMPLIFIED WARM-UP SYSTEM

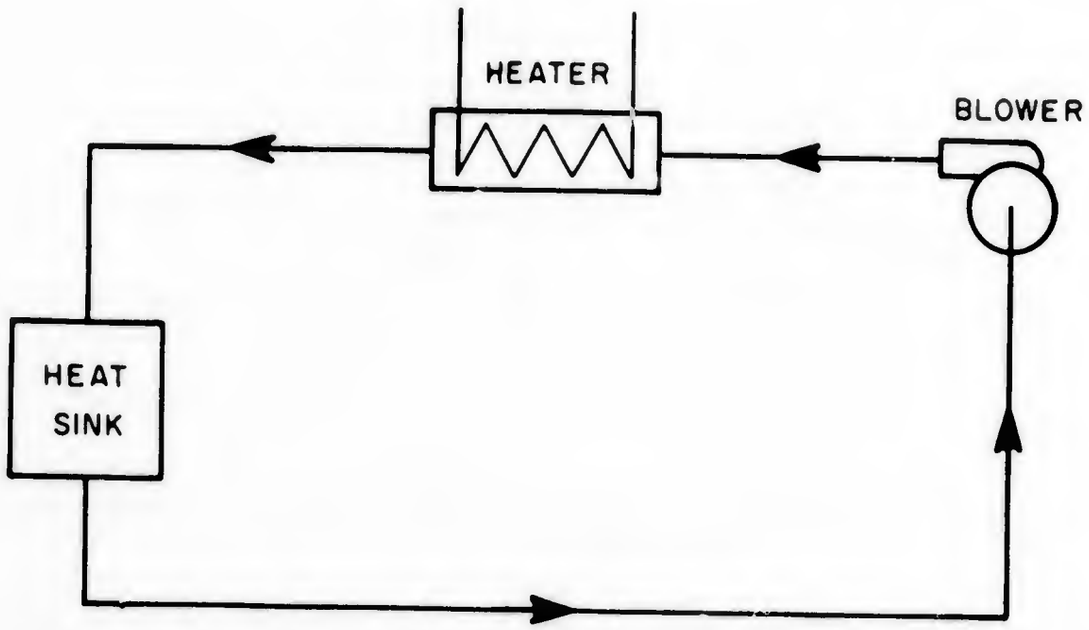

FIGURE 25-b. SCHEMATIC OF LOW PRESSURE WARM-UP SYSTEM

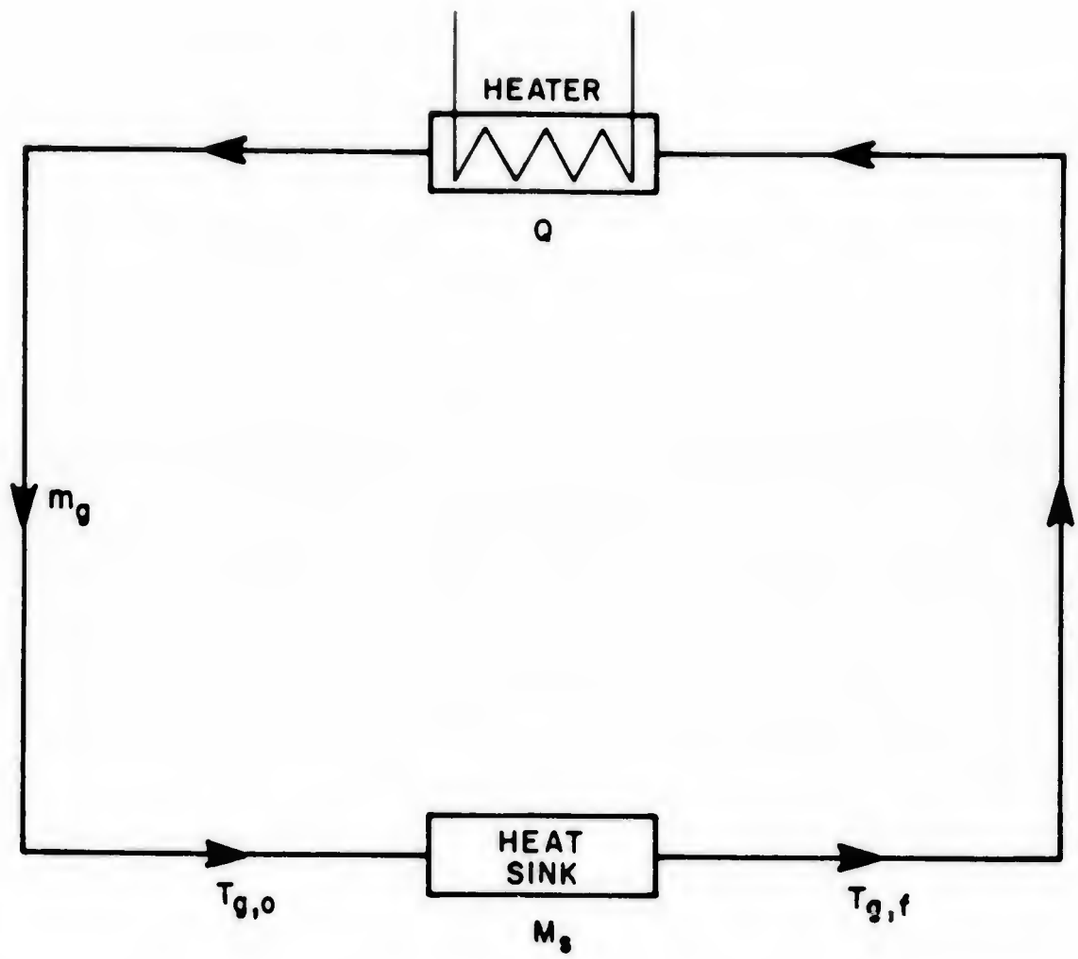

FIGURE 26. WARM-UP CIRCULATION DIAGRAM

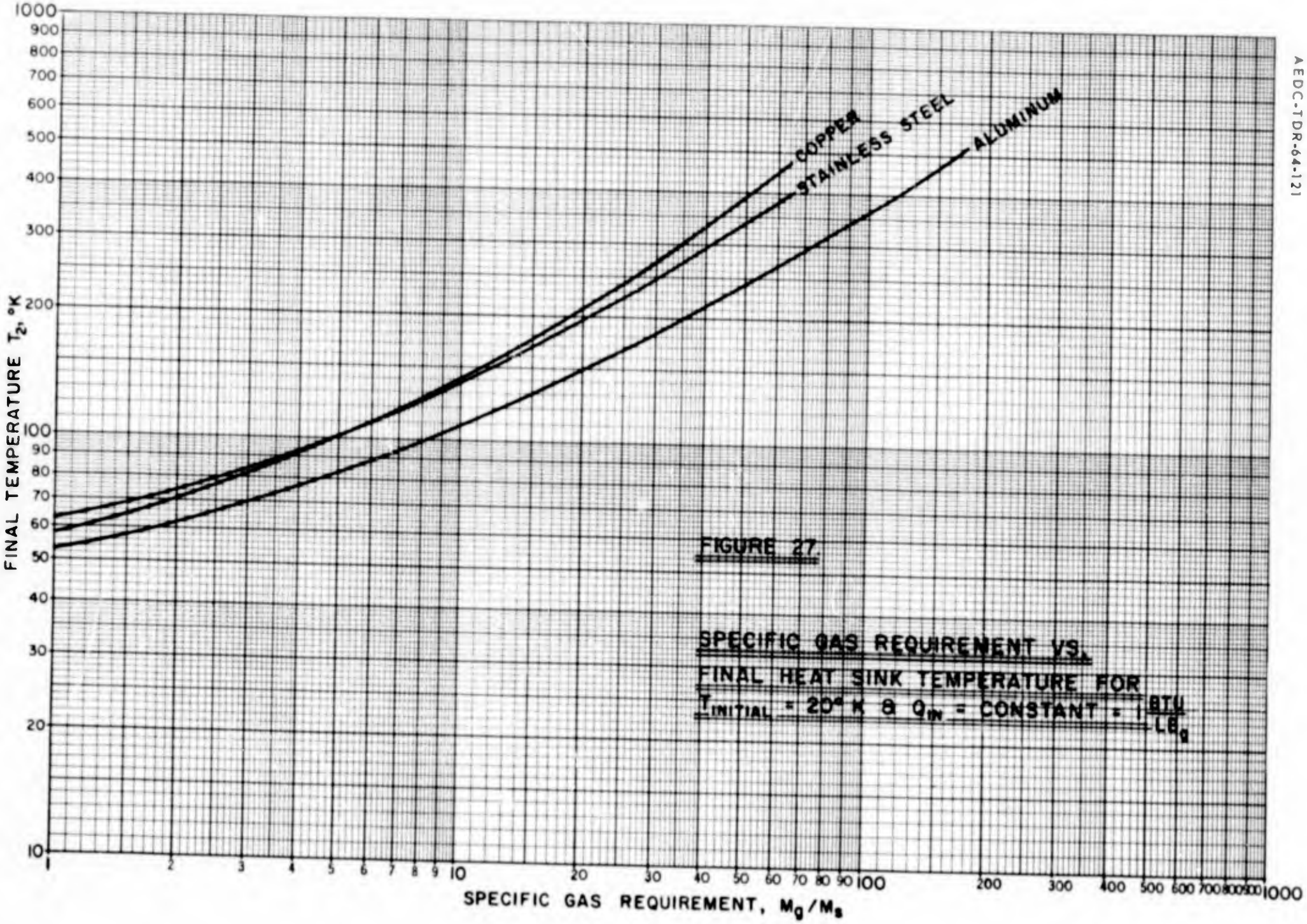

FIGURE 27.

SPECIFIC GAS REQUIREMENT VS. FINAL HEAT SINK TEMPERATURE FOR $T_{INITIAL}$ = 20° K & Q_{IN} = CONSTANT = 1 $\frac{BTU}{LB_g}$

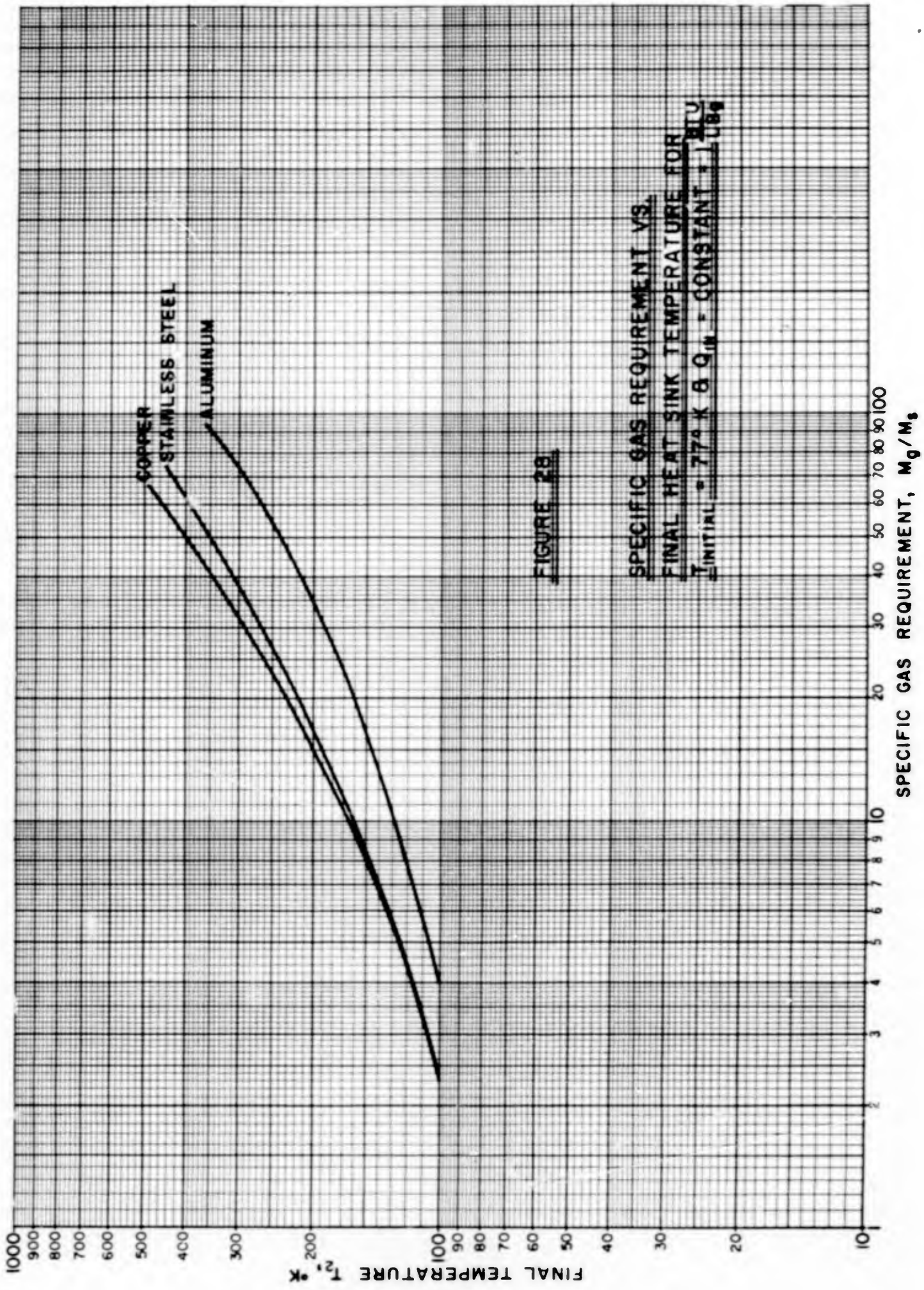
COPPER
STAINLESS STEEL
ALUMINUM
SPECIFIC GAS REQUIREMENT VS.
FINAL HEAT SINK TEMPERATURE FOR
T INITIAL = 77° K & Q IN = CONSTANT = 1 BTU / LBm
FINAL TEMPERATURE T2, °K
SPECIFIC GAS REQUIREMENT, Mg/Ms
1000
900
800
700
600
500
400
300
200
100
90
80
70
60
50
40
30
20
10
1
2
3
4
5
6
7
8
9
10
20
30
40
50
60
70
80
90
100

FIGURE 28

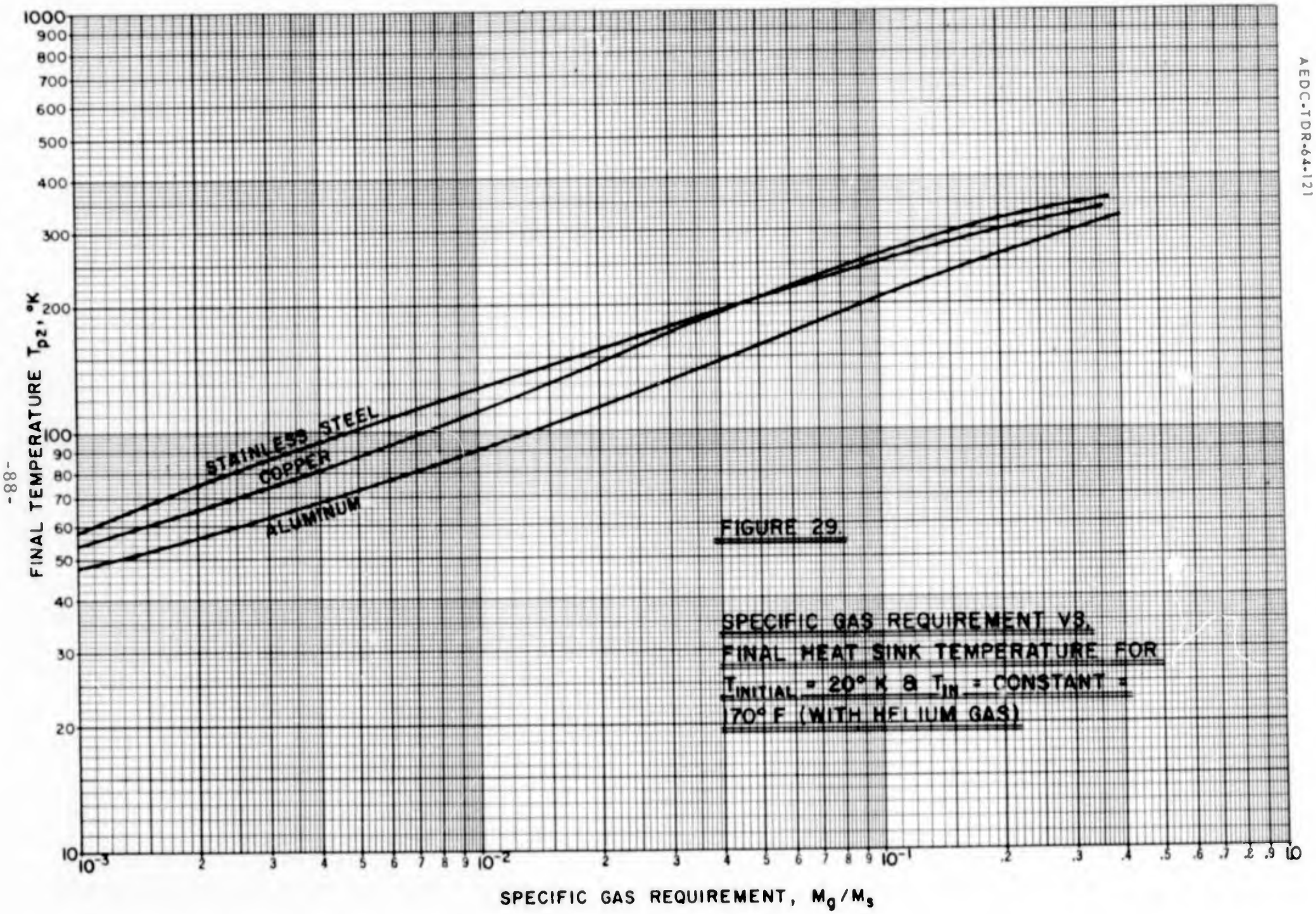

FIGURE 29.

SPECIFIC GAS REQUIREMENT VS. FINAL HEAT SINK TEMPERATURE FOR $T_{INITIAL}$ = 20° K & T_{IN} = CONSTANT = 70° F (WITH HELIUM GAS)

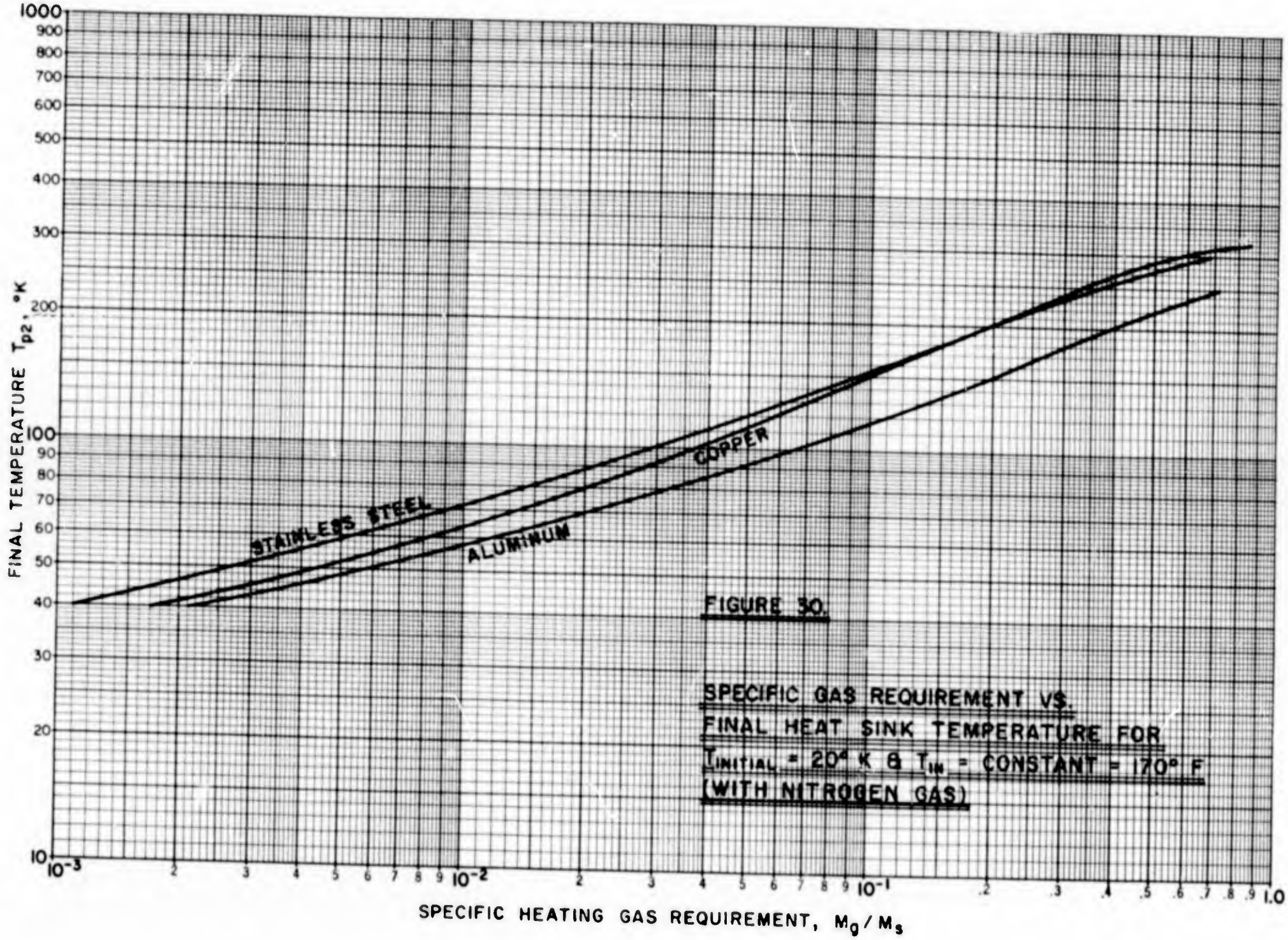

FIGURE 30.

SPECIFIC GAS REQUIREMENT VS. FINAL HEAT SINK TEMPERATURE FOR $T_{INITIAL}$ = 20° K & T_{IN} = CONSTANT = 170° F (WITH NITROGEN GAS)

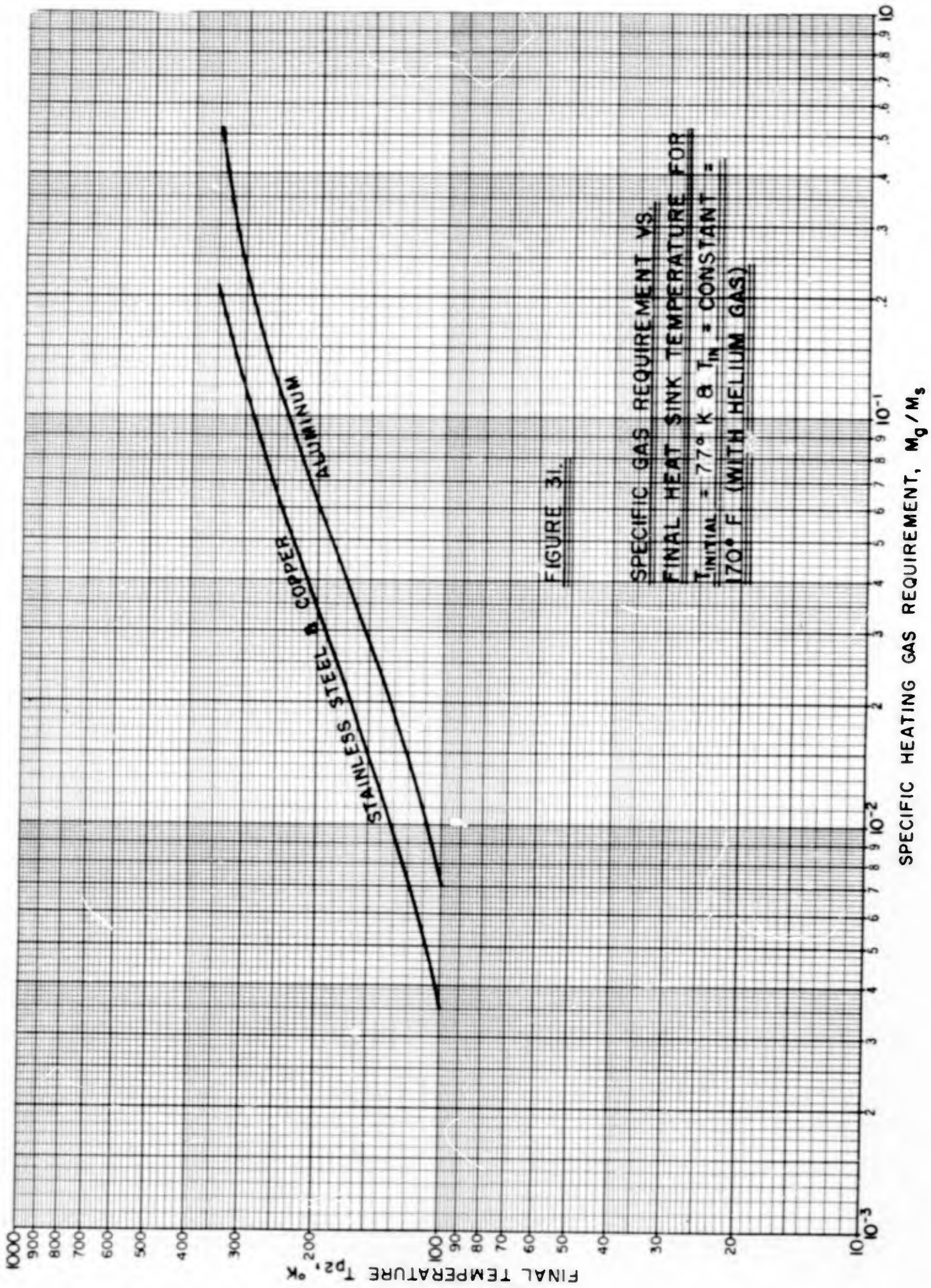

FIGURE 31.

SPECIFIC GAS REQUIREMENT VS.
FINAL HEAT SINK TEMPERATURE FOR
$T_{INITIAL}$ = 77° K & T_{IN} = CONSTANT =
170° F (WITH HELIUM GAS)

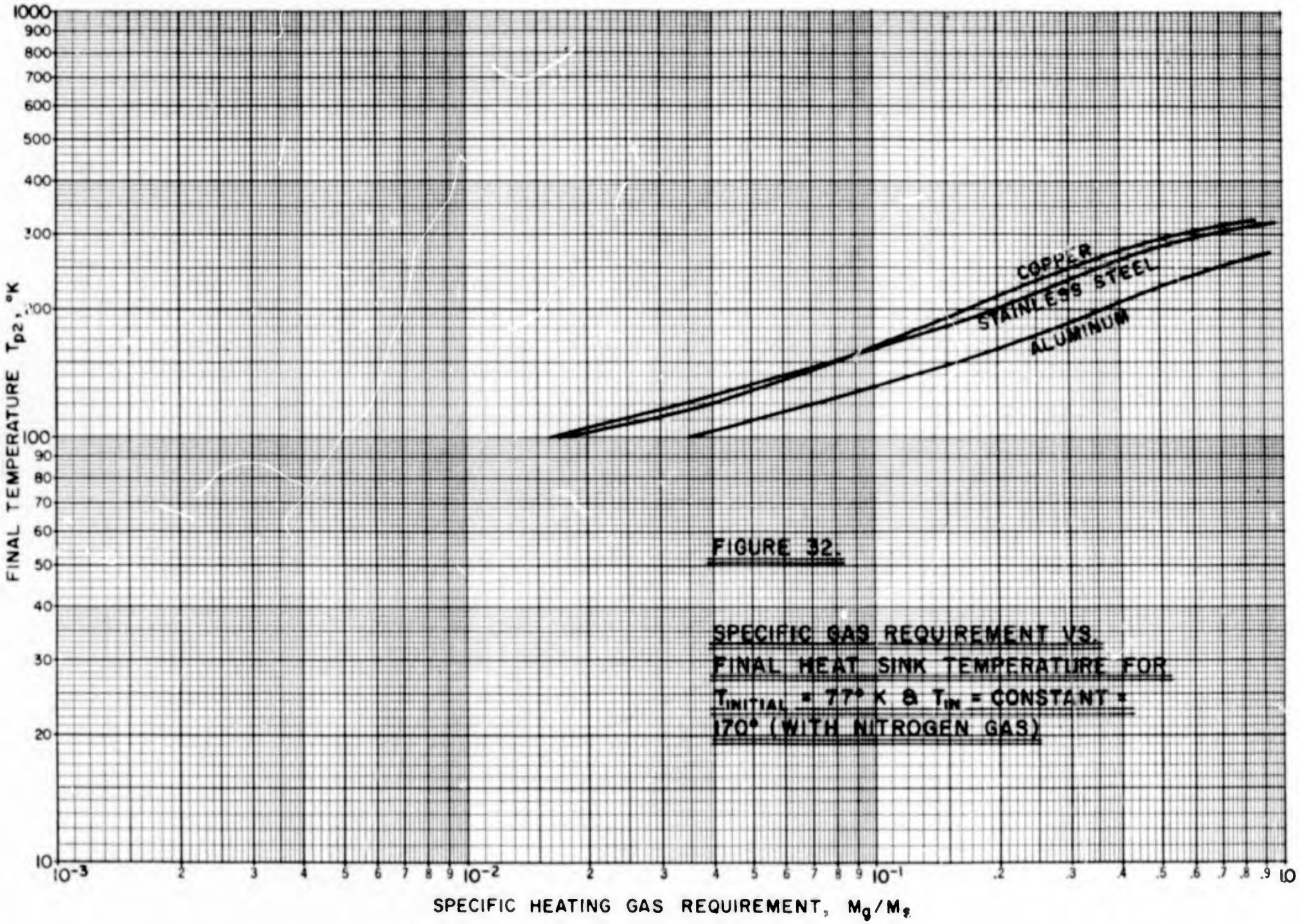

FIGURE 32.

SPECIFIC GAS REQUIREMENT VS. FINAL HEAT SINK TEMPERATURE FOR $T_{INITIAL}$ = 77° K & T_{IN} = CONSTANT = 170° (WITH NITROGEN GAS)

AEDC-TDR-64-121

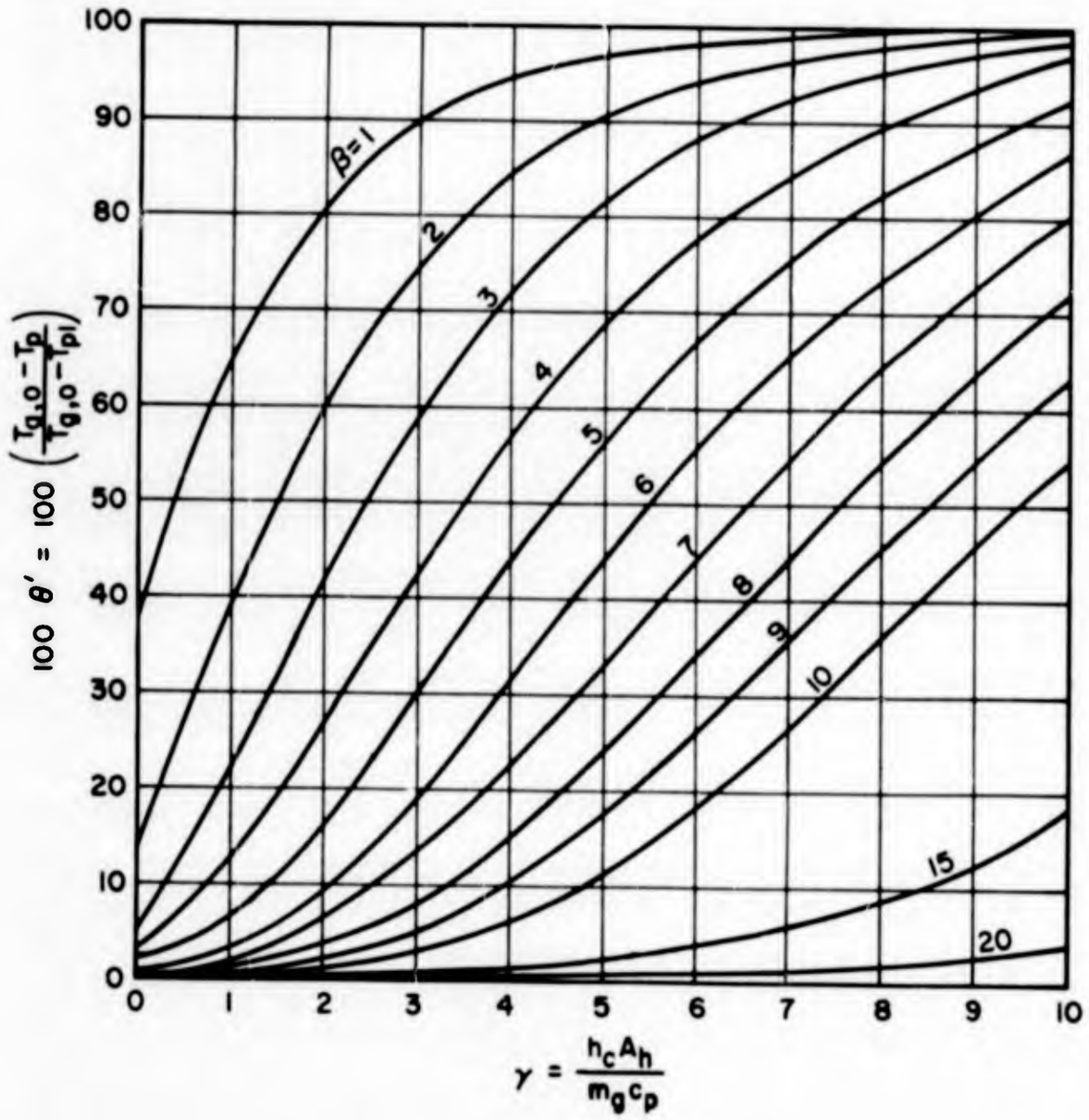

FIGURE 33. θ' VS. γ FOR DIFFERENT β $\left(\beta = \frac{h_c A_h t}{M_s \bar{c}_s}\right)$

BLANK PAGE

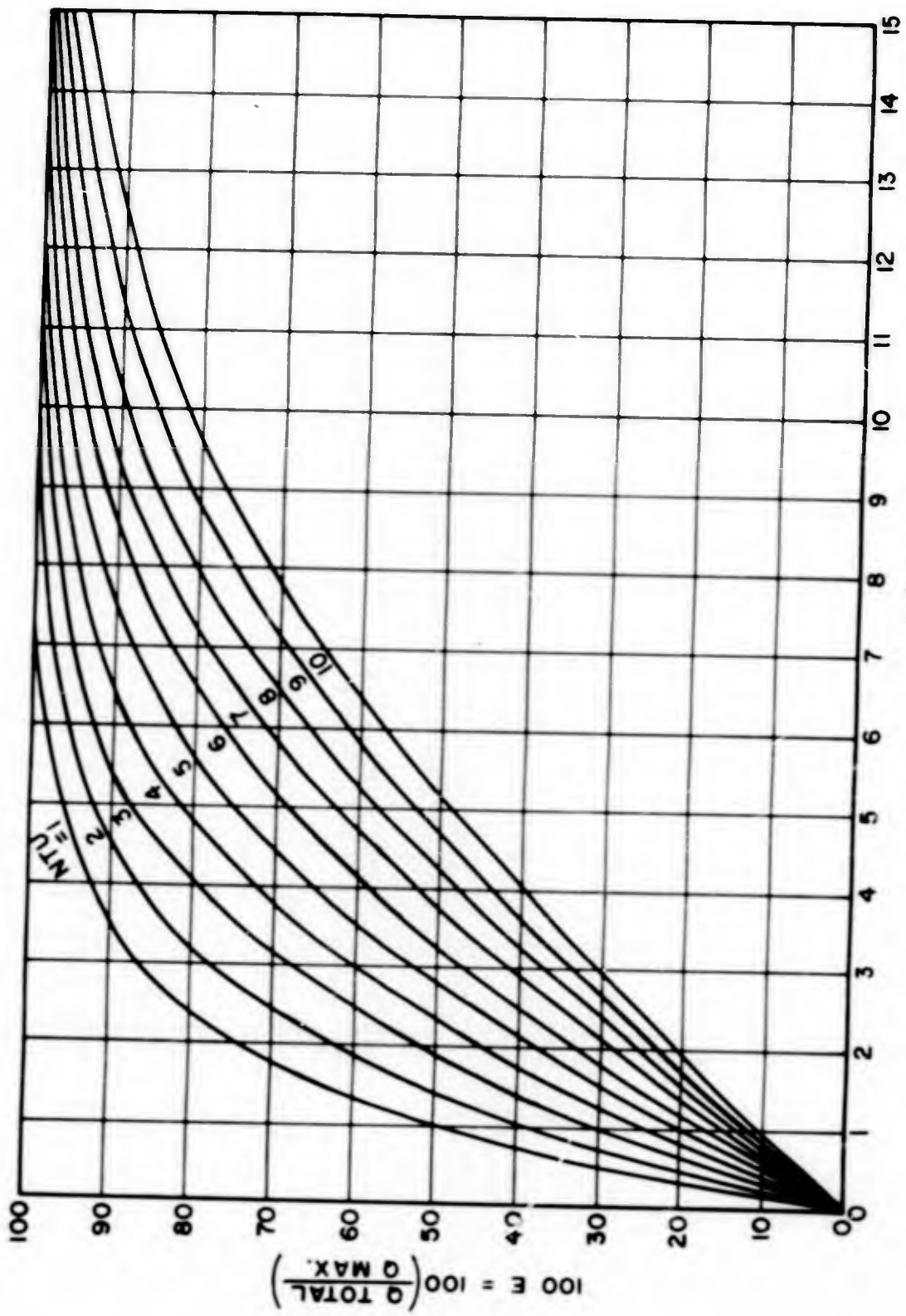

FIGURE 34. E VS. β FOR DIFFERENT NTU $\left(NTU = \frac{h_c A_h}{m_g c_p}\right)$

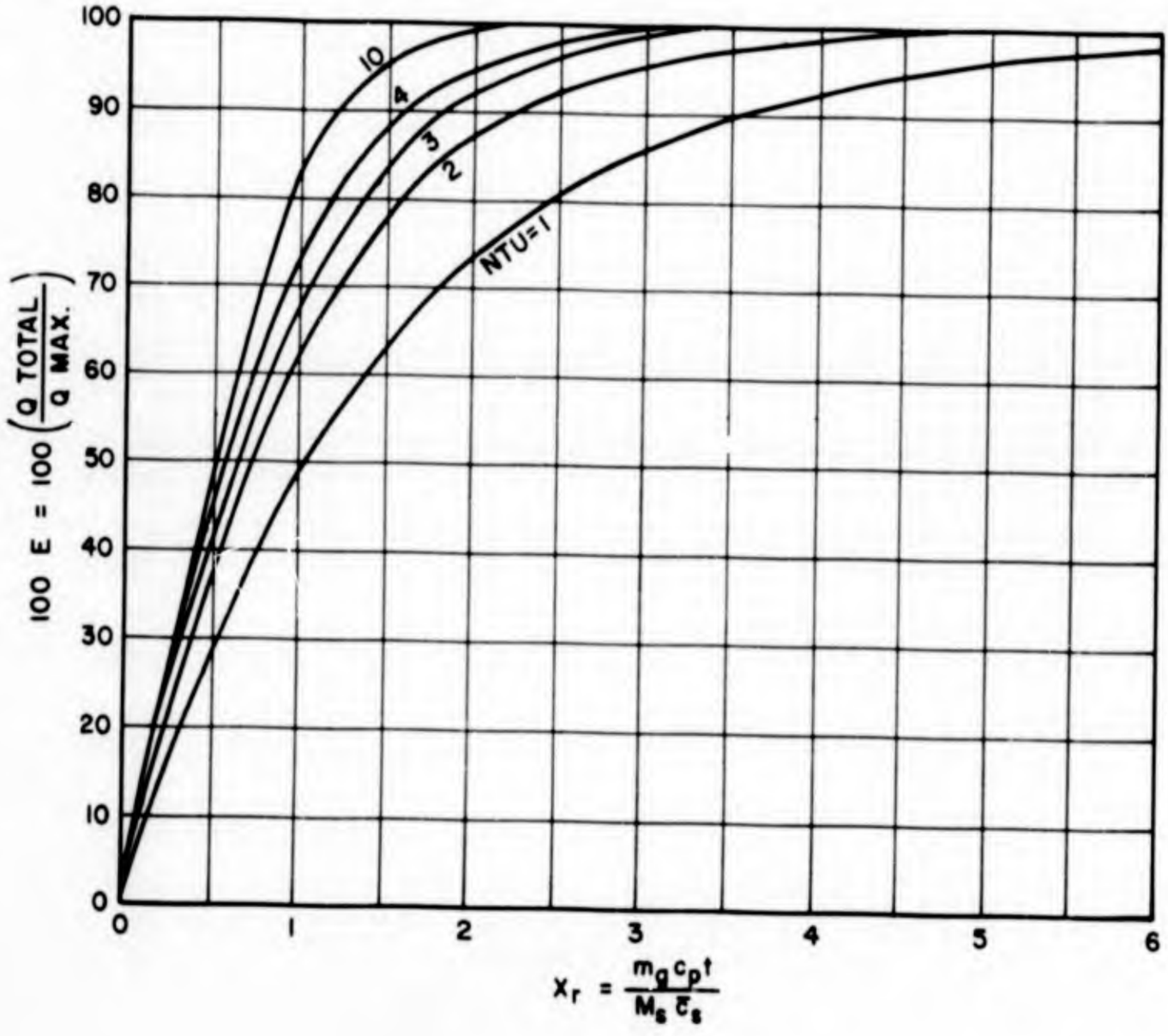

FIGURE 35. E VS. X_r FOR DIFFERENT NTU $\left(NTU = \frac{h_c A_h}{m_g c_p} \right)$

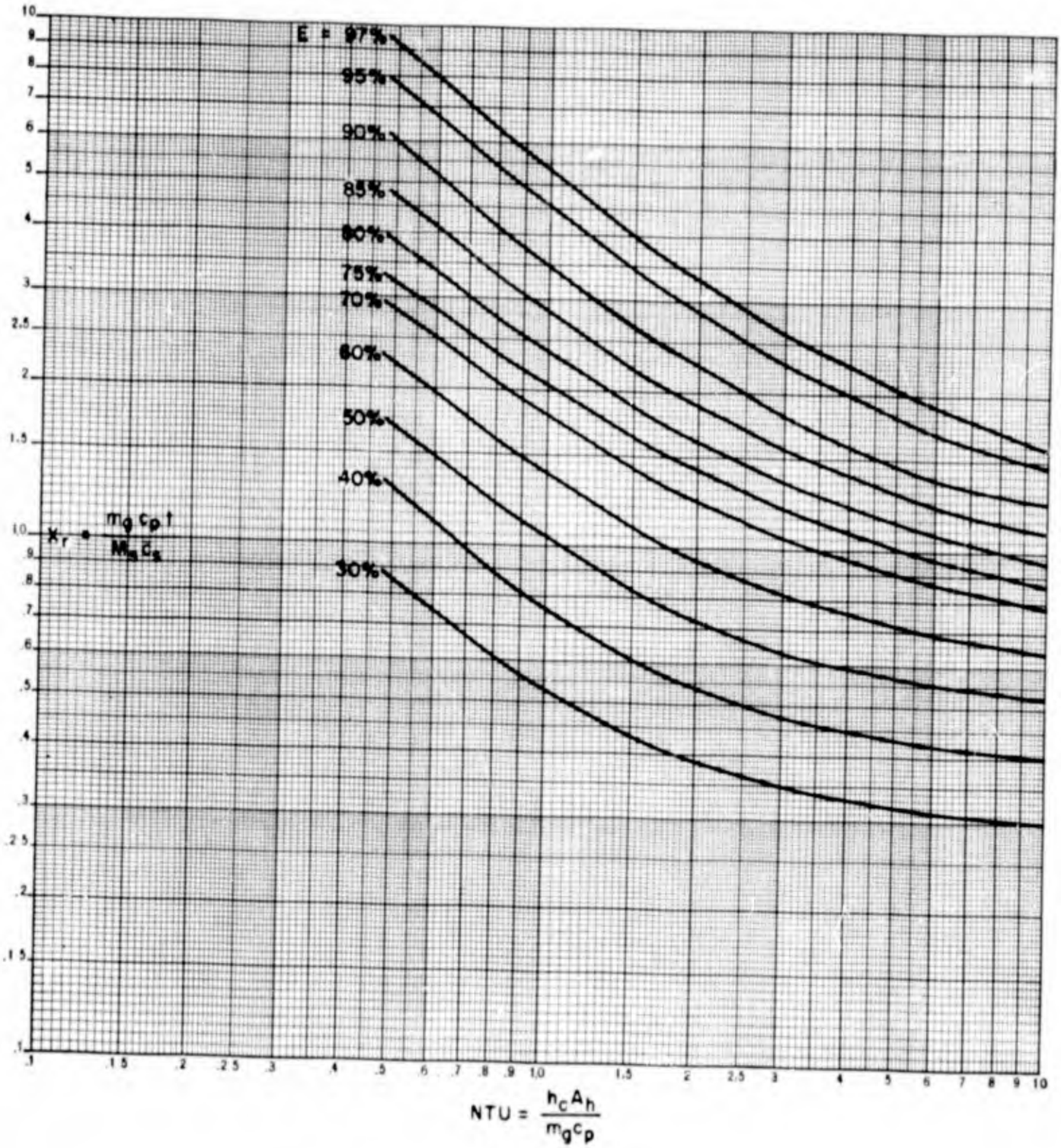

FIGURE 36. X_r VS. NTU FOR DIFFERENT E.

APPENDIX

SAMPLE CALCULATIONS

The use of the warm-up heat transfer calculations, included in Section 7.0 is amplified by the following three solutions to typical problems.

Example Problem # 1

Consider an aluminum heat sink panel ($\bar{c}_s$ = .214 BTU/lb_m-°R) which is to be warmed by nitrogen gas (c_p = .248 BTU/lb_g-°R). The panel is originally at a temperature of -320°F = T_{p1} and the panel inlet temperature of the gas is constant at 220°F = T_{go}. The mass of the heat sink heated by one pass of the gas is 300 lb_m = M_s. The mass flow rate of heating gas per pass is 300 lb/hr = M_g, the tube I. D. = .75" = D, and the length of the pass, L = 375". Determine the time, t required to warm the cryopanel to an average temperature of 120°F = T_{p2}.

The heat exchange effectiveness is given by

$$E = \frac{T_{p2} - T_{p1}}{T_{go} - T_{p1}} = \frac{580 - 140}{680 - 140} = \frac{440}{540} = .815$$

Next, the heat transfer coefficient must be determined so that (NTU) can be calculated. Using the McAdams equation for turbulent flow within a circular tube as given by Kreith.[1]

$$h_c = \frac{.023\, G c_p}{(N_{Re})^{.2} (N_{Pr})^{.66}}$$

where

$G = m_g/A$ = gas mass flow rate per unit cross-sectional area

(1) Kreith, Frank, Principles of Heat Transfer, p. 347 Int. Textbook Co., (1961)

BLANK PAGE

N_{Pr} = Prandtl number

N_{Re} = Reynolds number

Using appropriate values for the gas properties at an average temperature of -50°F, the heat transfer coefficient is calculated as

$$h_c = 62.7 \text{ BTU/hr-ft}^2\text{-°F}$$

The value of (NTU) can be calculated from

$$(NTU) = \frac{h_c A_h}{m_g \bar{c}_p}$$

The heat transfer area $A_h = \pi D L = 6.14 \text{ ft}^2$

$$(NTU) = \frac{62.7 \times 6.14}{300 \times .248} = 5.17$$

From Figure 36, at (NTU) = 5.17 and E = 81.5%, the heat capacity ratio, $X_r = 1.15$. Since

$$X_r = \frac{m_g \bar{c}_p t}{M_s \bar{c}_s}$$

the value of t can be calculated.

$$t = \frac{1.15 \times 300 \times .214}{300 \times .248} = \underline{\underline{.983 \text{ Hr}}}$$

Example Problem # 2

Consider an aluminum heat sink panel ($\bar{c}_s$ = .214 BTU/lb_m-°R) which is to be warmed by helium gas (c_p = 1.24 BTU/lb_g-°R). The mass of the panel is 300 lb_m and it is to be warmed from -320°F to 120°F.

The flow path is .75" I. D. and L = 375"
Determine the mass flow rate of gas required to effect warm-up in 1.0 hr.

As in example 1, E is given by

$$E = \frac{T_{p2} - T_{p1}}{T_{g'o} - T_{p1}} = \frac{440}{540} = .815$$

Since the mass flow rate is not known, a trial and error solution is indicated. Assume a value for G, the mass flow/unit cross-sectional flow area, of 2×10^4 lb/ft^2-hr. Using this value in the McAdams equation,as given in example (1), together with the properties of the gas at an average temperature of -100°F, the heat transfer coefficient is evaluated as

$$h_c = 46.1 \text{ BTU/hr-ft}^2\text{-°F}$$

The parameter β can now be calculated

$$\beta = \frac{h_c A_h t}{M_s \bar{c}_s} = \frac{46.1 \times 6.14 \times 1}{300 \times .214} = 4.41$$

From Figure 34, at a value of $\beta = 4.41$ and E = 81.5%

$$(NTU) = 3.25$$

and since

$$(NTU) = \frac{h_c A_h}{m_g c_p}$$

$$m_g = \frac{46.1 \times 6.14}{3.25 \times 1.24} = 70.3 \text{ lb}_m/\text{hr}$$

The value of G is calculated

$$G = \frac{70.3}{3.07 \times 10^{-3}} = 2.29 \times 10^4 \text{ lb}_m/\text{ft}^2\text{-hr}$$

which is not equal to the assumed value and the procedure is repeated assuming $G = 2.3 \times 10^4$. From this, a value of $m_g = 65.6\ lb_m/hr$ and $G = 2.14 \times 10^4$ is determined.

Again repeating the procedure, the correct value of m_g is found to be

$$m_g = 66.1\ lb_m/hr$$

Example Problem #3

For the conditions in example #2, determine the required mass flow rate, neglecting the effect of heat exchange effectiveness.

In this case, equation (104) may be used,

$$\frac{M_g}{M_s} = \frac{\bar{c}_s}{\bar{c}_p} \ln \left[\frac{T_{g,o} - T_{p1}}{T_{g,o} - T_{p2}} \right]$$

$$\frac{M_g}{M_s} = \frac{.214}{1.240} \ln \left[\frac{680 - 140}{680 - 580} \right]$$

$$= .173 \ln (5.4) = .292\ lb_g/lb_m$$

Thus

$$M_g = .292 \times 300 = 87.6\ lb_g$$

Since the required warm-up time is 1 hr, the mass flow rate is

$$m_g = \frac{M_g}{t} = \underline{\underline{87.6\ lb/hr}}$$